2009

Functional Antimicrobial Surfaces by Ultrafine Powder Coating

Jarrod A.J. Shugg

Functional Antimicrobial Surfaces by Ultrafine Powder Coating

(Spine title: Functional Antimicrobial Surfaces by Ultrafine Powder Coating)

(Thesis format: Monograph)

By

Jarrod A. J. Shugg

Graduate Program in Engineering Science
Department of Chemical and Biochemical Engineering

A thesis submitted in partial fulfilment
of the requirements for the degree of
Master of Engineering Science

The School of Graduate and Postdoctoral Studies
The University of Western Ontario
London, Ontario, Canada

ABSTRACT

The modern era of technology has amplified the significance of coated materials as well as their potential relevance and opportunity. With microbial infection arising as one of North America's biggest public concerns, by the ongoing spread of harmful microorganisms, the need for a marketably simple and durable antimicrobial surface has arisen for applications including inanimate objects and/or biomaterials.

Antimicrobial surfaces cater to public safety by protection/prevention of infectious disease by the reduction of transmission of harmful microorganisms and the intervention of microorganism contamination. This study exhibits the development of various powder coating formulation efficacies against *Escherichia coli* and corresponding bacterial reductions of over 99% after only hours of exposure on metallic substrates. The most effective formulations recognize differences in the inorganic active agent concentrations of silver ion or nano silver metal and accompanied additive percentages of corresponding carrier materials of natural chabazite zeolite or silica gel.

As an additional advantage to functional antimicrobial coatings, ultrafine powder coating is an environmentally friendly green technological coating, since it eliminates the use of toxic solvents that are responsible for the hazardous emissions of volatile organic compounds.

Key Words: antimicrobial surface/coating, ultrafine powder coating, silver ion, nano silver, E. coli inactivation, bactericidal

ACKNOWLEDGEMENTS

I would like to articulate my sincerest appreciation and inmost gratitude to my supervisor Dr. Jesse Zhu. His experienced guidance and dedicated support have made the completion of this research work a reality. I commend him for passing on inspirational knowledge of life and providing me with the necessary levels of focus and determination to conclude this work.

My perpetual gratefulness goes to Mohammad Rahbari for initializing and providing crucial elements of knowledge at the beginning and throughout this long process. His undoubted belief in the project and expertise in the area greatly helped me along my journey. I would also like to thank Dr. Hui Zhang for mentoring me in aspects of powder coating. Whether it was problems I encountered or simply adding unique ideas with creativity, Dr. Zhang's contributions were welcomed as he always pointed me in the right direction.

Tesfa Haille was a great mentor throughout my research and I would like to thank him greatly for always finding time for me. His experience with zeolitic materials and ionic silver allowed me to learn much and continue with my project without indignant barriers.

My dearest appreciation directed to Mehran Soleimani for mentoring me the techniques of microbiology. His knowledge and patience was encouraging. Also to many individuals under the Particle Research Facility and Powder Group your willingness to help was much appreciated.

I also extend my hand in thanks to all of my great friends back home and friends and colleagues throughout my university years away from home. Your moral support, friendship and fun were and will always be much appreciated and remembered.

Finally, I whole heartedly devote and dedicate this research work to my family. To my mother and father Patricia and Paul, brothers Ryan and Justin, sister Kaylee, and my grandparents, your unreserved support and love has made my mission thus far a success. I could not have done it without you. Thank you.

TABLE OF CONTENTS

LIST OF FIGURES

LIST OF TABLES

NOMENCLATURE & ABBREVIATIONS

ASTM	American Standard Test Method
BC	Before Christ
BET	Brunauer Emmet Teller
CNTs	Carbon Nano Tubes
CO_2	Carbon dioxide
CFU	Colony forming unit
DNA	Deoxyribonucleic Acid
EDX	Energy dispersive X-Ray spectroscopy
E.coli	*Escherichia coli*
EMB	Eosin methylene blue
HV	hydroxyvaleric acid
HAPs	hazardous air pollutants
Hap	hydroxy apatite
HGF	human gingival fibroblast cells
ICP-AES	Inductively coupled plasma atomic emission spectroscopy
IUPAC	International Union of Pure and Applied Chemistry
k	First order inactivation rate constant (min^{-1})
LPS	lipopolysaccahride
LB	Luria Bertani
MCP	monocrotophos
MRSA	methicillin-resistant *staphyloccus aureus*
N_0	viable colony forming units at 0 hour
N_t	viable colony forming units at time t
PMMA	polymethyl methacrylate
PHBV	poly(3-hydroxybutyrate)
PVD	Physical Vapour Deposition
ROS	reactive oxygen species
RNA	Ribonucleic Acid
SARS	Severe Acute Respiratory Syndrome

SEM	Scanning Electron Microscope
STP	Standard temperature and pressure
US	United States
UVA	Visible ultra violet
UWO	University of Western Ontario
VRE	Vancomycin resistant *Enterococci*
VOC	Volatile organic compounds
VCC	Viable colony count
TGIC	Triglycidyl Isocyanurate
TEOS	tetraethoxysilane
TMOS	tetramethyl orthosilicate
XRPD	X-Ray powdered diffraction

1 INTRODUCTION

In today's North American society infection is considered to be one of the biggest public enemies. Most informative sources available to the public including television, the internet, newspapers and health articles, show the increasing attention to and awareness of harmful microorganisms. Their widespread, adaptive and increasingly resistant properties are a mounting concern. An estimated five million trillion bacteria are ubiquitously living on earth forming much of the world's biomass (Whitman WB, Coleman DC, Wiebe WJ, 1998). Although the largest pool of bacteria is found in the depths of the oceans, a surprising number are living in places one would not initially expect or concern themselves with that may cause or lead to infection and disease.

In a typical North American office work space, an average desk top surface is home to 84000 bacteria per square centimetre, office telephone includes 10000 bacteria per square centimetre, and 40% of office coffee cups include traces of *Escherichia coli* coliforms (Lee, 2004). Similarly, there are many interesting points to note associated with a typical U.S. household. The Hygiene Council (2007), reported by Hitti (2007), researched 35 U.S. homes, swabbed for bacteria and made interesting discoveries. A bath tub surface included 770760 bacteria per square centimetre, and kitchen sink, kitchen faucet handle, kitchen floor, kitchen countertop, bathroom countertop, and an infant's highchair housed 115897, 85355, 5355, 3148, 2916 and 1226 bacteria per square centimetre. Comparing those values with only 2652 and 1903 bacteria per square centimetre in a garbage bin and on a toilet seat the numbers show plenty of room for improvement in the home and office - especially since some bacteria can survive on such surfaces, dry and wet, for days.

A vast majority of the North American general public are worried about bacteria overall and similarly a large percentage consider food contamination to be a serious health risk. Microbes are everywhere and are continuously being transferred from inanimate fomitic objects to human hands, and vice versa. The nature of microorganisms allows them easy transport from the air, contaminated surfaces or

host beings to uncontaminated or sanitary surfaces extremely quickly. Due to bacterial single cell division it is possible for them to double every twenty minutes.

Accompanying the scare of bacteria in our communities is the expanded research area that has arisen. More and more articles about bacteria are being published then in the past and numerous new age sanitary products are being introduced. It is fair to say that due to the worry of infection from the general population in North America, the antimicrobial product industry, specifically functional antimicrobial surfaces, has great potential. There is need for scientists to be more proactive in prevention and control of bacterial growth. U.W.O. research has shown that an untreated substrate may hold up to 200% more bacteria per square centimetre after just hours of cleaning, than an applied functional antimicrobial surface, both under ideal growth conditions.

A very serious and underlying problem with North American healthcare facilities is that proven to be nosocomial infections. A nosocomial infection is an infection resulting from treatment in a hospital; secondary to the patients original condition. From the biomedical market newsletter, Schachter (2003) reports that there are approximately 2 million cases each year in the United States. From this reported number 30,000 – 80,000 related deaths occur each year. The correlated rate stands at approximately 5-10% of hospital admissions succumb to a type of nosocomial infection during their visit. Antimicrobial coated surfaces within hospitals and medical related devices, fixtures and tools could help in preventing the spread of bacteria and viruses and in turn infection, disease, and death. The market calls for a durable and simple coating solution to microbe contamination risks and problems.

The production of a functional antimicrobial surface coating first lies in the application method of coating to the substrate of choice; this becomes an environmental issue. As it stands the majority liquid paints are organic solvent based. When a liquid paint is coated onto a substrate it needs time to dry to produce a solid coating. It is during this time period that the organic solvent evaporates and releases volatile organic compounds (VOC) into the atmosphere contributing in the long run to global warming. The increasing amount of attention that climate change is receiving from the media, general public and government forces one to notice the

seriousness of our environmental actions and the detrimental effects they may or may not have. The main causes of climate change include carbon dioxide (CO_2), hydrocarbons, emission of fine particulates and VOC's; the latter being the worst of the pollutants. Due to the facts, stringent regulations to reduce VOC emissions are being implemented by governments around the world.

Powder coatings are an environmentally viable solution to organic solvent borne liquid coatings. Powder coatings not only have the environmentally friendly alternative of zero VOC emissions but over sprayed powder from a substrate may be easily reclaimed and recycled yielding negligible waste. The application of powder to a part also has the advantage of reducing energy and labour costs as the process can be completed automatically. Powder is applied to a part by electrostatic spray guns which charge the individual particles, and blow them onto the grounded substrate by air pressure. The physical and mechanical properties of a powder coating lie in the particle size of the powder being sprayed. Regular powder coatings have an average particle size over 30μm while ultrafine powder coatings are below this value. Ultrafine powder is preferred over regular size due to augmented physical and mechanical capabilities possessed by the final coating.

Typically, most sanitary cleaning products utilize an organically based biocide agent. Continuously facilitating organic compounds to inactivate or kill bacteria becomes a serious global health threat as bacteria begin to build immunity and become resistant to that compound. For example this has been reported with certain antibiotics which are no longer allowed to be prescribed and administrated, in certain geographical locations. Not only do organic biocides give way for possible resistance complications but most are harmful and toxic to human beings and mammalian pets. Due to these reasons it is necessary to facilitate inorganic additives to an antimicrobial surface application. It has been known for centuries that certain heavy metals have antimicrobial effects and due to their inorganic and non toxic properties their use is ideal for our research purposes.

Incorporation of additives altering the physical and mechanical properties of a final coating may be accomplished one of two ways in the powder coating manufacturing

process: i) pre-extrusion, or ii) post-extrusion (dry-blended). Additives like inorganic antimicrobial fine powders dry-blended post extrusion with base resin powder paint offers a new insight to a premature technology.

The overall objective and main goal of this research work is to develop highly durable and simple antimicrobial surfaces; investigate the feasibility and effectiveness of dry-blending different inorganic antimicrobial additives with a polyester TGIC resin to produce a simple, durable, functional ultrafine powder coating. The antimicrobial efficacy of oligodynamic metals silver, zinc, copper and their respective ions will be evaluated, as well as metallic silver in nano and micro form, through American Standard Testing Method (ASTM) E2180 and the use of *Escherichia coli*. Essentially, the main goals of the project include:

- ◊ Chemically load silver, zinc and copper ions into natural chabazite zeolite particles and evaluate inactivation of *E. coli;* similarly conduct the same with synthetic zeolite – A,
- ◊ Evaluate differences between chabazite particles loaded at high and low concentrations of ionic silver,
- ◊ Produce Silica Glass by Sol-Gel method and house silver ions into the network structure; compare silica glass carrier with chabazite zeolite carrier with ionic silver, as well as comparisons of ionic silver with no carrier material.
- ◊ Investigate the drying effects of silica gel to pore size and surface area and consequently to bactericidal effectiveness,
- ◊ Produce a powder coating system with nano metallic silver, micro metallic silver and carbon nano tubes coated with silver and compare effects,
- ◊ Vary silver concentrations, consequently additive concentrations, and evaluate effects in powder coatings against *E. coli,*
- ◊ Conduct durability testing of main antimicrobial additives by repeat testing and leaching of coatings,
- ◊ Compare U.W.O. produced antimicrobial coatings in this research to top Industrial antimicrobial powders,

- ◊ Conduct repeatability tests to verify accuracy of obtained results,
- ◊ Apply obtained results to a bacterial kinetic model to further analyze growth curves.

2 LITERATURE REVIEW

2.1 Nosocomial Infection

Bio-contamination of facilities and structures threaten the health of those individuals within and may also force abandonment or disuse for some episode of time. Examples of facility bio-contamination was noticed with the postal service in Washington DC by anthrax (Centers of Disease Control and Prevention, 2002); and by an onslaught of Ebola at a primate facility near Washington DC (Preston, 1994). Facilities like the ones mentioned above only go recognized once disease is recognized by outbreaks of community acquired infection or nosocomial infection. Most healthcare facility bio-contamination events are not as striking as the ones previously mentioned but are very common. Widespread outbreaks of sickness recurrently enter healthcare facilities and go unrecognized for hours and even days, allowing to spread before being identified (Shen Z, Ning F, Zhou W, He X, Lin C, Chin DP, Zhu Z, Schuchat A, 2003).

When dealing with nosocomial types of infection, typically surface contamination plays a main factor but the overall degree to which it does is not clear. The biomedical market newsletter reports that there are approximately 2 million cases each year in the United States (Schachter, 2003). From this reported number 30,000 related deaths occur each year. The rate stands at approximately 5-10% of hospital admissions succumb to a nosocomial infection. However a conflicting number of deaths due to nosocomial infection were recognized by Feied (2004), Starfield (2000), and Bennett JV & Brachman PS (1992), at 80,000 per year. The inflicted economic cost from these infections was estimated at $5 billion annually (Wenzel, 1995).

Hospital acquired bloodstream infections are ranked the eighth leading cause of death in the U.S. (Wenzel, RP and Edmond MB, 2001) and the primary mode of transmission is through physical contact. Physical transmission of infection can be direct or indirect; person to person or person to object to person. The object involved in the indirect

transmission of infection is simply any "inanimate object (as a dish, toy, book, doorknob, or clothing) that may be contaminated with infectious organisms and serve in their transmission," (Merriam-Webster, 2005). This definition corresponds to the term fomite.

2.1.1 Surface Contamination by Fomites

Fomites may be macroscopic surfaces or individual loose particles. The surfaces have the potential to be passive or active; having the ability to simply accept contaminants with passiveness or the ability to accept, support growth and spread contaminants aggressively (Feied, 2004). Healthcare personnel are in constant contact with fomitic surfaces before direct physical contact with patients, thus yielding the opportunity for the spread of indirect contamination. This is shown by the little consideration sought towards common contact surfaces as "doorknobs, wallplates, faucets, countertops, bedrails, carts, telephones, pens and clipboards" (Feied, 2004) in a hospital. Additionally, objects like stethoscopes rarely receive any significant attention before and/or after periods of contact between patients thus adding a potential vector for infection. Studies with 55 stethoscopes and 42 otoscopes used by physicians in a community found that 100% and 90% were contaminated pathogenic bacterium and some even with methicillin-resistant *staphyloccus aureus* (MRSA) (Cohen HA, Amir J, Matalon A, Mayan R, Beni S, Barzilai, 1997).

Pathogens commonly found in a hospital setting can be supported by most typical fomite surfaces for extended periods of time. There are many examples and statistical data to support this but only a couple examples will suffice. Vancomycin resistant *Enterococci* (VRE) bacterial strains have been found to survive on surfaces and surgical equipment for 5 days to 2 months on dry surfaces (Bonilla HF, Zervos MJ, Kauffman CA, 1996). Wendt C, Wiesenthal B, Dietz E, and Ru-den H (1998), reported that VRE strains survived for atleast one week and up to 4 months on dry polyvinyl chloride. VRE strains of *faecalis* and *faecium* have also shown to survive on potential surfaces in a hospital where countertops allowed survival for 5-7 days, bed rails 24 hours, telephones and fingers (with/without gloves) 60 minutes, and stethoscope diaphragms for 30 minutes.

Coronaviruses including severe acute respiratory syndrome (SARS), pseudorabies virus, *Chlamydia,* varicella virus, parainfluenza, herpes complex, and MRSA were all found on and to possess a significant shelf life on typical fomite surfaces (Feied, 2004); *Staphylococcus epidermidis*, *Staphylococcus aureus*, *Alpha Streptococci*, *Corynebacterium acnes*, *Klebsiella pneumoniae*, *Pseudomonas aeruginosa*, *Escherichia coli*, and many others were found colonized on teddy bears that were in hospital rooms no longer than a week (Hughes WT, Williams B, Williams B, Pearson T, 1986).

There are many factual examples where fomite surfaces are directly blamed for the transmission of a particular disease. However any such case that exists has not been clinically proven to start and spread from a particular fomite source. Essentially, the reason why a fomite surface is blamed for such events is because they are the *most likely* cause of an outbreak or episode to take place. Due to the relevance of individuals associated with a particular minute location, the contamination involved and the correlating fomites presented, it only makes sense to blame these things for the extreme misfortune of spreading of disease. Examples include: outbreak of hepatitis A spread by contaminated drinking glasses in a public house (Sundkvist T, Hamilton GR, Hourihan BM, Hart IJ, 2000); outbreak of herpes simplex virus by radiator in neonatal nursery (Sakaoka H, Saheki Y, Uzuki K, Nakakita T, Saito H, Sekine K, Fujinaga K,1986); chlamydial eye infection by nonporous plastic surface in vitro (Novak KD, Kowalski RP, Karenchak LM, Gordon YJ, 1995); and indirect transmission of SARS coronavirus (Dutronc H, Dupon M, Cipriano G, Lafarie S, Lafon ME, Fleury HJ, Bocquentin F, Neau D, Ragnaud JM, 2004).

2.1.2 Manual Cleansing Not Sufficient

Particularly in microbiological laboratories and areas of intensive medical use, regular and thorough disinfection of surfaces is required in order to reduce the numbers of bacteria and to prevent bacterial transmission and contamination. Conventional methods such as disinfection by wiping are not effective in the long term, cannot be standardized, are time and staff intensive and use repeated aggressive chemicals (Kuhn, 2003).

Disinfection by hard ultraviolet C light is not satisfactory as depth of penetration is insufficient and there are occupational medicine risks. Additionally, every year it is becoming more difficult to fight infection as MRSA and VRE exhibit increasing rates of resistance to commonly used antimicrobials that are mainly found in healthcare facilities (Conly JM, Johnston LB, 2000).

The current approaches to limiting nosocomial infections are traditional and insufficient. The focus lies in quarantine of air borne infection by introducing respiratory blockades (face masks) and by simple reduction of direct person to person contact and hand washing (Feied, 2004). Nosocomial infections are presently a continuing epidemic and there is enough evidence to support the fact that the current approaches to limiting nosocomial infections in our healthcare facilities is failing and the adequacy is not there to eradicate the problem. The secondary problem facing nosocomial infection is the objective of eliminating a bio-contamination event once it is officially recognized in a facility and to keep that decontamination procedure ongoing if it is to be effective against contamination that is also on going. Indefinite contamination is likely by cracks and crevices in healthcare units. Routine manual disinfection is especially impractical for heavy populated emergency departments or intensive care units in a hospital. It is impossible to prevent all episodes of contamination but it is possible to keep it under control and introduce a significant reduction - Antimicrobial activity by a surface presents a pathogen death rate by reducing survival time and thus continuous reduction of transmission of disease. The term *infectious dose* is a measure of the number of organisms required to cause an infection or disease (Hardy SP, 2002). It describes the ability of an organism to occupy itself in a new host as all microorganisms pathogenic or not have a different infectivity. Therefore, reduction of the number of organisms available for establishment into a vulnerable host reduces the likelihood of possible infection and/ or transmission of by limiting the infectious dose. As such, photocatalytic oxidation on surfaces coated with metal oxides may be a possible alternative solution (Kuhn, 2003). Additionally any functional, effective and durable antimicrobial surface may serve a significant and worthwhile healthcare purpose.

2.1.3 Biomaterials

Fifty percent (50%) of all nosocomial infections are accounted for by biomaterials, or medical implant-associated infections (Gollwitzer H, Ibrahim K, Meyer H, Mettelmeier W, Busch R, Stemberger A, 2003). Biomaterial is termed as any substance (not a drug) or combination of substances synthetic or natural which can be used for any time period as a whole or part of a system that treats, augments, or replaces any tissue, organ or function of the body (Von Recum AF and LaBerge M, 1995). Most prosthetic devices in common use are made from a narrow range of biomaterials: silicone elastomer, polyurethanes, fabricated polytetrafluoroethylene (teflon) or polyethylene terephthalates (Dacron), titanium, stainless steel, ceramics and composite materials containing carbon or glass fibres. Examples of such devices are large joint (hip, knee etc.) replacements for arthritis, spinal fixation to stabilize spine after cancer or trauma, prosthetic heart valves, pacemakers, central venous catheters for parenteral nutrition, shunts, catheters, and many more (Bayston R and Allison D, 2000).

Infection of a biomaterial is the second most common cause of implant failure (Neuta D, van de Belt H, Stokroos I, van Horn JR, van der Mei HC, Busscher HJ, 2001). Infection rates can reach 5-10 % in dental implants, 10-30 % in bladder catheters, 25-50 % in heart-assist devices and even 100% for external fixation pins (Ratner BD, Hoffman AS, Schoen FJ, Lemons JE, 2004). Due to the high rates of infection for biomaterials, it is fair to conclude that the use of implantable medical devices may result in infectious complications.

There are two contamination modalites that may occur in order for a biomaterial infection to take place (Rimondini L, Fini M, Giardino R, 2005):

1) Introduced during implantation in the surgical environment,
2) or carried to biomaterial surface once implanted by bacteraemia. Where bacteraemia is simply bacteria in the bloodstream.

The microorganisms involved in infection can range from viruses, fungi, protozoas, and bacteria. The most frequent microorganisms involved in infections are endogenous

bacteria. This means that the bacterial infection arises from within the body, and may be due to the normal flora of the secific physiological department of implantation. *Staphylococcus epidermidis* is a type of bacteria that will most often adhere to polymers contrasting *Staphylococcus aureus* that will adhere to metals (Rimondini et al, 2005).

2.1.4 Biofilm

It is well known that most pathogenic bacteria diminish immediately when subjected onto a surface. However, it is possible for transmission of such species to still occur days or weeks after, especially in humid conditions. Humid conditions, in vitro, present the possibility of biofilm formation for many surfaces leading to microbial induced corrosion of pipelines, food and water contamination and a variety of biomaterial related infections (Gottenbos B, van der Mei HC, Busscher HJ, 1999). Infection of biomaterials always occurs in relation to biofilm formation (Inabo, 2006). Biofilm formation results in a bacteria community glued in a matrix like slime. The film acts as one multicellular organism rather then thousands of separate bacterial cells. Essentially it is a very protected mode for the bacteria to survive. The steps of biofilm formation for biomaterials are very similar to those steps that would occur in an in vitro aqueous environment, thus biofilm is serious problem for both fomitic surfaces and biomaterials.

The first and primary step to biofilm formation is adhesion. Adhesion rarely takes place between bacterium and naked biomaterial. Within seconds of a biomaterial being surgically implanted into the body, a surge of plasma-derived glycoproteins interact with its surface, leading to a steady state conditioning film (Bayston et al, 2000). Bacteria and microbes adhere to the components of this film and irreversible attachment has taken place. The organisms which are not killed by phagocytosis multiply developing micro-colonies. Production of exopolymers then allows adherence of the organisms to one another, constructing the biofilm. The major exopolymer involved in cell-cell adhesion is polysaccharide intercellular adhesion (Bayston et al, 2000).

Complications of Biofilm Formation

There can be many implications once biofilm is formed on a biomaterial device. There is potential for biomaterial breakdown as bacteria may try to use the implant for nutritional purposes (Carbon, Nitrogen) with persistent infection. Film can break off once matured and spread infection to surrounding areas and other susceptible sites; leading to chronic infection. There may also be absence of tissue integration with implant, and if the implant capsule needed to be porous then it will suffer from reduced vascularity.

Antibiotic resistance is a main issue in the medical industry today and with treating biofilms. Related studies show that antibiotic therapy simply leads to incomplete killing of the organism, which further leads to withdrawal of the antibiotic. Exposing the bacteria to an antibiotic and then withdrawing the drug when the bacteria are not completely irradicated, help the bacteria to become resistant to that drug. The bacteria mutate into evolved bacteria that have seen that specific mode of attack and can resist it. In order for antibiotic therapy to be effective and kill off the biofilm, treatment would have to be increased 1000 fold (Noble, 2004). Additionally, since the human body's defences cannot eliminate the biofilm either, the only option left is removal of the biomaterial device. If the device was left it may not function properly and chronic infection symptoms would persist.

There are various strategies available for biofilm contamination prevention: physical surface properties may be altered to prevent or limit bacterial adhesion, or chemical modifications can be made to the surface or bulk matrix of the implant material. Chemical modifications mainly exhibit the release of antimicrobial agents to the surrounding environment. Antimicrobial agents include traditional antibiotics, inorganic metals, organic antiseptics or adhesion inhibitors. Currently there are vast areas of research in the field of Antimicrobial biomaterials. With antibiotic resistance becoming a major concern, inorganic antimicrobial chemicals are being researched extensively.

2.2 Antimicrobial Systems and Chemicals

The production of an antimicrobial part can be manufactured in two different ways. One class includes the active agent throughout the entire work piece (ie. plastics) and the other involves surface coatings. Parts that are manufactured with antimicrobial agents(s) throughout the whole of the part still rely on the concentration of such agent at the surface. The biocidal agent may be coupled into an acrylic polymer matrix where it is possible for migration to occur in amorphous parts of the polymer. The antimicrobial action in acrylic polymer for example is claimed to last the lifetime of the part. If agent is removed from the surface by friction, abrasion or general wear, more of the agent will migrate to the surface until the agent's internal vapor pressure reaches equilibrium (Watterson and Hanrahan, 2002). Organic antimicrobial substances, free of heavy metal are most often used when incorporating antimicrobials throughout an entire part because inclusion of heavy metals or inorganic compounds would surely alter the mechanical properties of the work piece.

Surface coatings for antimicrobial parts may be more of an economically feasible method of application. The coating application may vary from dipping, spraying, or various nano technological methods (physical vapor deposition, chemical vapor deposition etc.), thus being more cost effective as a smaller biocidal concentration is necessary. Paints have been used for surface coatings and their application area is immense. Applications include any inanimate object where bio-contamination may be transmitted; treatments in public and healthcare facilities, households, biomaterials and others. Organic or inorganic agents may be included into a surface coating without worry of leaching or affecting the mechanical properties of the whole part.

Organic substances can be effectively used in many settings but problems exist under high wear settings or longer life applications as the substances are unstable under certain temperatures and pressures. Organic biocides are most often used when the hole of the part is manufactured as an antimicrobial product. They are included within plastics and fabrics during the manufacturing stages. Organic agents are used because they have a

smaller effect over inorganic additives to the mechanical properties of a part. In contrast inorganic additives are predominantly used in surface coatings.

Antimicrobial powder coatings have only recently become commercially available. The addition of antimicrobial chemicals to powder coatings has potential to inactivate microbes from surfaces finished with the antimicrobial powder. Antimicrobial additives can be classified as either organic or inorganic. With significant human exposure, such biocidal additives should be inorganic. Organic additives such as bleach or methyl urea are toxic to humans, animals and plants. Not only are organic chemicals toxic, but they also degrade organic components of the powder coating over time. The most important reason for incorporation of inorganic antimicrobial additives into the powder coating is so microbes cannot build up immunity or resistance with lengthy exposure. Inorganic additives will mainly be discussed in this paper.

There are many different types of inorganic additives that one may incorporate into a powder coating that can potentially kill microbes. A microbe includes bacteria, archea, fungi and protists. Bacteria are included in archea, while protists describe algae, amoebas, molds and protozoa. Viruses are also a major type of microbe, but there is much discretion whether they are living or not. All additives aimed at destruction of microbes may or may not be totally effective against viruses.

2.2.1 Ionic Metals

Working ionic metal species may include any oligodynamic metal such as: silver, copper, zinc, mercury, tin, lead, bismuth, cadmium, chromium, cobalt, nickel, iron, manganese, arsenic, antimony and barium (Mawatari M, Hamazaki C, Furuyama T, 1997). Of silver, zinc and copper, silver is the least cytotoxic (Williams RL, Doherty PJ, Vince DG, Grashoff GJ and Williams DF, 1989) and copper has the best antifungal effect. Inorganic compounds including cadmium, mercury and arsenic are strong antimicrobial agents but they are toxic and unsafe.

Silver Ion

Silver has several oxidation states including zero valent Ag^0, monovalent Ag^+, as well as higher oxidation states Ag^{2+} and Ag^{3+} and is one of the strongest antimicrobial agents. Silver in its colloidal form (dispersion of nano silver particles in water) is most commonly used to create antibacterial characteristics. Silver's history of use as an antimicrobial dates back to fifth century BC for applications of water storage (Feied, 2004).

Among the various antimicrobial additives, silver is special because of its natural properties of high thermal stability and long term activity (Radheshkumar C, and Munstedt H, 2006). Silver is a versatile antimicrobial agent because it has intense antimicrobial properties and little toxicity to mammalian cells and tissues. Bacteria inactivated by ionic silver show a low tendency to develop immunity or resistance (Ijaz MK, Brunner AH, Sattar SA, Nair RC, Johnson-Lussenburg CM, 1985). Not only does ionic silver show little cytotoxicity but due to its unique action, binding to and denaturing DNA and RNA, ionic silver presents a possible mechanism for inactivation of viruses (Modak SM, 1973).

Silver ions produce most toxic effects once inside a cell. Systems that usually transport essential ions for a cell such as passive transport and active transport systems are means of transportation for silver ions to enter the cytoplasm inside. Silver ions have the ability to bind to electron donor groups (containing sulphur, nitrogen or oxygen). They also have the ability to bind to negative charged groups (containing phosphate or chloride).

Ionic silver is especially important as an antimicrobial agent for biomaterials. Clinically silver exhibits low toxicity in the human body and minimal risk is expected due to clinical exposure (Lansdown, 2006), thus making it a great antimicrobial candidate in vivo. Chung RJ, Hsieh M, Huang CW, Perng Li-H, Wen Hsiao-W, Chin Tsung-S, (2005), report that 100 ppm silver ion creates a significant antibacterial effect, but 1000 ppm silver shows evidence of extreme cytotoxicity. However in a separate article by Feng QL and Cui FZ (1999), reports show that up to the concentration of 20 ppm $AgNO_3$

(12.7 ppm Ag) there is excellent biocompatibility; where no significant morphological changes of macrophages and osteoblasts were noticed, suggesting that the function of bone cells were not affected. They also report that this specific concentration presents an effective antimicrobial effect. Thus, Ag-treatment of implant materials to prevent infections should be limited to the amount of 20 ppm $AgNO_3$ or 12.7 ppm Ag.

Mechanisms of Inactivation

The silver ion is lethal to all bacteria, including MRSA and VRE; few incidences of resistance have ever been recorded (Baranoski S, Ayello E, 2007). Not only is silver ion lethal to all bacteria and resistant strains but it is proven to be extremely toxic against coronaviruses specifically that of SARS (Feied, 2004). Studies show complete inactivation of SARS coronavirus by silver zeolite antimicrobial powder in bulk suspension testing within as little as two hours.

Feng QL, Wu J, Chen GQ, Cui FZ, Kim TN, Kim JO, (2000), directly investigated the mechanisms of inhibition of silver ions on microorganisms. Two strains of bacteria were used in the study namely gram-negative *Escherichia coli K-12* and gram-positive *Staphylococcus aureus*. After Ag^+ treatment, both types of bacteria underwent similar morphological changes: the cytoplasm membrane detached from the cell wall, an electron light region appeared in the center of the cells containing condensed deoxyribonucleic acid (DNA) molecules, electron-dense granules were found around the cell wall, large amount of electron dense granules inside the cell and an extremely damaged cell wall. Thus the existence of elements of silver and sulfur in such electron-dense granules and cytoplasm suggest essentially that a) DNA loses its replication ability and by disrupting DNA strands the cell division is inhibited b) protein and enzyme dysfunction leading to disrupted cell metabolism and c) damaged and degraded cell wall preventing respiration by inhibiting transport functions in the cell wall. The prime molecular target for the silver ions exist in cellular thiol (-SH) groups commonly found in enzymes, inactivating them and inhibiting energy sources. When interacting with DNA, a marked enhancement of pyrimidine dimerization occurs by photodynamic reaction that may prevent DNA replication (Matsumura Y, Yoshikata K, Kunisaki S, and Tsuchido T, 2003).

2.2.2 Nano Metallic Silver

Silver nanoparticles can exhibit broad morphologies in the nano meter scale. They are known to have a highly reactive and sensitive surface. Silver nano particles have been identified to act primarily in three ways against gram- negative bacteria: (i) in the range of 1-10nm, silver attaches to the surface of the cell membrane and interrupts proper functions like permeability and respiration; (ii) they penetrate into the bacteria and cause damage by interacting with sulfur and phosphorus containing compounds – DNA – inhibiting replication; (iii) release of silver ions which have additional biocidal effects against bacteria (Morones JR, Elechiguerra JL, Camacho A, Holt K, Kouri JB, Ram´ırez JT and Yacaman MJ, 2005). When distributed in a surface coating, silver nano particles also present electronic effects – defined as changes in the local electronic structure of the surface due to size. This further enhances the reactivity of the surfaces and their antibacterial action. Current developments in the area of nano technology have facilitated the use of silver into plastics, fabrics and coatings without the necessary requirement of zeolite (Wagener M, Steinruecke P, Bechert T, 2004).

Production of metallic silver particles can be done a variety of ways by chemical means. One method involves the oxidation of a specific silver-ammonia complex ion. This complex ion is termed Tollen's reagent. It is well known as a silver mirror reaction where metallic silver is formed as a silver metal film. The experiment involves production of this Tollen's reagent and the addition of an aldehyde. Aldehydes are easily oxidized to carboxylic acids. When an aldehyde is added, silver oxidizes the aldehyde to a soluble carboxylate anion and the silver cation is reduced to metallic silver. The subsequent silver precipitates in solution and along the side of the housing glassware (Johnson WA, 1998).

Reducing silver in Tollen's reagent is simply an oxidation-reduction reaction (redox reaction) where formaldehyde may be the reducing agent. Silver cation as its ammonium complex can be changed into its free metallic form by addition of electrons by the reducing agent. When Tollens reagent is reduced by an aldehyde it will form metallic silver but there is nothing involved in the reaction to prevent or protect the silver from assembling into large micro structures. Mainly micro structures exist separately or within

deposited films when reducing the silver in Tollens reagent without the use of capping agents to prevent assembly (Buckley F, 2006). There are many capping agents described in literature that prevent assembly of silver when it is reduced to produce a final nano form. Capping agents include citrate and polyvinyl pyrrolidone (Sun Y, Yin Y, Mayers B, Herricks T, Xia Y, 2002). Capping agents make silver particles repel each other so they do not accumulate and precipitate as metallic films or micro structures during the chemical reaction.

2.2.3 Metal Oxides

Metal oxides will have a greater antimicrobial effect in the presence of light, while metallic ions can kill bacteria in the absence of UV rays. Of the metal oxides, TiO_2 and ZnO will be reviewed most but it should be noted that other forms of oxides yield an antimicrobial effect - other forms vary from but are not limited to: magnesium, calcium, germanium, aluminum, and copper (Mawatari M, Hamazaki C, Furuyama T, 1997).

Titanium Dioxide

Titanium dioxide (TiO_2) is a photocatalyst which can deactivate microbes. As a photocatalyst, TiO2 is photo-activated meaning it works in the presence of UV light. Specifically, UV light with a wavelength shorter than approximately 380 nanometers activates TiO_2. Light at the required wavelength provides the band gap energy (3.2eV) needed by an electron to jump from the valence band to the conduction band, in the chemical makeup of TiO_2. The absorbed photons generate excited pairs of electrons and holes or electron-hole pairs. It is from these generated holes that TiO2 releases an antimicrobial effect. The holes react with water (moisture in the environment i.e. humidity) to produce hydroxyl radicals (OH^-) and electrons react with oxygen yielding super oxide radical anions (O_2^-). Perhydroxy radicals (OOH) and H_2O_2 are also formed in the process (Vohre A, Goswami DY, Deshpande DA, Block SS, 2005). These radicals are highly reactive and in the presence of oxygen they initiate a complex of oxidation reactions resulting in oxidization of microbes and organic material. In the presence of

water and oxygen, highly reactive radicals are generated by TiO_2 and ultraviolet A light (UVA). These radicals have the ability to destroy bacteria and have the potential to reduce bacterial contamination in said environments.

TiO_2 has the confirmed ability to oxidize many types of bacteria (Kuhn KP, Chaberny IF, Massholder K, 2003). Hygiene specific bacteria, including: *E. coli, P. aeruginosa, S. aureus, E. faecium* and *C. albicans* were found to be significantly reduced by plexi-glass panels coated with nanometer sized TiO_2 powder. The bacteria were illuminated on the sample specimen by UVA light in different concentrations. The reduction efficiencies were found to decrease in the same order as the bacteria listed above, *E. coli* → *C. albicans*. Oxidation subsequent inactivation of *E. coli* was possible after only one hour and the inactivation of the other types of bacteria showed similar results only with different reduction efficiencies. Using a light and scanning electron microscope the cell wall of bacteria was examined throughout experiments where exposure to UVA light was conducted. The complexity and density of the cell wall of the bacteria increases in the same order of precedence: *E. coli, P. aeruginosa, S. aureus, E. faecium* and *C. albicans*. Therefore observing the rate of oxidation on the types of bacteria and the density and complexity of the cell walls of the bacteria, after TiO_2 exposure, the clear effect of TiO_2 is noticed - the primary step in photocatalytic decomposition consists of an attack by OH radicals on the cell wall, leading to punctures. As the cell wall increases with bacteria, the potential for oxidation and inactivation decreases (Kuhn et al, 2003).

There are many mechanisms of photocatalytic inactivation of microorganisms proposed in literature. Huang Z, Maness PC, Blake DM, Edward J, Wolfrum EJ, Smolinski SL, and Jacoby WA, (2000), state that the initial oxidative damage due to photocatalysis takes place on the cell wall and further damage occurs to the underlying cytoplasmic membrane. Cell permeability increases as a result and allows the free flux of intracellular contents bringing on cell death. Maness PC, Smolinski S, Blake DM, Huang Z, Wolfrum EJ and Jacoby WA, (1999), concluded that the lipid peroxidation reaction is the main mechanism of death of *Escherichia coli* K-12 cells in the presence of TiO_2 and an irradiation light source. Photocatalysis induces peroxidation of the polyunsaturated

phospholipid component of the lipid membrane of the bacterial cell wall. Cell wall damage subsequently leads to loss of respiratory activity.

Zinc Oxide

Zinc oxide is a photocatalyst, is activated with UVA light and can also inactivate microorganisms. ZnO nanoparticles damage the cell wall of bacteria (Zhang L, Jiang Y, Ding Y, Povey M, York D, 2007) in the same fashion as TiO_2. The mechanisms of photocatalytic inactivation of microorganisms are the same as described prior. ZnO copes well in very harsh environmental conditions, and has the ability to remain stable in pH ranges from 4 – 14.

ZnO operates very similar to Titanium dioxide (TiO_2) described earlier. A main difference, when comparing TiO_2 and ZnO, is that ZnO has wider band gap energy of 3.37eV. This theoretically means that it should take more energy to promote en electron to jump from the valence to the conduction band; yielding electron hole pairs. However, ZnO is a young chemical in the new antimicrobial industry and new journal papers comparing the two chemicals suggest that ZnO is an overall better choice in the matter: the rate of degradation of pollutants is faster with ZnO than with TiO_2. This is due to the fact that ZnO produces H_2O_2 more efficiently (Anandan S, Vinu A, Venkatachalam N, Arabindoo B, Murugesan V, 2006). One would think, like previously mentioned, that it should not work as well as TiO_2 under same operating conditions of UVA light, but due to ZnO's greater quantum efficiency, it exhibits higher photo catalysis. Quantum efficiency is a quantity defined for a photosensitive device or material, as the percentage of photons hitting the photo-reactive surface that will produce an electron hole pair. Simply put, ZnO is a more sensitive photocatalyst.

Studies at Duke University have confirmed ZnO`s greater quantum efficiency over TiO2 (Pinnel SR, Fairhurst D, Gilles R, 2000). UVA attenuation measured by diffuse reflectance spectroscopy, on normal human skin in vivo, showed that zinc oxide demonstrates superior protection compared to titanium dioxide. A superior ability of ZnO to absorb UVA light has been shown. Zinc oxide provides lower transmittance of UVA

light than titanium dioxide thus ZnO produces electron hole pairs more efficiently. In turn this fact should allow ZnO to produce free radicals faster, and kill microbes more efficiently.

Antibacterial effects of six different inorganic antibacterial agents show that silver ion additives into broth agar dilution tests prevail in antimicrobial effectiveness, with six bacteria associated with oral disease, over metal oxide additive ZnO (Fang M, Chen JH, Xu XL, Yang PH, Hildebrand H, 2006). In order of antibiotic power, the six inorganic agents used to kill these bacteria were: Longbei powder (silver ion), ZnOw complex AT-83, Ionpure-H (containing silver ion), basic magnesium hypochlorite, ZnOw AT-88, and Antim-AmS2 (containing silver ion). Thus although metal oxides are powerful inorganic antimicrobial agents, literature shows ionic silver as a superior alternative.

2.2.4 Carrier Materials

In order to optimize the performance of antimicrobial additives to be used in a powder coating, ceramic crystal carriers are often used. Such carriers include zeolites, silica glass, hydroxylapatite, and zirconium phosphates. Organic or inorganic chemicals can be put into these carriers in order to overcome and provide certain properties:

Increase surface area - When a carrier is holding any type of antimicrobial agent, the carrier may provide three dimensional release function independent of agent concentration,

Protection of Additives - Zeolite is a ceramic material that can withstand temperatures to 800°C, and pH values of 3 – 10 while retaining full antimicrobial effectiveness,

Protection of Substrate (powder coating) - Use of ceramic carriers also minimizes degradation of organic material. The substrate is not necessarily in direct contact with the additives that may oxidize organic material,

Increase Life expectancy - Carriers create a release environment for chemicals to work, adding to an increased life expectancy.

Silica Glass/Gel

Monolithic inorganic gels may be formed from raw materials and converted to glasses through chemical reaction. The resultant glasses present homogeneous inorganic oxide materials. Properties include hardness, optical transparency, chemical durability, custom porosity and thermal stability. These properties make silica glass an excellent candidate as carrier material for antimicrobial chemicals.

Production of silica glass from sol-gel processing includes inorganic networks by formation of colloidal suspension which is deemed the sol, and gelation of this sol to a gel or continuous liquid phase, and final drying of the gel to rigid glass; termed silica gel or silica glass. Thus synthesis is sequenced into three steps: i) Gel preparation - sol is initially prepared by silica solution and addition of catalyst, followed by subsequent gelation. Gels are classified according to the dispersion medium used; hydrogel, alcogel and aerogel for water, alcohol and air respectively; ii) Aging of gel - where gel is aged in the original mother solution, fortifying the gel so shrinkage is minimized during the drying stage; iii) Drying of the gel - liquid is freed from pores of the gel using one of several techniques (Dorcheh AS and Abbasi MH, 2008).

Silica gel involves hydrolysis and poly condensation reactions of organo metallic compounds. Precursors for creation of the colloids include a metalloid element, specifically metal alkoxides and a range of reacting ligands. Metal alkoxides specifically silicon alkoxides are used because they react readily with water. In the production of silica gel from sol gel, tetraethoxysilane (TEOS) (Kawashita M, Tsuneyama S, Miyaji F, Kokubo T, Kozuka H, and Yamamoto K, 2000) or tetramethyl orthosilicate (TMOS) (Folgar C, Folz D, Suchicital D, Clark D, 2007) are mostly used.

The sol-gel process begins with the hydrolysis reaction where, through the addition of water to the silicon alkoxide precursor, alkoxide groups are replaced with hydroxyl groups (OH). Consequently condensation reactions are followed involving silanol groups

(Si-OH) which produce siloxane bonds (Si-O-Si) plus by products of the solvents (water and alcohol). The alcohol is utilized as a mutual solvent with the precursor (alkoxide) due to its immiscibility with water. As condensation continues during the sol process, a three dimensional network is formed through a reaction called polymerization. Polymerization is the bridging and aggregation of molecules by increased number of siloxane bonds. As polymerization continues, gelation of the sol occurs. Thus aging of the gel is required for further polymerization reactions to result in the evolution of the micro structure; or interconnected solid matrix (Folgar C, Folz D, Suchicital D, Clark D, 2007). The wet gel is then dried using one of several methods. Xerogel are sol gels produced by drying in a conventional oven where cracking due to capillary pressure is likely. Aerogels are produced when gels are dried and liquid removed as a gas phase through supercritical conditions and reduced capillary pressure. Resultant aerogels would successively have high surface area and high porosity.

Characteristics of a sol gel network relate to pH, temperature, time of reaction, reagent concentrations, catalyst (acid/base), molar ratio water to silica, aging time and drying. Use of acid or base catalysts, increasing or decreasing pH, generally speeds the process time to form the gel network by increasing rate of condensation reactions (Brinker CJ and Scherer GW, 1990).

A dried silica gel generally consists of amorphous silica matrix and accompanied pores distributed throughout. High specific surface area is characterized from 300-1200 m^2/g. Drying of the gel is a crucial step, where capillary pressures determine the pore sizes. High capillary pressures induce shrinkage and cracking. In supercritical drying the liquids removed above critical temperature and pressure create no liquid-vapor interface, and diminished capillary pressure. Ambient pressure drying creates surface tension between liquid and vapour and causes high capillary forces prone to fracture of the structure. Simply, the drying method used to free the solvent can in turn manipulate the pore size distribution of the sample (Dorcheh AS and Abbasi MH, 2008). The final microstructure of the silica gel is strongly influenced by changes imposed upon it during the drying phase of processing.

Silica gel's high chemical durability and superior surface area and porosity properties are main reasons for its candidacy for antibacterial material for medical applications. By use of sol-gel method biocidal compounds can be incorporated to the pores of the silica network. Kawashita M, et al (2000), produced antibacterial powder by incorporating silver nitrate into silica gel by the sol gel method. Slow release of silver ions was shown during leaching tests credited by the silica glass network providing an excellent carrier material for the silver cations to perform their action.

Zeolite

Zeolite has good biocompatibility, high mechanical, thermal, and chemical stability, large surface areas and unique hydrophilic and electrostatic property (Xie Y, Liu H, Hu N, 2007). These properties make zeolite a favorable carrier for anitmicrobial additives. The atomic structure of zeolites is essentially based on a three dimensional framework of silica and alumina tetrahedra where silicon or aluminum ions are surrounded by four oxygen ions in a tetrahedra configuration. Each subsequent oxygen ion is bonded to two adjacent silicon or aluminum ions. Tetrahedra clusters appear to be linked like cubes, polyhedral units, that are in turn linked to form a zeolite framework. Zeolite framework is negatively charged by nature but this is balanced by the cations held in the cavities.

Zeolites are essentially hydrated alumino-silicate materials, where again silicon and aluminum atoms are tetrahedrally coordinated with each other through shared oxygen atoms. They are open structures that can accommodate a wide variety of cations. Exchange sites in the zeolite are primarily occupied by potassium (K^+), calcium (Ca^+) and/or sodium (Na^+) ions. There are hundreds of different types, and for the application here, both natural and synthetic options would work. However, if one had to be chosen, the more physically and chemically stable and cheaper of the two options is a natural and abundant zeolite material (i.e. Chabazite).

Zeolite is produced from the earth and can be manufactured as a natural product or a synthetic product. Depending on the application, one will choose between the two options. The difference is the ratio of silica to alumina (SiO_4^{4-} and AlO_4^{5}) that makes up the tetrahedral sharing edges of the crystal. Synthetic zeolites have a ratio of silica to

alumina of 1 to 1 while natural zeolites have a much higher ratio (ie. clinoptilolite 5 to 1, chabazite 7 to 1). Natural zeolites do not break down in acid environments where synthetic zeolites do. It is the higher ratio of silica in the natural zeolite that holds it together because it is acid resistant. High Si/Al ratios like chabazite and clinoptilolite natural zeolites create low anionic fields that present good selectivity towards cations of lower charge, monovalent cations, and poor selectivity towards higher charged cations, like divalent cations (Langella A, Pansini M, Cappelletti P, de Gennaro B, de Gennaro M, Colella C, 2000).

Approximately forty-five natural zeolites exist on earth; forming in a variety of low temperature geologic environments. Synthetic zeolites can have a wider range of properties and are produced to have larger cavities for efficient exchange. They were initially produced n the 1950s, and over one hundred types presently exist. Syntheitc zeolites are manufactured from energy consuming chemicals and natural zeolites from natural ore material. Zeolite particles can be utilized for many applications. They interact with water to absorb or release ions, and they can selectively absorb ions acting as molecular sieves. Zeolites are specifically used as water softeners removing calcium ions which react with soap to form scum. They are also used to remove radioactive strontium and cesium from radioactive waste solutions, and absorb sulfur dioxide to purify gases from power plants.

Their tertiary structure network of interconnected tunnels and cavities allow organic or inorganic materials to be readily encapsulated within and permanently trapped (Shen B, Scaiano JC, English AM, 2006). Guests can be incorporated into the zeolite through variety of methods, but the main method used is termed ion exchange synthesis: Zeolites are brought into contact with an aqueous mixed solution containing the cationic species wanting to be absorbed into the zeolite matrix; each ionic species is generally used in the form of a salt and vigorous mechanical mixing is required for adequate time periods. The final content into the zeolite is predominantly determined by the concentration of ionic species mixed with the zeolite (Niira R, Niira Y, Yamamato T, Uchida M, 1990). Metal oxides can also be formed in zeolite cavities. Anandan S, Vinu A, Venkatachalam N, Arabindoo B, Murugesan V, (2006), used ion exchange originally to capture zinc ions in

the pores of zeolites and then drying was carried out under flowing O_2 to produce zinc oxide. Bouvy C, Marine B, Sporken R, Su BL, (2007), also found incorporation of metal oxide rather than just metal ions if dried and calcined under flowing O_2 at high temperature.

2.2.5 Ionic Metal(s) in Zeolite

Silver filled materials have to release the silver ions to a pathogenic environment in order to be effective. This condition is satisfied in aqueous medium where there is interaction between the water molecules and subsequent production of silver ions. Zeolites enhance the water uptake properties resulting in an increase in silver ion release. Zeolite used as the carrier materials for silver provides channels for the water molecules to enter the polymer matrix thus improving water diffusion characteristics. Silver zeolites act as an ion pump providing controlled time release of silver ions to an aqueous environment (Radheshkumar C and Munstedt H, 2006).

The process of releasing silver ion from the silver loaded material is composed of basically three steps: i) The diffusion of water into the composite specimen, ii) the reaction between silver and water molecules leading to the ionic exchange and iii) the migration of silver ions to the aqueous environment. The carrier material can be affective in accelerating the diffusion of water molecules and migration of silver ions through the polymer matrix (Radheshkumar C and Munstedt H, 2006).

A silver zeolite releases silver ions whenever common environmental cations such as sodium, potassium and calcium are readily available for exchange with ionic silver in the zeolite; in the presence of moisture. This step is considered to create a controlled release mechanism for ionic antimicrobial species in zeolite particles. Further, the release of one ionic species with another in a zeolite is dependent on charge and so release will not happen unless there are ions available to take the place of ones in a zeolite matrix (Feied, 2004). The cations that promote ionic exchange with a zeolite found in certain environmental conditions are the same cations that favour growth and survival of

microorganisms. In conditions where microorganisms cannot normally grow and survive, very dry conditions, ions would not be released from a zeolite particle as moisture and any such cationic species are not present. Due to the release properties of zeolite and the aforementioned details, it is believed that the longevity of the product is vast, measurable up to decades of time (Feied, 2004).

Silver zeolite can not only produce bactericidal action by releasing and exchanging ions but also from generation of reactive oxygen species (ROS) from silver in the zeolite matrix (Kourai H, Manabe Y, and Yamada Y, 1994). Two methods of generation of ROS and accompanied mechanisms of action were studied by Matsumura Y, Yoshikata K, Kunisaki S, and Tsuchido T, 2003: ROS are possibly produced through inhibition of a respiratory enzyme(s) in a bacterial cell by silver ion which in turn attacks the cell itself. Also, silver ion's known ability to inhibit thiol group- containing enzymes, such as NADH dehydrogenase II in the respiratory system, brings a theoretical contestant for the site of production of ROS.

Hu CH, Xu ZR, Xia MS, (2005), proposes two mechanisms of inactivation of *E. coli* from a natural monmorillonite zeolite loaded with copper ions. The first being the common ion dissociation factor where release of ionic species exerts its effect. However they also propose that the surplus positive charge of the zeolite due to the cationic species forces an attraction with the negatively charged cell wall of the bacteria. Since the opposite charges attract, adsorption of bacteria from a solution and immobilization on surface of the zeolite was presumed to occur. This phenomenon would also hold true with cationic silver species with net positive charges.

Silver and zinc containing zeolite shows excellent antimicrobial efficacy (2.5% weight of silver and 14% weight of zinc). Silver-zinc-zeolite coated onto stainless steel coupons was performed by both a wet coated process and a powder coated process and the antimicrobial efficacy against *E.coli, S. aureus, P. aeruginosa* and *L. monocytogenes* was conducted (Cowan M, Abshire KZ, Houk SL, Evans SM, 2003). Silver-zinc zeolite reduces microbial colony forming units when compared to control or uncoated steel surfaces under all circumstances. Also, the powder coated coupons performed

significantly better then with the wet coated items, after durability washing trials. The percent reduction of both processes yield 99.99 to 100% inactivation of bacteria, with the powder coated process performing marginally better for such bacteria tested. However there is a significant difference between the two processes (liquid coating and powder coating) when performing durability trials by washing the surface with a towel or toothbrush. The durability of the coating declined most with the wet coating process scrubbed between uses with a test tube brush. Powder coated surfaces cleaned with a towel retained a high degree of activity after five cycles of use. Notably on the 5^{th} trial, the powder coated surface did significantly better then the wet coated surface after 4h exposure; both washed with a towel. Thus it is fair to say that the durability of powder coated antimicrobial additives has an edge over wet process coated items, through the reviewed study by Cowan et al (2003).

Fang M, et al (2006), presents research showing that silver ion reduces to metallic silver over time and presents a drastic color change to the substrate. This is due to the loosely held cations in the zeolite framework. However water immersion testing of antimicrobial zeolite coating present excellent results. O'Neil C, Beving DE, Chen W, Yan Y, (2006), immerse Ag-exchanged zeolite A into deionized water for eight weeks that subsequently shows highly durable properties under such wet conditions, maintaining their hydrophilic and antimicrobial properties. Haile T, and Nakhla G, (2008), confirmed that the presence of bacteria is necessary for leaching of Ag from zeolite and that antimicrobial action of Ag is dependent upon contact between the zeolite and the biomass.

Zeolites exchanged with silver are highly hydrophilic and toxic to *Escherichia coli* specifically (McDonnell AMP, Beving D, Wang A, Chen W, Yan Y, 2005) which solidify the work completed in the subsequent research. Silver zeolite coatings have also found to be effective even under loads containing fats and oils on the surface which disrupt ion release and provide nutrients to bacteria. Feied (2004) inoculated surfaces of silver metal zeolite with ground beef extract and still found rapid reduction of bacterial species despite the soil load. Also according to Feied (2004) silver zeolite coatings are safe as they are approved FDA for food packaging materials and given a class (I) title for use by invasive medical devices, not requiring application.

2.2.6 Metal Oxides in Zeolite

TiO_2 encapsulated within zeolite particles has shown ability to generate reactice oxygen species (ROS; O_2^-, HO^-, H_2O_2) (Shen B, et al, 2006). Encapsulation of TiO_2 within zeolites alters its photocatalytic activity and thus the effects on ROS formation in cells under UVA-irradiation. The photooxidizing power of TiO_2, under UVA light to produce electron hole pairs, varies with both crystal size and form of the TiO_2 particles. UV irradiation of anatase TiO_2 produces more free radicals than rutile form. Nano form (32 nm) anatase TiO_2 particles increase ROS formation in fibroblasts (human cells) on UVA irradiation, whereas TiO_2 in zeolite (500nm) has the opposite effect. Encapsulation of TiO_2 in zeolite significantly attenuates or decreases UVA-induced ROS production (Shen B, et al, 2006).

Encapsulation of metal oxides into zeolite protects the organic substrate of the powder. Additionally, if the powder is to be coated onto an organic item of sorts, zeolites could help slow and decrease damage to such a piece. TiO_2 within zeolite has a bandgap of 4.66-4.81eV vs. 3.2eV for free anatase TiO_2; thus less free radicals are produced by UVA irradiation, as it requires more energy to promote electrons to the conduction band (Shen B, et al, 2006). An antimicrobial effect of TiO_2 encapsulated into a zeolite will be attenuated rather than TiO_2 on its own. However, the lifetime of the powder coating will be significantly increased, and bacteria can still be destroyed; over a slightly longer period of time. ZnO may be more efficient at producing ROS than TiO_2 in zeolite, even with a larger band gap. ZnO supported zeolite exhibits better photocatalytic activity than TiO_2 supported zeolite (Anandan, et al, 2006); however there is only limited literature available for the photocatalytic degradation of organic pollutants using ZnO supported zeolite. Experimentation investigating degradation of monocrotophos (MCP), a toxic organic pollutant insecticide by photocatalytic degradation with ZnO zeolites exists. Studies prove that ZnO supported zeolite required shorter time exposure to UVA light, for complete mineralization or degradation of MCP than ZnO alone. This is due to the good adsorption of anions and intermediates on zeolite surfaces where OH radicals are available for breaking MCP molecules. The hydrophilic/hydrophobic properties aid zeolite in capabilities to oxidize species through improved adsorption properties and

efficient delocalisation of photogenerated electrons by a metal oxide. The OH radical is strong enough to break bonds in species adsorbed on the surface of ZnO leading to complete degradation of the organic material (Anandan, et al, 2006).

2.3 Biomaterial Contamination Prevention

Currently there is research underway to eliminate biofilm once it is already formed on a biomaterial, and even more research developing to prevent biofilm formation all together. Contamination prevention is sought in two ways: Physical modifications and chemical modifications.

2.3.1 Physical Modifications

Physically, the surface of the device can be altered to meet requirements of antimicrobial action. It has been shown that correlation exists between the hydrophillic properties of the material surface and the initial adhesion of cells spreading onto the surface. This is determined by water contact angle. Appropriate physical polishing of the substrate is necessary. Biofilm formation increases significantly with increase in surface roughness. Reduction of concavity and other modifications of physical properties such as surface free energy also affect bacterial adhesion; increase surface free energy, increases wet ability (Rimondini et al, 2005).

The charge of the surface also affects bacterial adhesion and growth. Gottenbos B, Grijpma DW, van der Mei, Henny C, Feijen J, Busscher HJ, (2001), compared the antimicrobial effects of adhering bacteria of a positively charged poly(methacrylate) surface (+12 mV) against negatively charged poly (methyl methacrylate) (-12 mV) and a highly negative charged poly(methacrylate) (-18 mV) surface. Results of adhesion of various bacteria strains, including *Staphylococcus aureus, Staphylococcus epidermis, Escherichia coli* and *Pseudomonas aeruginosa* were most rapid to the positively charged surface. Most bacteria carry a net negative surface charge therefore adhesion is

encouraged on positively charged surfaces. However there was no subsequent surface growth of the gram negative strains on the positively charged surfaces. Surface growth was exponential for both gram negative and gram positive bacterial strains on the negatively charged surfaces. Thus, positively charged biomaterial surfaces exhibit antimicrobial effects on gram negative bacterial strains only. Gram positive bacteria are encased in a plasma membrane covered with a thick wall of peptidoglycan, while gram negative bacteria are encased in a plasma membrane, covered by a thin layer of peptidoglycan which is further covered by a third layer (outermost layer) containing lipopolysaccahride (LPS).

2.3.2 Chemical Modifications

Chemical modifications can be made to the surface of the biomaterial or to the bulk of the material by impregnation methods. The main goal of both is the release of antimicrobial agents. Essentially there are four different antimicrobial agents that may be incorporated to the biomaterial: Traditional antibiotics, inorganic oligodynamic metals, organic chemicals and adhesion inhibiting chemicals. The most frequent antibiotics found in literature for use in this area of research are gentamicin, teicoplanin, rifampicin, novobiocin, vancomycin, clindamycin, minocycline and oxacillin. The use of such antibiotics will be dependent on where the biomaterial is implanted and bacterial strains most associated with that implant material and physiological department; since different antibiotics target different bacterial strains.

With antibiotic resistance on the rise and the scare that is protruding in the medical field, inorganic metals are gaining popularity. Such metals include silver, copper and zinc. Silver metal is predominantly used and its mode of action against microbes is relative to the bioactive silver ion (Ag^{+}) released and its availability to interact with bacterial or fungal cell membranes. Silver metal and inorganic silver compounds ionize in the presence of water, body fluids or tissue exudates (Lansdown, 2006).

Organic chemical compounds may also be used as antimicrobial agents, such as antiseptics; however these types of agents are not selective in their toxicity and will kill and harm human cells as much as any pathogen. Adhesion inhibitors are other chemicals used as means to prevent bacterial adhesion and development, specifically biosurfactants. Biosurfactants are surface-active substances synthesized by living cells that work at the interface of the biomaterial and surrounding environment. Microbial amphiphilic polymers (hydrophobic and hydrophilic) and polyphilic polymers compose the biosurfactants. Essentially they affect the wet-ability and surface energy, preventing adhesion (Rodrigues, 2006). Difference between affecting adhesion of bacterial cells and human cells is not known. This technology is relatively new.

Surface Modification

Like discussed prior, chemical modifications occur to either the surface or to the bulk material of the medical implant device. When modifying the surface of the biomaterial a chemical coating to house the antimicrobial agent may or may not be used. When a coating matrix is used, specific biodegradable polymers may be used. Gollwitzer et al, (2003), experiments with PDLLA which is a polymer with a mixture of the D- and L-enantiomers of lactic acid. Rossi Shawn, Azghani Ali O, Abdelwahab Omri, (2004), demonstrate the use of PHBV which is poly(3-hydroxybutyrate) and numbers of hydroxyvalerate or hydroxyvaleric acid (HV) molecules. Both of these specific polymers are biocompatible and may promote bone growth when coated on medical implants. It is also most common to have antibiotics, as antimicrobial agents, uniformly distributed within the polymer matrix exhibiting matrix dissolved delivery system of drug release to the environment. Additionally, hydrophilic polymers are used for coatings as well as hydroxy apatite and porous particles like zeolites. Hydroxy Apatite is a coating of choice as it is the main inorganic of hard tissues in vertebrates. Antibiotics or oligodynamic metallic salts may be incorporated into such a coating. Hydroxy Apatite has also shown good compatibility results of early bone growth, greater fixation and prevention of foreign-body-acute-effect caused by metals (Chung et al, 2005).

The surface of the implantable material can be coated in many different fashions. The type of coating technology used is dependent on the type of coating to be treated on the biomaterial. Nanotechnologies including ion beam assisted deposition, plasma treatments, chemical vapor deposition, physical vapor deposition, and electrochemical deposition are all methods used to make thin films. These methods are able to produce thin films as thin as 2 microns. Oligodynamic metals often makeup these thin film coatings. Ewald A, Gluckermann SK, Thull R, Gbureck U, (2006), used Physical Vapor Deposition (PVD) to deposit silver nanoparticles on the surface of cylindrical titanium specimens. PVD is the transfer of growth species from a source or target and deposit on a substrate. There are two types of PVD; evaporation and sputtering. Sputtering uses energetic ions to knock atoms/ molecules out from the target (acts as electrode) and deposit on the substrate (acts as electrode). Sputtering was used by Ewald, et al (2006), in their efforts to test a metallic silver coating on application on load-bearing implants, e.g. in hip or knee arthroplasty. PVD is a good coating technology as it yields strong adhesion of particles. Implantation into the bone results in high (abrasive) shear forces between bone and the implant surface for hip and knee arthroplasty and PVD technique fulfills the mechanical criteria for load bearing implants as it creates a strong, hard coating.

Solvent casting techniques are other methods to coat implant materials. This is a good method for oddly shaped implants. Where the implant is basically dipped into the gel or aqueous polymeric mixture containing the antimicrobial agent; homogeneously dispersed within.

Bulk Material Modification

Rather than simply modify the surface of a biomaterial; the entire bulk of the material can be modified creating antimicrobial effects. Incorporation of antimicrobial agents into polymeric materials is accomplished during the manufacturing stage. During manufacture of the implant, or specifically during polymer synthesis, the antimicrobial agent can be homogeneously dispersed within the matrix. Examples of specific polymers used for such purposes are polyurethanes and polymethyl methacrylates (PMMA). Diffusion processes can also be used with polymers. Antibiotics are predominantly used when incorporating

into polymeric materials. However there is one method, which is the only method known to impregnate polymers with silver, which is with use of silicone elastomers. Furno F, Morley K, Wong B, Sharp B, Arnold P, Howdle S, Bayston R, Brown P, Winship P, Reid H, (2004), used a solution of organometallic precursors of silver to swell and permeate the silicone polymer. After exposure to hydrogen gas the organometallic precursors of silver decompose leading to homogeneous distribution of silver nanoparticles (10-100nm). Use of chloroform can also cause silicone to swell, and when mixed with antibiotic solutions a homogeneous dispersion of antibiotic within the polymer is the result. Other bulk materials that are often modified with antimicrobial agents include bone cement (calcium phosphate) and Dacron grafts (vascular graft). It should also be noted that bulk material modification alters the mechanical properties of the medical device itself. Therefore this mode of introducing antimicrobial agents to the environment should only be used under non-load bearing conditions.

2.3.3 Antimicrobial Testing and Biocompatibility

The length of antimicrobial activity required for an implant is obviously as long as possible. When a medical device is surgically implanted into human physiology, bacteria and the human cells compete for attachment on the surface. Therefore immediate antimicrobial effectiveness is required. However, half of all biomaterial related infections occur months to even years after deep tissue implantation – termed late biomaterial centered infection. There is controversy concerning the origin of the infecting micro-organism during these late infections; there is no significant evidence pointing to one mode. It is thought that the implant becomes infected either through hematogenous pathways or by appearance of perioperatively introduced bacteria (Gottenbos B, Klatter F, van der Mei HC, Busscher HJ, Nieuwenhuis P, 2001). Since infections occur months to years after implantation, it is difficult to specifically say how long antimicrobial effectiveness is required. Essentially it is required throughout the lifetime of the biomaterial. Since antibiotic loaded implants are delivered over a certain length of time, the initial burst of antimicrobial effectiveness is sometimes enough to prevent attachment, yielding enough time for bodily tissues to cover the implant. For example, silicone

polymer loaded with antibiotics rifampicin and vancomicin, by method of swelling with chloroform, is able to prevent bacterial colonization for over 50 days (Bayston R, Ashraf W, Bhundia C, 2004). This method would be favoured for a short time period.

Ewald, et al (2006), studied cylindrical titanium specimens as this form of material is most often used for hip or knee arthroplasty. Physical Vapor Deposition of Ag (Sputtering) was used to make a thin film of silver nanoparticles on the surface. Silver ion release was dependent on the percentage of silver nanoparticles loaded on the surface. Also, the silver ion release marginally decreased after 6 days indicating that it should last for long periods of time.

Antimicrobial effectiveness against *K. pneumonia* showed that 3% silver content is most effective with less than 40% bacteria resulting, but at 9% silver content 85% bacteria remain. Indicating that there may be an optimal concentration of silver allowed to be most effective. However against *S. epidermis* the bacteria percentage decreases proportionally with increased silver content.
Biocompatibility studies of the titanium-silver samples were conducted on epithelial cells and osteoblasts showing good short term biocompatibility results. Epithelial cell activity and total protein (ug/mL) was not significantly reduced on any of the silver surfaces. However the 9% and 18% silver content does show noticeable cytotoxicity when treated with the osteoblast cells and their cell activity and total protein (ug/mL).

Chung, et al (2005), researches hydroxy apatite (Hap) sol-gel coatings on titanium alloy substrates for dental applications. An aqueous hydroxy apatite mixture is combined with silver nitrate and/or zinc nitrate to produce a coating consisting of ions from the salts. Hydroxy apatite gels containing these ions are simply spin coated onto the titanium alloy substrate and allowed to dry. The antimicrobial tests were conducted using *Streptococcus mutans* bacteria which are often found on the surface of dental implants - 100 ppm Ag is enough to limit bacterial growth, but 1000 ppm of zinc shows no zone of inhibition. Both 10,000 ppm of Ag and Zn showed large areas of inhibited growth of *S. mutans.*

Short term biocompatibility studies of the hydroxy apatite coatings loaded with silver and zinc ions were performed on human gingival fibroblast cells (HGF); which is a formative cell that moderates wound healing in the mouth. The morphology and attachment of these cells was investigated using an optical microscope, after crystal violet staining, thus 1000 ppm Ag and 10,000 ppm of Ag results in cytotoxicity to HGF cells. Neither of the Zn concentrations exhibit cytotoxicty, as the pseudopods of the HGF cells extends relatively well.

Chung, et al (2005), also reports that the number of attached HGF cells onto Hydroxy apatite-Ag coatings of 100 ppm Ag is less than pure Hap coatings. They do not report of an optimal concentration. However in a separate article by Feng, et al (1999), they report with other reference as well, that up to the concentration of 20 ppm $AgNO_3$ (12.7 ppm Ag) there was no significant morphological changes of macrophages and osteoblasts, suggesting that the function of bone cells was not affected. Thus, they suggest that the Ag-treatment of implant materials to prevent infections should be limited to the amount of 20 ppm $AgNO_3$ or 12.7 ppm Ag. Furthermore it is evident that there is a limit to the silver content that may be implanted into the human body.

2.4 Powder Coating

Powder coatings are an environmentally acceptable finishing method, devloped since the mid 1950s. These coatings are simply dry paints formulated with the same resins, pigments and additives as solvent borne paints, but without the solvent. There are two general classes of powder coatings: thermo plastic and thermo setting. Thermo plastic can re-melt upon heat exposure while thermo setting polymers melt and chemically react, unable to re-melt; these make the majority of powder coatings (Berins ML, 1991).

2.4.1 Advantages

Powder coating presents many advantages over solvent based paint coatings like environmental, economic, operational and finishing advantages. Powder coatings do not incorporate solvents in the premixing, application or clean up stages of operation thus the elimination of volatile organic compounds (VOCs) and hazardous air pollutants (HAPs) are one of the main environmental benefits. In conventional coating it is these solvent vapours that are released when paint is naturally drying. Additionally to the zero VOC emissions to the atmosphere, environmental benefits include reduction of waste by recycling overspray powder, higher efficiency during application and overall process is essentially safer and cleaner. Economically, powder coatings present lower costs in labour, energy, production, waste disposal, and regulation compliance which presently make powder coatings one of the least expensive coating application methods. Operating advantages include a less labour intensive process, as no mixing of solvents with resin is required, the powder may be applied as is once obtained from manufacturer. Finally, the finishing advantages include a coating with better physical consistency, better mechanical properties and good resistance to corrosion. Powder coatings are produced from solid material therefore they have higher molecular weight then liquid coatings, providing a denser cross linking of the polymer resin and curing agent. Thus oxygen transmission is lower and coatings have a higher resistance to hydrolysis (Liberto N, 2003).

2.4.2 Manufacturing

Powder coatings are processed by one of three methods: dry blending, solution or melt mixing. Melt mixing is the most popular method with thermo setting polymers therefore it will be discussed and because it was utilized in this research. The melt mix manufacturing process of powder paint occurs through the following sequence of events: weighing, premixing, melt mixing (extrusion), cooling, chipping, fine grinding (pulverizing), and classification/sieving.

The manufacturing process begins with measuring out, by weight, the appropriate amounts of raw materials including resin, pigment, fillers and additives. Once accurately weighed, materials are mixed together. The goal of this step is to create a homogeneous, uniform solid blend of the materials. Mixed raw materials are then transferred into the extruder, also known as hot melt compounding. This stage completely homogenizes the materials melting the resin and curing agent and dispersing the additives, fillers, and pigments within. This homogeneous molten extrudate material is then cooled by chiller rollers pressing the molten plastic into a thin work piece. Once further cooled, the sheets of plastic are broken down into smaller chips, and transported for further grinding. Grinding is conducted by air classifying mills, opposed nozzle jet mills, or simply high powered, high shear grinders. Opposed nozzle jet milling method uses compressed air to create gradients of high pressure to break apart particles. Particle size is affected by the change in feed rate of particles to the system. When the rate of particles entering a high pressure chamber is reduced, finer particles result due to higher energy available per particle to accelerate the particles and mass of the whole. Collisions between particles are more violent and gradients in pressure become larger. Once fine grinding is sufficient, fine powders are classified or sieved to retain a small particle size distribution range. The end product is an ultrafine powder formulation ready for application.

2.4.3 Electrostatic Spraying

The four basic methods for applying powder to a part are fluidized bed, electrostatic spray, friction static spray and electrostatic fluidized bed. Since electrostatic spray was utilized in this research, it will be discussed extensively. Without use of electrostatics, processes usually involve preheating the substrate to a temperature higher than the melting point of the powder and dipping into the fluidized bed or by spraying air suspended powder onto the surface where the powder melts immediately once contact is made (Schram PJ and Earley MW, 1997.)

In the 1960s, principles of electrostatics were applied to application processes of powder coatings. Since most powders are insulators with high volume resistivity values, they

accept a positive or negative charge (polarity) and are allowed to be attracted to a grounded workpiece or oppositely charged workpiece. Typical spray systems include a powder reservoir, powder feed mechanism to the reservoir, the gun design to spray the powder, powder generator to charge particles and powder recycling equipment gathering overspray. The corona charge occurs internally at the tip of the gun or by means of an electrode at the end of the gun. The power pack producing charge to the gun ranges in kilovolts and microamp measures; voltage can range from 35 kV to 100 kV. The final thickness of the powder film is dependent on the speed of the powder cloud produced, cloud pattern created by the gun tip, feed rate, charge, type of spray gun and resistivity of the powder (Berins ML, 1991).

The main advantage with electrostatic spraying is the capability to make very uniform, thin film coatings to a cold workpiece. Transfer efficiency of the spray is initially 5 - 85% but with a recovery system will reach 100% (Berins ML, 1991). The recycling system is usually integrated into the spray booth. Once the powder is transferred to the substrate at desired thickness, the part is cured by thermal means of a convection oven. Oven temperatures and exposure times range for complete curing (cross-linking) depending on the resin and binder used forming the finished coating.

2.4.4 Composition

Polymeric resin and the curing agent comprise the main component of powder coatings which is the binder. The binder composition in a powder coating usually accounts for 50% of the total weight, however when a clear coat powder coating is desired the binder content is at least 95% the total weight.

The binder is formed from cross linking of the resin and curing agent under thermal conditions creating an endothermic reaction. Once the powder melts creating the thin film, the curing process begins. This type of chemistry is represented by four different systems: epoxy, polyester, polyester-epoxy hybrid and polyurethane. Since a polyester system was used in this research only polyester curing reactions will be discussed.

Polyester paints are most known for their resistance to UV rays and resistance to weathering. Thus outdoor applications are ideal for such a resin. Most often polyester is cured with Triglycidyl Isocyanurate (TGIC). This type of curing agent is common and also known as a trifunctional crystalline heterocyclic polyepoxide. When appropriate thermal conditions are met, the carboxylic functional group of the polyester reacts with the epoxy group from the TGIC. Typical ratio of polyester to TGIC is 93:7. Polyester may also be cured with other curing agents such as β-hydroxy-alkylamide and Araldite PT 910.

The mechanical properties of polyester powder coatings are excellent with good flexibility and toughness. Their low melt viscosity makes them to have a very good flow during the melting and curing process that translates into very smooth glossy finishes. Lehr W, (1991), presents qualitative performance of a generic polyester powder coating finish indicating that the curing chemistry shows excellent flexibility, excellent hardness, excellent outdoor resistance, excellent corrosion resistance, very good chemical resistance and excellence in over baking situations. However polyester coatings have not so great resistance to solvents.

Pigments, specific additives and fillers are also components in a powder coating composition. Pigments give color to the paint and present an aesthetic quality only. Additives in the powder may include flow agents, degassing agents, matting agents, texturing agents, light stabilizers, and catalysts. These ingredients are found at low concentrations and are meant to effect different properties of the final coating. Flow agents strive to avoid surface defects, degassing agents help with gas release during curing, matting agents reduce gloss, texturing agents modify surface so it is not smooth, light stabilizers protect from UV rays, and catalysts yield faster cure times. Fillers simply cut manufacturing costs by replacing some parts of the binder which is the most expensive and by adding hardness (Howell D, 2000). Moreover, other additives may be incorporated to yield a specific functionality of the finished coating changing properties and creating different effects.

2.4.5 Functional Coatings

Almost every object encountered by an individual in his/her daily life, including household objects and materials like toothbrushes, cars, furniture or pots and pans, exist with some kind of coated material. Coating is defined as a material which is applied onto a surface and appears as either a continuous or discontinuous film after drying (Ghosh SK, 2006). Depending on their compositions, paint coatings are classified as solvent borne, water borne and solvent free. Solvent borne paints include resin, additives and pigments dispersed in organic solvents, water borne the agents are dispersed in water and with solvent free formulations the paints include no solvent or water – powder coatings – where everything is dispersed with the resin.

Coatings may occur in organic or inorganic forms. These properties are determined by the kinds of binders, pigments and additives used in the formulations. The end properties of a coating depend on the substrate (pre-treatments), application technique and conditions of film development. Inorganic coatings are mainly applied for protective purposes where organic coatings, including powder coatings, are used for functional purposes (Wilson AD, Nicholson JW, Prosser HJ, 1987).

A functional coating is a system which possesses, besides the classical properties of a coating (decoration and protection), an additional critical functionality. Apart from their unique functional properties these types of coating are expected to satisfy additional requirements; examples include durability, reproducibility, easy application, cost effectiveness, customized surface morphology, and environmental friendliness (Ghosh SK, 2006). Further, functional coatings are classified as several categories depending on the functioning characteristic. These categories include optical properties, thermal properties, physio-chemical properties, structural/mechanical properties, electrical/mechanical properties, and hygienic properties. Included in the hygienic category are antimicrobial coatings which perform their action at the air-film interface. Evaluating the degree of effectiveness for functional coated surfaces, specifically antimicrobial coated surfaces, may be carried out using standard testing methods.

2.4.6 Standard Efficacy Testing

Effectiveness and durability of functional antimicrobial parts in industry today are wide-ranging and comparisons are hard to make. This is due to the fact that there is no internationally recognized standard for testing such parts, so most claims made by various companies are made using inapplicable test methods. There are a number of antimicrobial surface tests that do exist. The antimicrobial surface tests include:

- ASTM E 2149: Standard Test Method for Determining the Antimicrobial Activity of Immobilized Antimicrobial Agents Under Dynamic Contact Conditions
- ASTM E 2180: Standard Test Method for Determining the Activity of Incorporated Antimicrobial Agents in Polymeric or Hydrophobic Materials
- JIS Z 2801: Japanese Standard Test for Antimicrobial Product Activity and Efficacy
- Minimum Inhibitory Concentration test (MIC Test)
- Kirby-Bauer: Zone of Inhibition (ZOI) Testing

The antimicrobial fabric tests include:

- AATCC 100: Assessment of Antibacterial Finishes on Textile Materials
- AATCC 147: Antimicrobial Fabric Test (Parallel Streak Method for Antibacterial Activity Assessment of Textile Materials)

MIC values are obtained by bulk dispersion of an antimicrobial agent in liquid media where many different types of bacteria may be used. This procedure under estimates real world effectiveness of the same substance used as an antimicrobial surface. This is because ion concentrations achieve elevated levels more quickly in thin film (or droplet) environments on a treated surface than in a bulk dispersion analysis (Feied, 2004).

ASTM E 2180 was used in the present research. This method is designed to assess quantitatively the antimicrobial efficacy of agents incorporated or bound like a coating into or onto flat (two dimensional) hydrophobic or polymeric surfaces. Mainly antibacterial activity is assessed but others may also be used. Bacteria are applied to

surfaces by an agar slurry which reduces surface tension and allows a pseudo biofilm to be formed providing even contact of the inoculums bacteria with the test surface. Quantitative analyses can be made between control and treated surfaces and long term stability can also be determined through testing washed surfaces over time.

In the real world bacteria on controlled surfaces usually die off over time due to resentment of environmental conditions. Survival at steady state or extreme growth that was noticed by control samples using ASTM E 2180 does not imitate what would occur in the real-world as conditions and inoculation are too favourable. It should also be noted that the killing times and rates noticed with this research would occur much faster in the real world; again as conditions would not be as positive for bacteria to subsist.

Although there are certain testing standards in place for antimicrobial surfaces and fabrics, international comparison is nearly impossible. The standards may be accurate in determining one time efficacy but none of the standards include surface soiling testing or durability tests and how long the surface or part may keep it's antimicrobial properties. Suggestions are included with some standards but they are very elemental and not detailed.

Through ASTM E 2180 antimicrobial powders would be developed and tested aiming at the main goal of a functional, simple, highly durable antimicrobial surface; aspiring essentially to out due current market industrial antimicrobial powders by advancements in processing inorganic additives into powder coatings. The call and need has been outlined prior by various fomitic surfaces and biomaterials.

3 EXPERIMENTAL FORMULATIONS AND TEST PROCEDURES

Unless specified, all chemicals were reagent grade and obtained from VWR Scientific (VWR Canada, Mississauga, ON). Standard temperature and pressure (STP) were used as 20 °C (293.15 K, 68 °F) and 101.325 kPa (14.696 psi) (atmospheric pressure) by National Institute of Standards and Technology (Wright JD, Johnson AN, Moldover MR, 2003).

Inorganic antimicrobial additives were produced and/or obtained in a variety of different methods and/or means. The general concept for each additive produced involves the inclusion into an ultrafine powder coating and testing effectiveness against a strain of *Escherichia coli* bacterium. Through dry-blending or freeze drying methods of incorporating the additives with the base binder powder, a simple highly durable antimicrobial surface would be produced.

3.1 Antimicrobial Additive Powder Production

3.1.1 Chabazite Zeolite

As previously mentioned chabazite is a highly stable, natural zeolite. Due to its immense abundance in nature and high silica to alumina ratio, chabazite was chosen as a test carrier for antimicrobial cationic species.

Jet Milling

Chabazite zeolite that was originally obtained (GSA Resources Inc., Arizona, USA) had a mean particle diameter of 27 micron and a density of 1730 kg/m^3. Opposed nozzle jet milling was used to reduce the particle size. A captured image of the system is shown in Figure 7.1 in Appendix A.

Compressed air was used as the source of fluid energy for the system. Vibratory feeder was used to control the rate of material fed to the system. A free hanging filter bag was used to entrap ultrafine chabazite particles once they reached ultrafine size. After milling the chabazite particles were reduced to D(v,0.5) particle size of 2.76 microns.

Functionalization

Chabazite (Ca, Na_2, K_2, Mg)$Al_2Si_4O_{12}\cdot 6H_2O$ was loaded with ionic species of silver, zinc or copper. Silver Nitrate ($AgNO_3$), Copper(II) Nitrate hemipentahydrate 98% ($Cu(NO_3)_2 \cdot 2.5H_2O$) or Zinc Nitrate Hydrate 99% ($Zn(NO_3)_2 \cdot xH_2O$) salts were used to ion exchange their respective ions into chabazite.

Ion exchange was carried out in the dark for all respective salt species in order to avoid any chance of photooxidation (Li Z and Flytzani-Stephanopoulos M, 1997). The following steps were carried out to deposit metallic ions into chabazite:

1. Chabazite zeolite (20 g) was brought into contact with aqueous mixed suspensions (500 mL) of respective ionic species at specific molar concentrations (C) calculated using the following simple formula:

   Mass (g) = C (mol/L) · Volume (L) · MolarMass (g/mol)

   Ion-exchange was carried out by vigorous magnetic stirring at 500 rpm in 1000 mL glass beakers overnight (24 hours). Unless specified the water bath temperature of each experiment below was kept constant at an ambient temperature of 20°C.

   a. Silver Nitrate ($AgNO_3$) – 0.05 M - 60°C
   b. Silver Nitrate ($AgNO_3$) – 0.05 M
   c. Silver Nitrate ($AgNO_3$) – 0.011 M
   d. Copper(II) Nitrate hemipentahydrate ($Cu(NO_3)_2 \cdot 2.5H_2O$) – 0.05 M
   e. Zinc Nitrate Hydrate ($Zn(NO_3)_2 \cdot xH_2O$) – 0.011 M
2. The pH was measured during each experiment to ensure proper pH levels. i.e. ion exchange of silver was measured to be pH of 5-7 in all cases which was below the

maximum natural precipitation limit therefore silver was in its monovalent form. This also prevents silver or the like from forming or depositing on the surface or in pores of zeolite (Niira et al, 1990).

3. The solid phase was separated from the liquid phase after ion exchange by centrifugation at 7000 rpm for 5 minutes. Solid phase samples were washed extensively with mega pure deionized water. Washing was carried out several times with repeated centrifugation to ensure only chemisorbed ions within the zeolite particles. I.e. NaCl suspension in water at 0.1 M was used to identify any ionic silver species in supernatant fluid after centrifugation and washing. NaCl suspension in water indicated if silver ion was present after washing by producing a perceived cloudy mixture with the supernatant.
4. The chabazite particles were then dried in an oven over night (24 hours) at 105°C under normal pressure.
5. After sufficient drying, the chabazite particles were easily broken down into their initial respective particle sizes by small coffee grinder.

Loading chabazite with specific metallic ions theoretically possesses uncontrollable variables of the final product including surface area, density and porosity. However by manipulating the variables we may control, like the concentration of salt species used during ion exchange, the concentration of loaded material in the final chabazite after ion exchange may be subsequently altered.

3.1.2 Synthetic Zeolite

Functionalization

The same procedure as outlined above was used to functionalize synthetic zeolite with silver ion. The initial particle size during exchange was approximately 4 micron and the silver nitrate concentration in aqueous solution was 0.011 M.

The synthetic zeolite used was obtained from PQ corporation. This synthetic zeolite was of type A and contained only sodium cations for exchange. Characterization would confirm these properties and a perfect cube like structure.

3.1.3 Silica Glass

Functionalization

Silica gel despite its name is a solid highly porous material. Contact with silver nitrate solution would presumably cause physical impregnation of silver ions into the porous silica structure. Amorphous silica gel (SiO_2) powder was brought into contact with 0.05 M aqueous silver nitrate solutions while mechanically agitated at 500 rpm and ambient temperature 20°C and normal pressure. The contact times were varied from 24 hours, 48 hours and 72 hours to optimize impregnation results. After mixing, the solid phase was separated from the liquid phase by centrifugation and corresponding solids were washed once with deionized water to eliminate ions on the surface. The silica gels were then dried over night at 105°C in an oven at normal pressure. The impregnation results are summarized in the table below:

Table 3.1: EDX Results of loaded Silver Ion into Baked Silica Gel by various contact times with 0.05 M Silver Nitrate

EDX Analysis	Sample 1	Sample 2	Sample 3
	24 hours	*48 hours*	72 hours
Ag Concentration	0.44	0.82	0.00
(Weight %)	0.00	0.00	0.47
	0.26	0.11	0.33
Mean	**0.23**	**0.31**	**0.26**
Stdev	**0.22**	**0.44**	**0.24**

The procedure above failed to impregnate silver ions into silica gel. EDX analysis showed negligible amounts of silver in all three samples (24, 48 and 72 hours) of silica gel powders after impregnation efforts. Therefore an alternative method was used to create a similar additive.

Sol-Gel Method

The procedure used to prepare silica glass particles containing silver ion was carried forth with help from Suratwala, T.I. (2003) and Kawashita M, Tsuneyama S, Miyaji F, Kokubo T, Kozuka H, and Yamamoto K, (2000). The molar ratios of the starting solutions used to produce the silver silica glass are shown below:

Table 3.2: Molar ratios of starting solutions to produce silver loaded silica glass

$(C_2H_5O)_4Si$	H_2O	HNO_3	C_3H_7OH	$AgNO_3$
1	8	0.01	2	0.025

The above molar ratios were used to prepare silica glass. The procedure that was followed to make all silica samples used in this research is outlined below; unless otherwise specified:

1. Tetraethoxysilane (TEOS) ($C_8H_{20}O_4Si$) was mixed by magnetic stirrer with Iso-propanol (C_3H_7OH) making solution (a) in 1000 mL glass beaker.
2. Silver nitrate salt was then added to water (H_2O) in a separate 250 mL flask. Once silver nitrate was fully dissolved in the water, 68% nitric acid (HNO_3) was added to form solution (b).
3. Solution (b) was then slowly added drop-wise into solution (a) while vigorous agitation was applied at room temperature. Strong mixing was continued for at least 3 hours.

4. The resultant tetraethoxysilane based solution was kept in the original beaker and allowed to gel and age for seven days at room temperature 20°C and atmospheric pressure.
5. Various drying techniques were utilized unto the gels in order to optimize the ultimate microstructure.

The microstructure (porosity, surface area) of the finished sol gel would clearly be affected by changes upon the structural template during the drying phase of production. Five different biocidal silica samples were produced, varying only by the drying method from gel unless otherwise stated. Drying methods are summarized in Table 3.3:

Table 3.3: Methods of drying utilized unto Silver-Silica Gels at the end of the Sol-Gel Process

Silica- Gel Sample (#)	Temperature (°C)	Pressure (mbar), (kPA)	Drying Time (hours)
(1)	200	1013.25 ,101.325	2
(2)	200	1013.25, 101.325	2
(3)	100	1013.25, 101.325	2
(4)	20	1013.25, 101.325	24
(5)	20	215, 21.5	72
(6)	-50	215, 21.5	72

A standard oven with open ventilation was used to obtain temperatures as high as 200°C for drying. Only 2 hour drying times were used for samples (1) – (3) because fractions of these silica samples began to show thermal oxidation of silver by color changes from clear to light yellow/brown. A ModulyoD Freeze Dryer (by Thermo Electron Corporation) was used to dry silica gel at -50°C and a low pressure of 215mbar or 21.5kPa. Samples (5) and (6) utilized the freeze dryer but only silica sample (6) was initially flash frozen using liquid nitrogen; liquid nitrogen was dispersed around plastic vials holding the silica gel inside as not to let the liquid nitrogen directly touch the sample. Freeze drying the sol gel simulates supercritical drying and 72 hours was sufficient enough to maximize drying.

6. After drying, the finalized powders were all pulverized using Retsch PM 200 Ball Mill. Dry Ball milling was performed in both chambers for 30 minutes, 450 rpm, 16 grams powder and 25 balls per chamber for each silica sample. A picture of the ball mill equipment is shown in Appendix A Figure 7.2.

The exception of the above condition was met by silica sample (1) where a manual crucible was used to grind the powder to its generated particle size.

An important point to note is that sample (4), that was allowed to dry at room temperature and pressure (STP), was dispersed into petri dishes after step number 3 of the sol-gel procedure. After adequate mixing, the sol solution was allowed to evaporate and gel much quicker in petri dishes (while in a safety hood) as more of the surface was exposed to air. Overnight (24 hours drying) it was observed that the sample was completely dry, cracking into perfectly transparent, large smooth pieces of silica glass.

3.1.4 Metallic Silver Nanoparticles

Metallic silver nanoparticles ranging in size from 2-10 nanometres were obtained from Company V. - for confidentiality purposes. The nano particles were obtained as a deep orange solution where 1.5 mg by weight of particles may be found in 1 mL of solution. According to the material safety data sheet there are three components to the nano particle suspension: water 99% by weight, silver (as nanocrystal compound) less than 0.1% by weight and a type of polymer less than 1.0% by weight. As indicated by Company V directly, silver makes up 31% by weight of the solid phase nano particles in the suspension.

The nanoparticles are produced through chemical reaction by initially dispersing a negatively charged polymer in water and adding a positively charged metal species. The polymer chain then collapses around the metal species as opposites attract. The polymer shell that surrounds the silver nano crystals gives the particles a water dispersible property. The charged metal species can then be easily reduced by oxidation means to create a metal nanoparticle.

The metallic silver nanoparticles were formulated into a final polyester TGIC powder by first very vigorously mixing the two components together. Depending on how much silver was to be theoretically found in the final powder coating, the volume of the nano particle suspension added to a specific amount of polyester powder was carefully measured. To produce a 0.5% by weight silver powder with polyester, 268.82 mL of the suspension was added to 25 g of polyester TGIC ultrafine powder. This was accomplished by incorporating the components proportionally into 14 polymer freeze drying vials, and covering with a parafilm lid. Vials with the suspension and polyester powder were shaken very strenuously and vortexed for at least 1 minute each on the highest speed; mixing was continued until powder was completely dissolved into the suspension. The vials were then flash frozen with liquid nitrogen and placed in ModulyoD Freeze Dryer (by thermo Electron Corporation) at -50°C and 215mbar or 21.5 kPa. Freeze drying equipment is given in Figure 7.3 in Appendix A.

This procedure producing silver nanoparticles homogeneously dispersed into polyester resin powder at a specific weight percentage of silver was repeated for silver concentrations of 0.1%, 0.05% and 0.005% by weight silver in final coating.

It was necessary to flash freeze and freeze dry the formulation described above because if allowed time to settle the polyester particles would sink to the bottom due to density and gravity. Most importantly, silver nanoparticles are oxidized very easily therefore for precautionary measures freeze drying was carried out. It should also be noted that the metallic silver nanoparticles were assumed to melt at temperatures above 180°C, says company V. Furthermore, current studies from their research department show that the particles may be subject to melting at temperatures as low as 100°C after 10 minutes of exposure (data not shown).

3.1.5 Metallic Silver from Tollen's Reagent

Tollen's Reagent was produced/reduced with help from literature by Johnson WA (1998). The procedure that was followed to produce metallic silver precipitate from Tollen's reagent is outlined below:

1. 0.80 g of $AgNO_3$ was dissolved in 70 mL of distilled water to get a clear solution. Continued agitation was applied to the 500 mL beaker throughout the experiment.
2. $NH_3 \cdot H_2O$ was added to the $AgNO_3$ solution until silver oxide was formed - a deep-brown precipitate.

   Relative reaction: $2AgNO_3 + 2NH_3 \cdot H_2O = Ag_2O(s)\downarrow + 2NH_4NO_3 + H_2O$

3. $NH_3 \cdot H_2O$ was continued to be added, drop wise, to the precipitate solution until all precipitation totally dissolved to give a clear solution again which yielded Tollen's reagent ($2[Ag(NH_3)_2]^+OH^-$).

   Relative reaction: $Ag_2O + 4NH_3 \cdot H_2O = 2[Ag(NH_3)_2]^+OH^- + 3H_2O$

4. 0.85 g formaldehyde was added to approximately 10 mL of ethanol and mixed in a separate 250 mL flask. It should be noted that only 0.765 g of formaldehyde was calculated to be necessary to react with all the ionic silver in solution. Therefore 100% transfer efficiency was assumed for the reaction of ionic silver to metallic silver.
5. Formaldehyde solution was then added slowly drop wise method into the previous tollen's solution. Mixing continued for approximately 2 hours.

   Relative reaction: $HCHO + 2[Ag(NH_3)_2]^+OH^- = HCOO^- NH_4^+ + 2Ag(s) + 3NH_3 + H_2O$

Silver coated Carbon Nanotubes

The procedure outlined for Metallic Silver from Tollen's Reagent was used to produce silver coated carbon nanotubes (CNTs). 2.5 g of carbon nanotubes were added to step 3 (Tollen's reagent) and allowed to mix for 30 minutes ensuring good dispersion. After steps 4 and 5 the silver coated CNTs were separated by filteration. The solid phase obtained was rinsed several times with deionized water until the residual was neutral. The final product was then dried in oven at 100°C for 2 hours. After drying, small coffee grinder was sufficient to separate the CNTs. Obvious silver particles were perceived to be present and dispersed in the final powder. Silver coated CNTs were the goal of the experiment but it was apparent from simply observing the final powder that there was a micro dispersion of metallic silver.

Silver Microparticles dispersed with Polyester TGIC

The procedure outlined for Metallic Silver from Tollen's Reagent was used to produce a dispersion of metallic silver micro particles in a base Polyester TGIC resin powder. Using steps from the procedure used to try and produce silver coated carbon nanotubes this procedure was developed. 25 g of ultrafine polyester TGIC was added to step 3 and allowed to mix for 30 minutes ensuring good dispersion. After steps 4 and 5 the thick shiny solution was transferred to 10 polymer freeze drying vials. The vials were then flash frozen with liquid nitrogen and placed in the freeze dryer for 72 hours at -50°C and 215mbar or 21.5 kPa. The freeze dryer was utilized in this experiment because polyester TGIC would begin to cure at high temperatures that would have been required to dry the material and eliminate all H_2O molecules. The amount of polyester TGIC by weight that was added to the Tollen's solution yields a theoretical silver concentration by weight in the final powder formulation of approximately 2.0%. A 0.1% sample was also produced in similar fashion.

3.1.6 Ionic Silver with No carrier

Ionic silver without the help or use of carrier materials was incorporated with polyester TGIC resin powder. This was completed at a theoretical weight percent of silver into the polyester of 0.1%. Essentially, an aqueous suspension of silver nitrate would be mixed with polyester TGIC and freeze dried. 0.0394 g of silver nitrate salt was dissolved in deionized water. Through molar calculation of silver nitrate and silver it was determined that the weight percent of silver in silver nitrate is 63.48%, thus 0.0394 g of silver nitrate has 0.025 g silver. This amount of silver mixed with 25 g of polyester TGIC yielded the required fractions to produce the suspension desired. After the polyester powder was homogeneously dispersed in the silver nitrate solution, by vigorous shaking and vortexing in freeze drying vials, the samples were flash frozen and freeze dried for 72 hours at -50°C and 215mbar or 21.5 kPa.

3.1.7 Industrial Powders

For confidentiality issues, the industrial powders obtained will not be called upon by their real names or places of origination. However it should be noted that the powders obtained from each top powder manufacturer are claimed to posses high antimicrobial properties including longevity of the final coatings. Both powders are currently marketed and sold as antimicrobial powder coatings in many different colors for wide ranging applications.

Company P

The base resin system used by company P was white polyester.

Company D

The base resin system used by Company D was clear polyester. This resin system was purposely obtained to aid in efforts of worthy and accurate comparison as it is almost identical to our base resin system.

Company D's antimicrobial powders are patented under U.S. patent numbers (6093407, 6432416). Their antimicrobial effectiveness is claimed to be from zeolite particles that are loaded with both zinc and silver ions, where the additive is incorporated with the base resin system pre-extrusion.

3.2 Characterization of Additive Powders

3.2.1 Scanning Electron Microscope Images

A Field S-2600N Emission-Scanning Electron Microscope (SEM) by Hitachi High-Technologies Inc allowed detailed qualitative observations of antimicrobial additives. All sample powders were first sputtered with gold by an Emitech K550X Gold Sputter device to provide an electrically conductive thin film representative of the surface topography. The film in turn reduces thermal damage and enhances secondary electron emission. Captured images of the SEM and gold sputter equipment are shown in Appendix A Figures 7.4 and 7.5. SEM Images of additive powders are shown below in Figures 3.1 – 3.11:

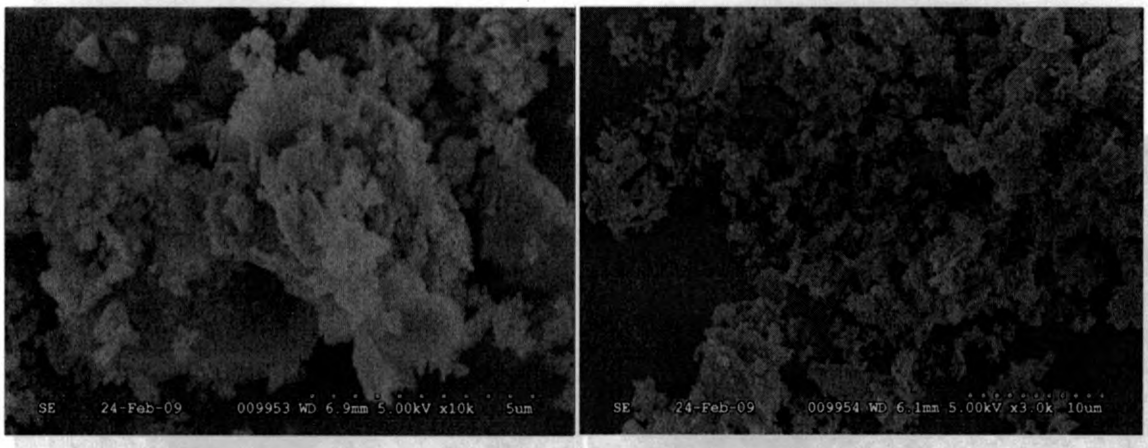

Figure 3.1: SEM Images (5 and 10um scale) Blank Chabazite Particles

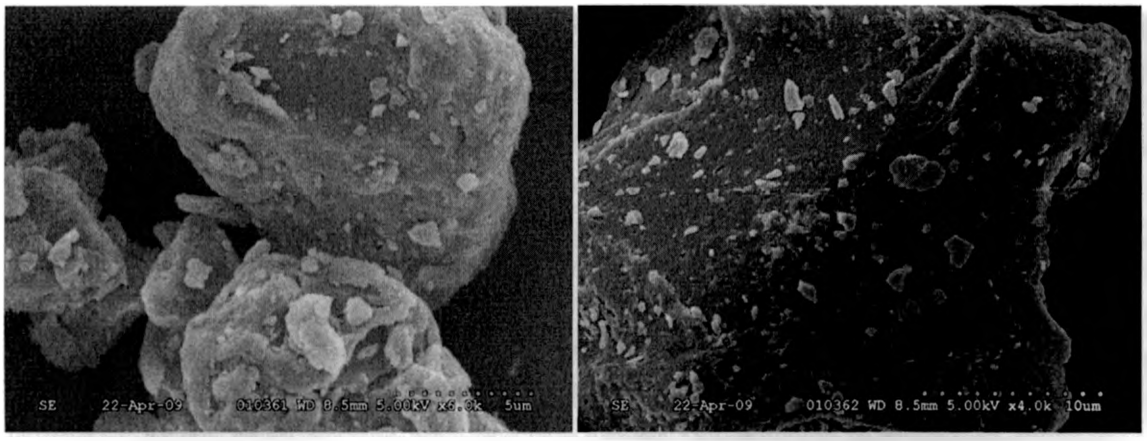

Figure 3.2: SEM Images (5 and 10um scale) 0.5% Ag Polyester Powder by Chab-20% Ag additive

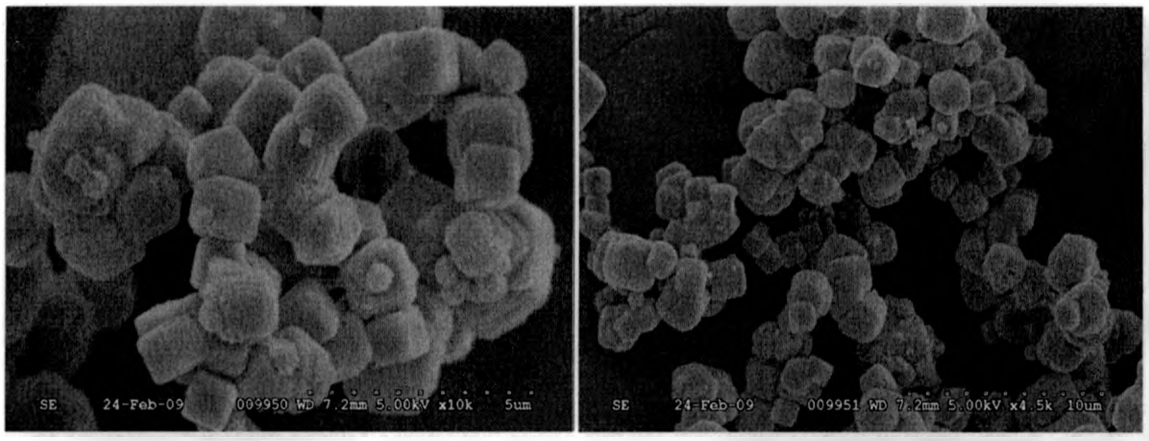

Figure 3.3: SEM Images (5 and 10 um scale) Synthetic Zeolite A – (Na) by PQ Corp

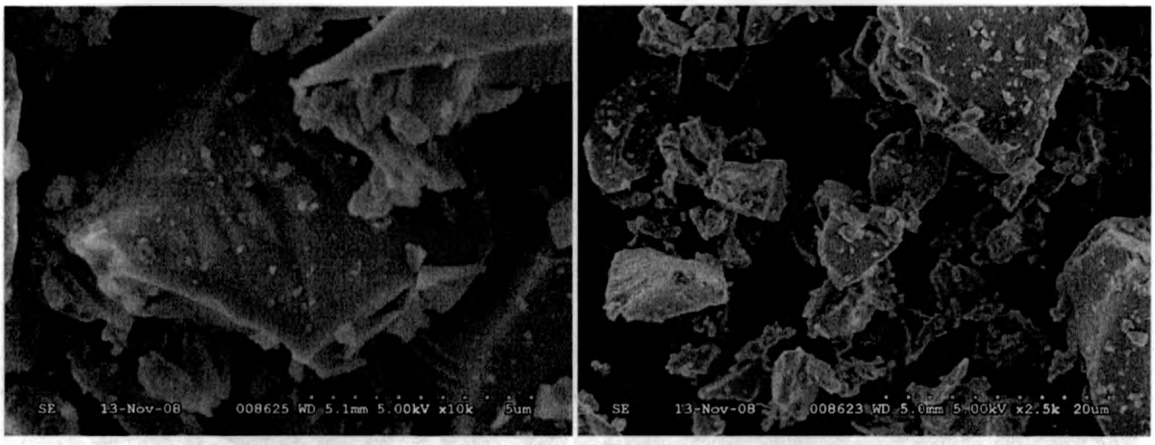

Figure 3.4: SEM Images (5 and 20 um scale) Silica Glass sample (1) – 200C, 1013.25mbar drying conditions

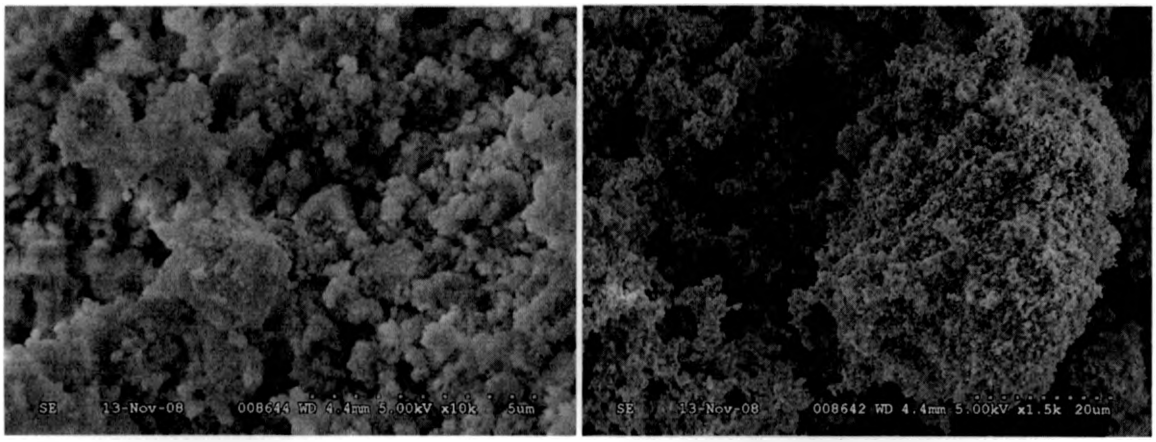

Figure 3.5: SEM Images (5 and 20 um scale) Silica Glass sample (2) – 200C, 1013.25mbar drying conditions

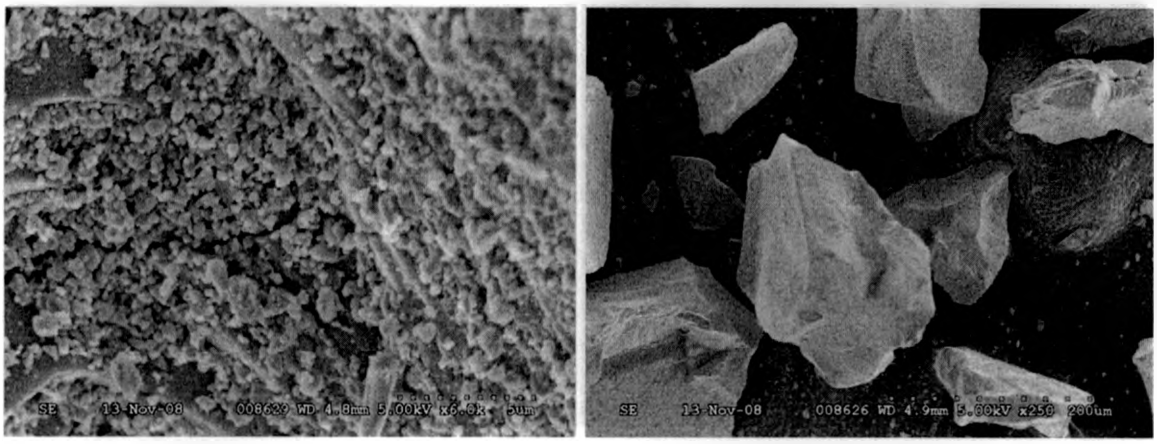

Figure 3.6: SEM Images (5 and 20 um) Silica Glass sample (3) – 100C, 1013.25mbar drying conditions

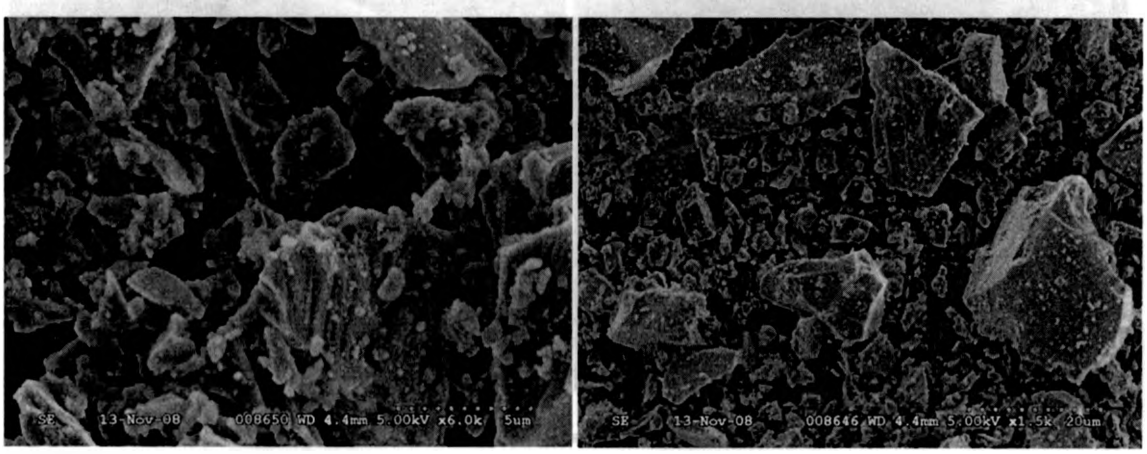

Figure 3.7: SEM Images (5 and 20 um scale) Silica Glass sample (4) – 20C, 1013.25mbar drying conditions

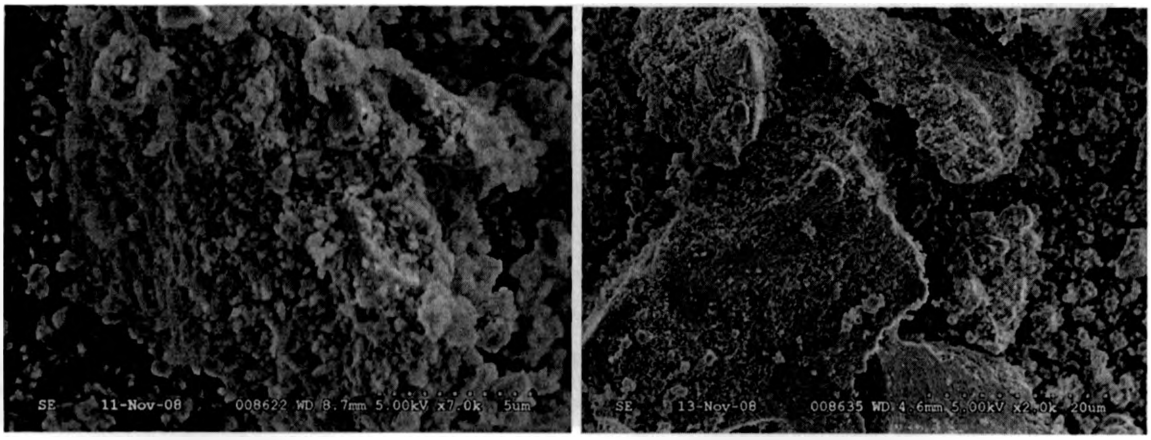

Figure 3.8: SEM Images (5 and 20 um scale) Silica Glass sample (5) – 20C, 215mbar drying conditions

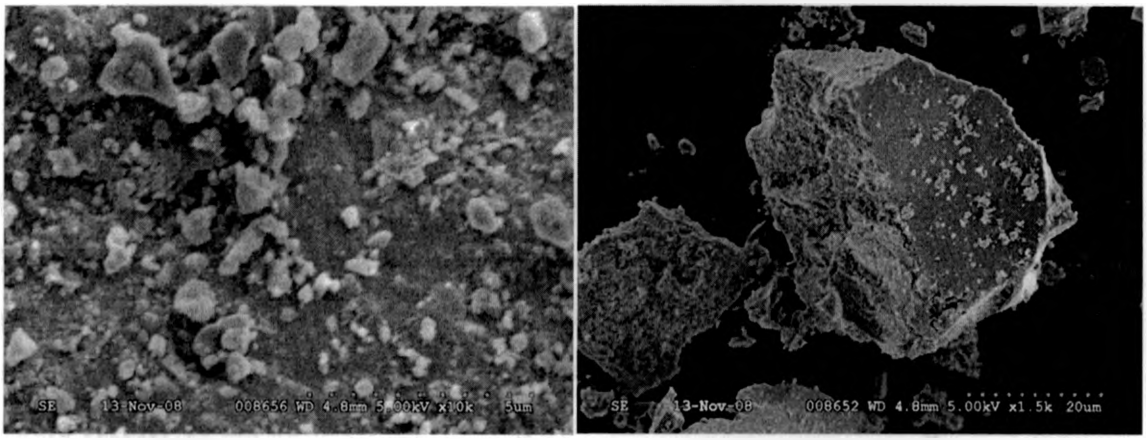

Figure 3.9: SEM Images (5 and 20 um scale) Silica Glass sample (6) – -50C, 215mbar drying conditions

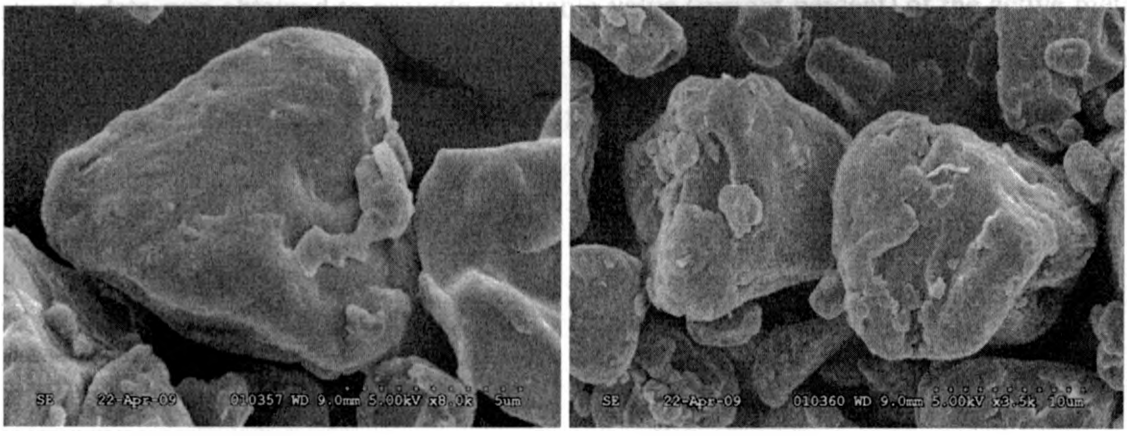

Figure 3.10: SEM Images (5 and 10 um scale) 0.5% Ag Polyester by Nanoparticles-31%Ag from Company V

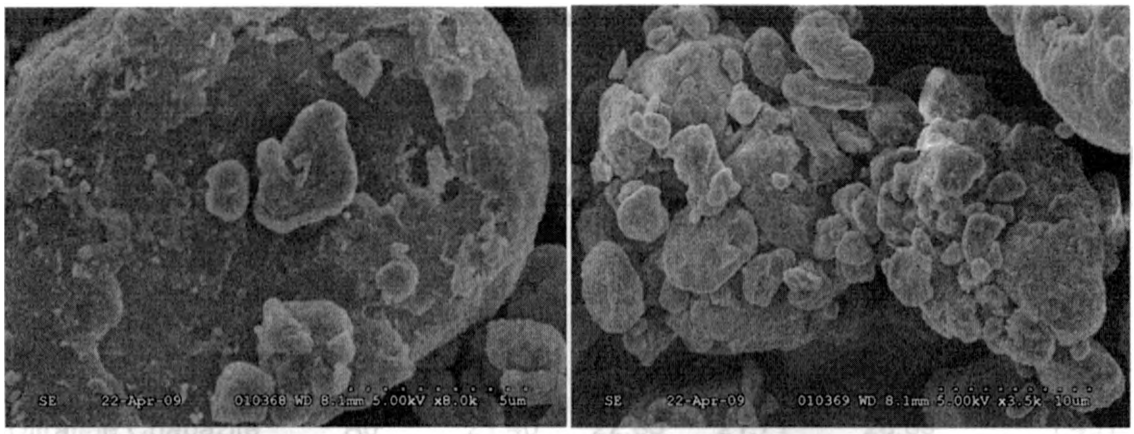

Figure 3.11: SEM Images (5 and 10 um scale) 2% Ag Polyester by metallic silver from Tollen's Reagent

3.2.2 Energy Dispersive X-Ray Spectroscopy

The microanalysis (EDX) of antimicrobial additive powders was undertaken using the field-emission scanning electron microscope. EDX was used for the elemental analysis and chemical characterization of the samples. It enabled a reliable weight percentage value (estimated quantitative number) to be assigned to each antimicrobial powder which would further be the basis for calculating the concentrations of active agents in the final powder coatings. Three SEM stubs were prepared for each antimicrobial powder analyzed and three EDX readings were taken from each stub. This was done to ensure enough data was obtained to provide a reliable value (weight percent) of the active metal agent incorporated therein. Further, yielding an accurate estimate of active material found at the surface of the coating. EDX results for additive powders are summarized in the following Table:

Table 3.4: EDX Analysis of Additive Powders determining Active Agent Metal weight Percentages

Powder Description	Metal Form	EDX Analysis Concentration (weight%)			Mean Average (weight%)	STDEV (weight%)
		(Stub1)	*(Stub2)*	*(Stub3)*		
Ultrafine Chabazite	Ag^+	19.98	23.04	18.40	20.83	1.844
0.05M Silver Nitrate		22.50	19.61	18.40		
60°C		21.04	21.39	23.10		
Ultrafine Chabazite	Ag^+	21.40	22.86	21.71	20.69	1.451
0.05M Silver Nitrate		21.77	19.81	19.67		
20°C		19.78	18.53			
Ultrafine Chabazite	Ag^+	4.11	4.27	4.43	4.49	0.274
0.011M Silver Nitrate		4.89	4.57	4.55		
20°C (1)		4.84	4.30			
Ultrafine Chabazite	Ag^+	5.31	3.05	2.60	3.42	0.983
0.011M Silver Nitrate		4.10	2.61	3.42		
20°C (2)		3.89	2.40			
Ultrafine Chabazite	Cu^{2+}	14.69	12.97	12.03	13.04	1.399
0.05M Copper II Nitrate		14.12	12.68	12.91		
20°C		15.77	14.17	11.29		
Ultrafine Chabazite	Zn^{2+}	5.81	4.33	4.43	4.53	0.635
0.05M Zinc II Nitrate		3.63	4.82	4.63		
20°C		4.05	4.54			
Synthetic Zeolite A	Ag^+	2.10	1.92	1.98	2.19	0.291
0.011M Silver Nitrate		2.10	2.35	2.10		
20°C		2.14	2.84			
Carbon Nanotubes	Ag°	78.38	79.12	87.19	77.18	5.315
		67.68	73.76	79.42		
		78.86	74.05	76.18		
Silica Glass	Ag^+	7.35	9.18	7.59	8.62	1.53
0.023M Silver Nitrate		6.80	10.45	9.65		
200°C (1)		10.63	7.35			

*** Metallic Silver Nano Particles include 31% Ag° loading produced by Company V.

From the above chabazite loaded particles, further analysis of ion exchange between cations in the zeolite was conducted. The ion exchange analysis may be observed in the following Table.

Table 3.5: EDX results before and after ion exchange with chabazite by various salt concentrations

Element	Chabazite 0.05M AgNO3		Chabazite 0.011M AgNO3		Chabazite 0.05M Cu (II) NO3		Chabazite 0.05M Zn (II) NO3	
	Weight % in Solid Phase							
	Before IE	*After IE*	*Before IE*	*After IE*	*Before IE*	*After IE*	*Before IE*	*After IE*
Ag, Cu or Zn	0	20.7±1.6	0	4.5±0.3	0	13.0±1.4	0	4.5±0.6
Na	1.6±0.6	0	1.6±0.6	0	1.6±0.6	0	1.6±0.6	0
K	8.4±3.0	1.9±1.1	8.4±3.0	5.9±1.0	8.4±3.0	3.2±0.9	8.4±3.0	6.4±1.3
Ca	0.9±0.4	1.3±0.6	0.9±0.4	1.1±0.6	0.9±0.4	0.8±0.6	0.9±0.4	0.3±0.1
Fe	5.7±2.3	3.5±0.2	5.7±2.3	5.6±2.7	5.7±2.3	3.9±2.7	5.7±2.3	6.1±2.0

Aluminum and Silica are not shown in the above table as they remained relatively constant throughout at weight % of 6.9±2.3 and 38.8±4.4 respectively. The oxygen weight % was very scattered for all samples. Additionally, the variances and increases of Calcium after ion exchange for chabazite (0.05M and 0.011M $AgNO_3$) in the above table relate to high standard deviations for such samples; when analyzing the calcium spectrums.

Similar to Table 3.4, Table 3.6 was generated which summarizes the EDX results of silver loadings for all produced silica gel powders:

Table 3.6: EDX Analysis of Silica Powders determining Silver Ion weight Percentage

Powder Description And Drying Method	Metal Form	EDX Analysis Concentration (weight%)			Mean Average (weight%)	STDEV (weight%)
		(Stub1)	*(Stub2)*	*(Stub3)*		
Silica Glass (1)	Ag^+	7.35	9.18	8.84	8.62	1.43
0.023M Silver Nitrate		6.80	10.45	8.40		
200°C		10.63	7.35			
Silica Glass (2)	Ag^+	2.56	3.19	3.30	3.25	0.432
0.023M Silver Nitrate		4.04	3.44	3.10		
200°C		2.74	3.35	3.49		
Silica Glass (3)	Ag^+	5.67	7.05	5.12	4.92	1.52
0.023M Silver Nitrate		4.82	7.08	3.94		
100°C		2.46	4.28	3.82		
Silica Glass (4)	Ag^+	3.04	3.73	3.88	3.61	0.312
0.023M Silver Nitrate		3.66	3.58	3.31		
20°C		4.03	3.62			
Silica Glass (5)	Ag^+	3.57	3.89	3.82	3.71	0.289
0.023M Silver Nitrate		3.53	3.93	3.61		
215mbar, 20°C		3.20	4.12			
Silica Glass (6)	Ag^+	1.75	1.71	2.97	2.16	0.889
0.023M Silver Nitrate		0.71	2.47	2.08		
215mbar, -50°C		2.47	1.53	3.77		

*** Silica samples were dried at 1013.25 mbar unless otherwise specified.

The above EDX results from Tables 3.4 and 3.6 correspond to U.W.O. produced antimicrobial powders. However a couple of antimicrobial claimed industrial powders were also tested. Company P's powder fails when tested against bacterial inactivation therefore its characterization was not conducted. Company D's powder worked therefore its EDX results are included in the following Table 3.7.

Table 3.7: EDX Analysis of Company D's Powder determining Silver and Zinc Ion weight Percentage

Powder Description And Drying Method	Metal Form	EDX Analysis Concentration (weight%)			Mean Average (weight%)	STDEV (weight%)
		(Stub1)	*(Stub2)*	*(Stub3)*		
Company D	Ag^{+}	0.39	0.23	0.50	0.505	0.212
		0.49	0.9	0.42		
		0.44	0.8	0.38		
	Zn^{2+}	0	0	0	0	0
		0	0	0		
		0	0	0		

The EDX spectrums of some of the antimicrobial powders tested are shown in the Appendix B. It would be redundant to include every powder tested so only necessary ones are incorporated. The EDX spectrums were the source of weight percent concentrations gathered for calculation of final reliable values assigned to each sample and for ion exchange comparisons with chabazite.

3.2.3 Particle Size Analyses

The particle sizes of the processed resin systems, and functionalized carrier materials were determined by two analysis devices: BT-9300S Laser Particle Size Analyzer and TSI 3603 Particle Size Distribution Analyzer. The pictures of equipment are found in Appendix A, Figures 7.6 and 7.7. Particle sizes of additive powders produced by BT-9300S system are shown in Table 3.8 below, while particles sizes produced by TSI 3603 are shown in Table 3.9.

Both tables include *D(v,0.5)* which is the average particle size defined as the average equivalent diameter where 50% mass of the particles have a larger equivalent diameter, and the other 50% mass have a smaller equivalent diameter. *D(v,0.9)* is that equivalent diameter where 90% mass of the particles have a smaller diameter and hence the remaining 10% is coarser. The definition of *D(v,0.03) D(v,0.05)* can be derived similarly.

D(4,3) is the volume moment mean of the particles, defined $\Box x_i d_i^4 / \Box x_i d_i^3$, and *D(3,2)* is the surface area moment mean or Sauter Mean Diameter defined $\Box x_i d_i^3 / \Box x_i d_i^2$; often used in applications where the active surface or surface area is important.

Table 3.8: Particle Size Analysis by BT-9300S System

Powder Description	Particle Size (µm)				
	D(v,0.03)	*D(v,0.5)*	*D(v,0.9)*	*D(4,3)*	*D(3,2)*
Polyester Resin 2401-2	1.51	24.96	78.85	34.74	9.10
Polyester Resin 2471-4	1.48	20.81	61.16	27.75	8.40
Chabazite Zeolite Stock Blank	0.73	27.29	120.80	46.84	5.34
Chabazite Zeolite Jet Mill Blank	0.27	2.76	7.28	3.47	1.39
Chabazite Zeolite 20.83% Ag, 60°C	0.23	2.07	5.18	2.53	1.14
Chabazite Zeolite 20.69% Ag, 20°C	0.24	2.26	5.73	2.78	1.21
Chabazite Zeolite 4.53% Zn, 20°C	0.27	2.31	5.77	5.81	1.24
Chabazite Zeolite 13.04% Cu, 20°C	0.25	2.27	5.69	2.77	1.22
Synthetic Zeolite A 2.19% Ag, 20°C	0.41	3.62	8.80	4.35	1.93
Carbon Nano Tubes 77.18% Ag	1.66	11.87	26.23	13.64	7.06

*** Company V`s Nanoparticles with 31% Ag^0 loading have particle size 2-10 nm.
*** CNT particle size reading may result from agglomeration of particles during processing.

Table 3.9: Particle Size Analysis of Silica Glass Additives by TSI Model 3603

Powder Description	Particle Size (µm)					Grinding Method
	D(v,0.05)	*D(v,0.5)*	*D(v,0.9)*	*D(4,3)*	*D(3,2)*	
Silica Glass (1) 8.62%Ag, 200°C	1.80	28.81	81.17	36.35	10.48	Crucible
Silica Glass (2) 3.25%Ag, 200°C	1.68	14.4	36.2	17.5	6.53	Ball Milled
Silica Glass (3) 4.92%Ag, 100°C	15.1	130.1	216.9	124.2	43.2	Ball Milled
Silica Glass (4) 3.61%Ag, 20°C	1.90	13.5	32.5	18.0	8.08	Ball Milled
Silica Glass (5) 3.71%Ag, 215mbar, 20°C	3.18	26.9	47.6	27.8	13.4	Ball Milled
Silica Glass (6) 2.16%Ag, 215mbar, -50°C	1.40	10.3	32.9	14.6	13.6	Ball Milled

*** Silica samples were dried at 1013.25 mbar unless otherwise specified.

3.2.4 Brunauer Emmet Teller

Brunauer Emmet Teller (BET) equipment was used to produce isotherm graphs, surface area and micropore area calculations for each silica gel additive. BET measures physical adsorption and desorption properties of material with gas molecules on solid surfaces of particles. The aforementioned drying techniques for each sol-gel were believed to produce very different structural properties of silica particles. The below table lists the monolayer Langmuir surface areas and BET micropore areas of each silica gel additive produced.

Table 3.10: Brunauer Emmet Teller (BET) Results of Different Drying Techniques of Silver loaded Silica Glass

Powder Description	Langmuir Surface Area (m^2/g)	Micropore Area (m^2/g)	IUPAC Isotherm Result
Silica Glass (1) 8.62%Ag, 200°C	41.58	0	Type II or III Nonporous
Silica Glass (2) 3.25 %Ag, 200°C	43.34	0	Type II or III Nonporous
Silica Glass (3) 4.92%Ag, 100°C	7.89	0	Type II,III or none Nonporous
Silica Glass (4) 3.61%Ag, 20°C	341.49	203.63	Type I Microporous
Silica Glass (5) 3.71%Ag, 215mbar, 20°C	30.15	0	Type II or III Nonporous
Silica Glass (6) 2.16%Ag, 215mbar, -50°C	7.57	0	Type II, III or none Nonporous

*** Silica samples were dried at 1013.25 mbar unless otherwise specified.

The adsorption-desorption isotherms generated by BET are found in Appendix C along with a re-drawn classification system by IUPAC for adsorption isotherms. Comparisons of the IUPAC classification system isotherms to the ones generated by BET tell of the porosity of that sample; results are listed in the above table.

3.2.5 X-Ray Powdered Diffraction

Chabazite zeolite additives underwent characterization by X-Ray powdered diffraction (XRPD). This technique was used to determine the crystal structure of chabazite before and after functionalization processes and show differences between ion exchange environments. The XRPD spectra were collected on a powder diffractometer with settings of 30 kV radiations and 15 mA. Scans were run from 0° - 70° (2 theta degree), increasing at a step size of 0.02° and counting time 2 seconds. The obtained data was then processed and the crystallographic structure of the powdered samples was recognized through peaks over 2 theta degree. The data may be found in Appendix D.

3.3 Powder Coating Procedure

3.3.1 Resin System

The same or similar polyester paint was used throughout the project. For production of the polyester paint powder, low viscosity polyester was selected to be cured with TGIC at a ratio of 93:7. Low viscosity resin should allow high additive percentages in the final coatings with high quality thin films. The chosen polyester resin was manufactured and supplied by Cytec Industries with the trade name Crylcoat™ 2401-2, and 2471-4. The physical properties of the polyester resins are listed in the table below.

Table 3.11: Cytec Polyester Resins for TGIC Powder Coatings

Crylcoat Number	Binder Ratio	Acid #	Viscosity	Tg (°C)	Curing (°C)
Powder Coating Resins					
2401-2	93/7	33	3500 200°C	60	200
2471-4	93/7	33	3500 200°C	58	200

Source: Cytec Product Guide. (2006). Binder Resins, Hardeners and Additives Americas. Cytec Surface Specialties Inc. UV Links

The above binder resins are claimed to have outstanding flow, high flexibility, low reactivity, excellent smoothness and clarity as a clear powder coating.

The curing agent was selected as Triglycidyl Isocyanurate (TGIC). It was manufactured by Huntsman Advanced Materials and it is commercialized under the trade name Araldite® PT 810. It was supplied in dust free pellet form with melting temperature of 86-96°C. A flowing agent and degassing agent was also required for the polyester powder paint system and the mix formulation sheet of ingredients is shown below.

Table 3.12: Mix Formulation Sheet yielding Polyester TGIC Clear Coat before extrusion

Class	Sub Classes	Name	Weight (g)	Class (Wt.%)	Total (Wt. %)
Binder	Resin	2401-2 2471-4	917.90	93.00	91.79
	Curing Agent	TGIC	69.10	7.00	6.91
	Matting Agent	-	0.00	0.00	0.00
	Catalyst	-	0.00	0.00	0.00
Additives	Flow Agent	P10	10.00	76.92	1.00
	Degassing	BEN	3.00	23.08	0.30
	Waxes	-	0.00	0.00	0.00
Fillers	-	-	0.00	0.00	0.00
Pigments	-	-	0.00	0.00	0.00
Total Binder			**987.00**		**98.70**
Total Additives			**13.00**		**1.30**
Total Filler			**0.00**		**0.00**
Total Pigments			**0.00**		**0.00**
Total Weight			**1000.00**		**100.00**

From the above table it is shown that 1000 grams or 1 kilogram was produced from the mix formulation sheet. These materials would be used twice – once using resin 2401-2 and once using 2471-4, producing a total of 2 kilograms of polyester powder paint for this research. Clear polyester powder paint was the main component in all antimicrobial coatings.

3.3.2 Premixing

Using the formulation sheet shown above, the components were weighed and shaken in a large plastic bag. This mixture was incorporated into a high shear grinder for approximately 10 seconds producing an adequate homogeneous dispersion and smaller

particle size. Once all raw material components had been mixed and sheared together they were then ready for extrusion.

3.3.3 Extrusion

Premixed raw materials were further processed by transfer into a twin screw extruder with cooling belt by DongHui Powder Coating Equipment (East Sun). Extrusion begins by first preheating the equipment to 80°C. Once the previous materials in the screws has melted and allows rotation the setting of the screws was set to 500rpm. The premixed raw materials were then slowly poured into the hopper. The hopper fed the mix into the extruder by the rotating movement of the twin screws. Once the material had left the extruder by passing through the rotating screws, the extrudate dripped down onto double chiller rollers, which were refrigerated with water, that rotate inwards forcing the extrudate to flatten through their forceful middle rotation. Once flattened, the thin extrudate was cooled as it moved along the cooling conveyer belt. The pieces were then collected from the belt and manually broken into smaller pieces, ready for further processing. An observation of the twin screw extruder is noticed in Figure 7.8 Appendix A.

3.3.4 Ultrafine Grinding

A high shear grinder was used to break the paint chips obtained from the extruder. Paint chips that were input to the high shear grinder were allowed to grind in increments of 10 seconds. Then one would have to wait for a few minutes before restarting the grinder. High temperatures reached inside the chamber would cause the paint to cure if long grinding times were performed. The chamber would be filled half way and the chips would be processed in the specified increments several times. Once the powder produced by the high shearing no longer felt grainy or sandy to the touch, it was transferred to a mechanical sieve for further processing. This grinding process was performed several

times or more to reach the desired level. The high shear grinder equipment is shown Appendix A, Figure 7.9.

3.3.5 Ultrafine Sieve Screening

The powders obtained from the high shear grinder were transferred to a Vorti-Siv by MiMi Industries Inc. using 325 mesh (45 micron) insert. Powder was transferred slowly/incrementally at a rate of approximately 1 g/min to the sieve and allowed to automatically vibrate with help of ultra sonic pulse, and pass through the screen. Steel washers were also added into the sieve chamber to aid in forcing powder through the screen. Once through the screen the powder was moved to the bag-house where a plastic bag trapped the ultrafine paint particles. Occasionally the screen would need to be cleaned of oversized clogged particles and remaining powder unable to pass through the screen would be sent back to the high shear grinding stage. A captured image of the sieve apparatus is shown in Appendix A, Figure 7.10.

3.3.6 Additive incorporation to Resin System

Dry Blending

Once processing of the resin system was completed, antimicrobial additives could be incorporated. Powder coating and dry blending functional additives is a unique step that has yet to be recorded in literature. All antimicrobial additives produced in powder form were dry blended with the polyester using a proprietary *Method and Apparatus for Uniformly Dispensing Additive Particles in Fine Powders* protected by Zhu J & Zhang H, 2006. Dry blending was conducted using a range of weight percents for various additives where the weight percent of each additive corresponded directly to how much of the active agent was included in that additive; silver ion, silver metal, zinc ion or copper ion.

The dry blending process initially involves weighing of additive powders and polyester resin using OHAUS Analytical Plus Balance (0.00000g). Polyester and each supposed

antimicrobial additive were then added into a small low powered coffee grinder and mixed for approximately 15 seconds while shaking. The goal of dry blending was to homogeneously disperse the smaller additives throughout the resin and in turn the functional particles would cover the surfaces of each polyester particle.

The antimicrobial additives that were dry blended with polyester included all zeolite based materials, all silica samples (1) to (6), and CNTs.

Freeze Drying

Although most of the functional antimicrobial additives were in powder form and allowed to be dry blended with the polyester resin, some additives that were found in liquid form needed to be flash frozen by liquid nitrogen and freeze dried once mixed with the polyester resin in an aqueous suspension. The additives included in this section included Silver ion with no carrier material, Tollen's Reagent reduced to silver metal, and metallic silver nano particles by Company V.

A table showing each additive used in the research and corresponding weight percent of active material and weight percent of the entire additive sample within the produced coatings will be shown and discussed in the Results section of the research paper.

3.3.7 Powder Application

Specimen/Substrate Preparation

Aluminum panels (8.6 cm long and 4.9 cm wide) supplied by Q-Lab Corporation specifically manufactured for powder coating testing were used. Square aluminum chips measuring 3.0cm · 3.0cm were cut from the aluminum panels by manual metal sheet cutters. For each antimicrobial powder sample that was prepared and tested, eighteen 3.0cm · 3.0cm aluminum substrate pieces were made.

In order to replicate the same coating conditions and produce identical coating results for each aluminum chip (for each powder sample sprayed), a unique setup was configured:

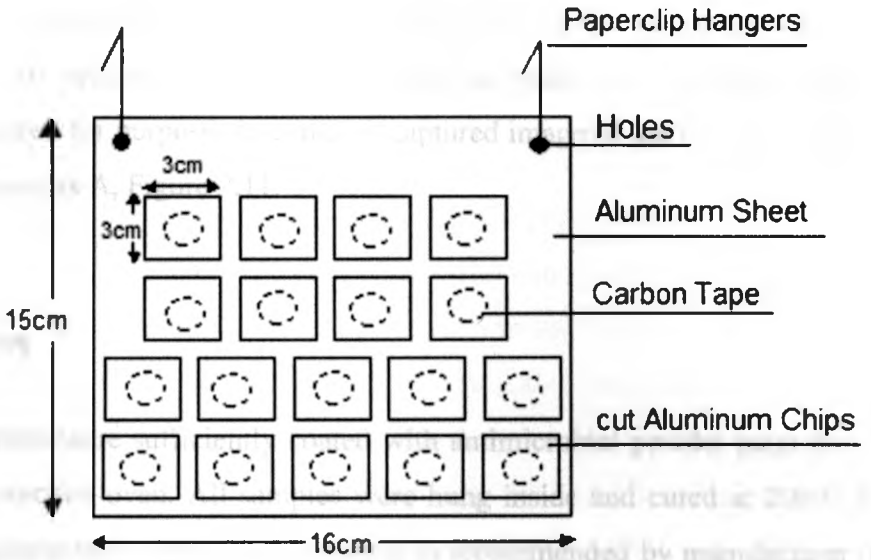

Figure 3.12: Experimental setup of spray sheets

Approximately ten to fifteen grams of powder would be sprayed out of the corona gun in order to fully coat the aluminum spray sheet and accompanied chips shown in Figure 3.12. Electrostatic field lines helped to determine powder coating completion on the substrate, as transfer efficiencies were different for all powder formulations. Once satisfied with charged powder, the sheets were hung and cured according to specifications of the base resin in the oven. 0.5 cm diameter holes were cut using CT022 N Drill Press in order to hang the apparatus in the spray booth by paper clips folded into hook shapes.

Electrostatic Spraying

Using the above specimen setup spraying of powders was initiated. Each powder sample that was electrostatically sprayed took place in a 146 mm (H) · 900 mm (D) · 750 mm (W) acrylic spray booth. The above substrate feature was hung inside the booth for each sample and grounded appropriately. A Nordson Surecoat corona spray gun (Nordson Corp, TWGEMA) was used to manually and directly coat the prepared specimens. The mixed powders were also manually deposited into the gun during the process. The corona spray gun used a cone deflector tip at the end of the gun. Powder spray was controlled by air pressures of fluidizing air and atomizing air sent through the gun. The corona charge

generator had constant settings for each spraying instance: 30 kV operating voltage, 8 uA current, and 55 air pressure strength. Only the front side of the substrate sheet was sprayed and required for purposes to come. A captured image of the booth and spray gun is evident in Appendix A, Figure 7.11.

3.3.8 Curing

Once the specimens were sufficiently coated with antimicrobial powder paint they were taken to the convection oven. All samples were hung inside and cured at 200°C for 10 minutes which guarantees a fully cured coating as recommended by manufacturer of the resin system. The only sample that did not succumb to this condition was the silver nanoparticle paint samples which were cured at 160°C for 20 minutes to try to avoid detrimental affects to the additive. A captured image of the convection oven is located in Appendix A, Figure 7.12.

3.4 Antimicrobial Efficacy Testing Procedure

3.4.1 Test Microorganism Used

Escherichia coli strain ATCC 10798 was purchased from the American Type Culture Collection (ATCC). This strain of bacteria would be used for all antimicrobial testing purposes throughout the research. *Escherichia coli* are gram negative, rod shaped, and facultative anaerobic bacterium. *E. Coli* are predominantly used as test microorganisms for most disinfection studies and predominantly noted in literature studies.

Revival

The *Escherichia coli* strain was received from shipping in frozen pellet form and was revived immediately. The propagation procedure used to revive the bacteria from this form into usable and sustainable colonies is outlined in Appendix E: Bacterial Culture Propagation Procedure.

Growth Curve

The growth curve of *E. coli* has four phases: Lag Phase occurring directly after inoculation when bacteria are not growing, Logarithmic (log) Phase where exponential growth and cell division occurs rapidly, Stationary Phase where growth slows and remains constant due to limited nutrient availability, and lastly Death Phase where nutrients are completely depleted and death occurs. The late log phase was the targeted time period for growth of the test microorganism, the reason being that this stage occurs at the end of the log phase where exponential growth is completed. This stage was tested for with the strain of *E. Coli* and using a Cary Win 50 UV-Vis spectrophotometer at 600nm was found to be occurring around 16 hours into inoculation: Liquid medium of Luria Bertani (LB) broth was inoculated with a loop full of bacteria into a Stuart Orbital Incubator 3150 at the recommended temperature of 37°C by ATCC. Sterile 250 mL flask was used and the appropriate sized sterile sponge stopper. Every hour a sample of the medium was withdrawn into a cuvette and placed in the spectrophotometer. The emitting light source from the spectrophotometer would pass through the cuvette, and the number of photons scattered by the light (absorbance at 600nm) was proportional to the mass of cells in the sample. The resulting growth curve plot was found:

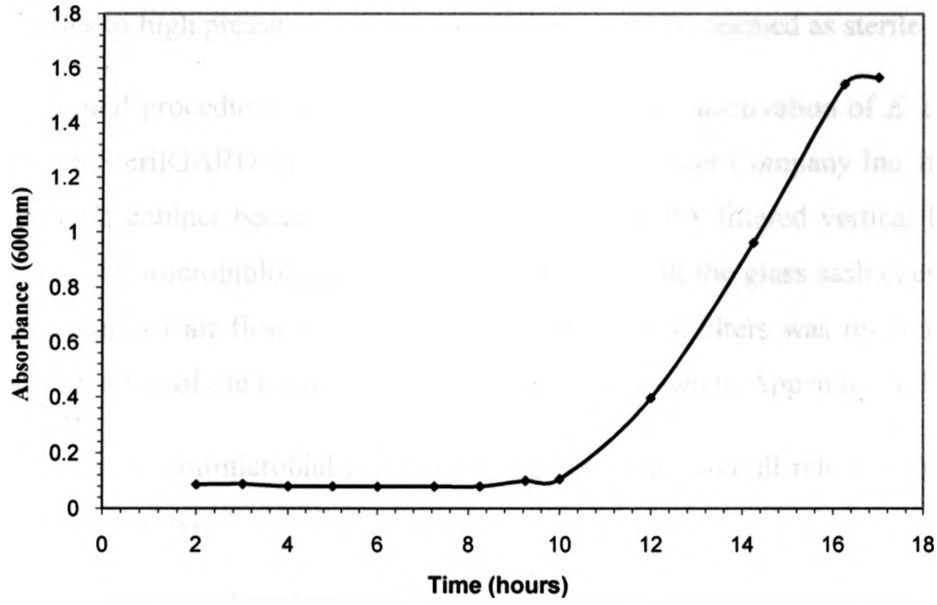

Figure 3.13: Growth curve of E. coli bacteria in LB medium determined from Cary Win 50 UV-Vis spectrophotometer readings at 600nm

Therefore inoculation of the test microorganism always took place 16 hours before starting any inactivation experiments with powder coatings. Similar experimentation in literature also uses the 16 hours inoculation period for *E. coli* (Pal A, Min X, Yu LE, Pehkonen SO, Ray M B, 2005).

3.4.2 Experimentation

ASTM E 2180-01

American Standard Testing Method (ASTM) E 2180-01 *Standard test method for determining the activity of incorporated antimicrobial agent(s) in polymeric or hydrophobic materials* was followed to obtain results for all antimicrobial powder coatings produced. All required materials and equipment to be used was prepared and sterilized days before the experiment was planned to take place. Sterilization was completed using an AMSCO 2041 Autoclave. An image of the autoclave used for sterilization of materials is included Appendix A, Figure 7.13.

The autoclave device was used to sterilize all materials and equipment that were used for or in direct contact with bacteria or bacterial suspensions. By subjecting solutions and supplies to high pressure steam at 121°C they could be deemed as sterile.

All related procedures and methods dealing with the inactivation of *E. coli* were carried out in a SterilGARD Biological Safety Cabinet by Baker Company Inc. It was considered a class II cabinet because it used re-circulated HEPA filtered vertical laminar air flow within. All microbiological work was conducted with the glass sash open 20-25 cm. The component of air flow exhausted through the HEPA filters was re-circulated inside the room. Picture of the hood used for all research is shown in Appendix A, Figure 7.14.

The detailed antimicrobial efficacy testing procedure and all relevant materials used are described below:

1. Sterile swab or loop was used to obtain bacterial culture of *E. coli* (ATCC 10798) from LB agar stock culture plates (stored at 3-5°C). A loop full of bacteria was

added to test tube of 10 mL sterile LB medium broth, covered with sterile foam stopper and inoculated for 16 hours in Stuart Orbital Incubator at 37°C. This step was completed the day before every experiment was scheduled to occur. The incubator device is shown in Appendix A, Figure 7.15.

It should be noted that the bacterial broth culture (inoculums) incubated overnight was enumerated prior to beginning any antibacterial testing and methods were adjusted to obtain the required amount of cells/mL of broth for each inoculation (~$100x10^7$ cells/mL).

2. Agar slurry was prepared by dissolving 0.85 g NaCl and 0.3 g granulated dry agar (agar-agar) in 100 mL of deionized water. The agar slurry was then sterilized by autoclaving for 15 minutes then was kept at equilibrium on a hot plate at 40 +/- 2°C.
3. The 3.0 cm · 3.0 cm specimens of each antimicrobial powder that were coated prior were gathered and placed into sterile petri dishes (15 mm · 100 mm): 3 coated chips per petri dish and 6 petri dishes total yielding 18 chips per sample. A sterile cotton swab was then dipped into sterile 0.85% saline solution to pre wet each test sample (powder coated chip). This aided in dispersing agar slurry evenly on the surface.
4. 1.0 mL of the inoculated culture, from step 1, was placed into the 100 mL agar slurry, equilibrated at 40 +/- 2°C.
5. 1.0 mL of inoculated agar slurry was pipetted evenly onto each chip sample. Application was slow and gentle at a low angle of incidence relative to the sample. Depth of the deposited film was no more than 1 mm. Once complete the contact time begun and was noted.
6. The petri dishes were then covered with their lid and edges closed with strands of pre-cut parafilm pieces. All samples except for 1 petri dish - "0 hour" (3 chip samples), were placed into the incubator at 37°C. Low humidity caused drying of the agar slurry inoculums on samples during exhibition trial runs, therefore open reservoirs of water were placed inside for all experimental runs thereafter.
7. Following the specific pre-determined contact times, the samples were removed from the incubator and aseptically transferred from the petri dishes into sterile 120

mL specimen cups (1 chip per cup). Each cup contained a sufficient volume of Dey/Engley (D/E) neutralizing broth to form an initial 1:10 dilution of the original inoculums slurry from each chip. D/E neutralization broth was used because it has the ability to neutralize antimicrobial chemicals. The next step includes extensive integration between antimicrobial surface and inoculums and so the prevention of any further inactivation was required.

8. Specimen cups containing the recovered test samples were then placed into a non-cavitating sonic bath and sonicated for 1 minute. Sonication was followed by 1 minute of vigorous mechanical vortexing. This step facilitated the complete release of the agar slurry from the sample. Release efficiency was tested for at random instances by imprint culture on eosin methylene blue (EMB) agar, but no colony forming units were present after incubation (results not presented).
9. Three serial dilutions were made from each specimen cup where 1 mL was pipette into sterile test tubes containing 9 mL of sterile 0.85% NaCl solution. Vortex was used to homogenously disperse the cells before each dilution.
10. 0.1 mL was pipette from each end dilution and spread onto 3 separate EMB agar plates using a sterile spread stick. This worked out to 9 EMB agar plates per sample contact time (n=9) and at least 63 EMB agar plates per one powder tested.
11. EMB agar plates were then covered with their lid, edges wrapped with parafilm strips and placed into the incubator at 37°C for 24 – 48 hours.
12. The following days the plates were studied, analyzed and colony forming units counted accordingly and recorded. The enumeration of bacteria on each plate corresponded to 10^7 colony forming units, as the end dilution spread onto each plate was 10^{-7} cells.

An "initial" determination of cells produced by each overnight inoculum was necessary just in case there was an error with the "0 hour" plate results. Therefore at the beginning of the experiment, 6 serial dilutions were made by transfer of 1 mL inoculums to sterile test tubes containing sterile 9 mL NaCl solution; this was done 3 times for accuracy of data. Vortex method was used to ensure homogeneous mixture of cells before each

dilution. 0.1 mL of the three separate end dilutions was plated onto 3 EMB agar plates to make 9 plates of 10^7 colony forming units.

A schematic to help understand the above method for one sample at one contact time is shown below.

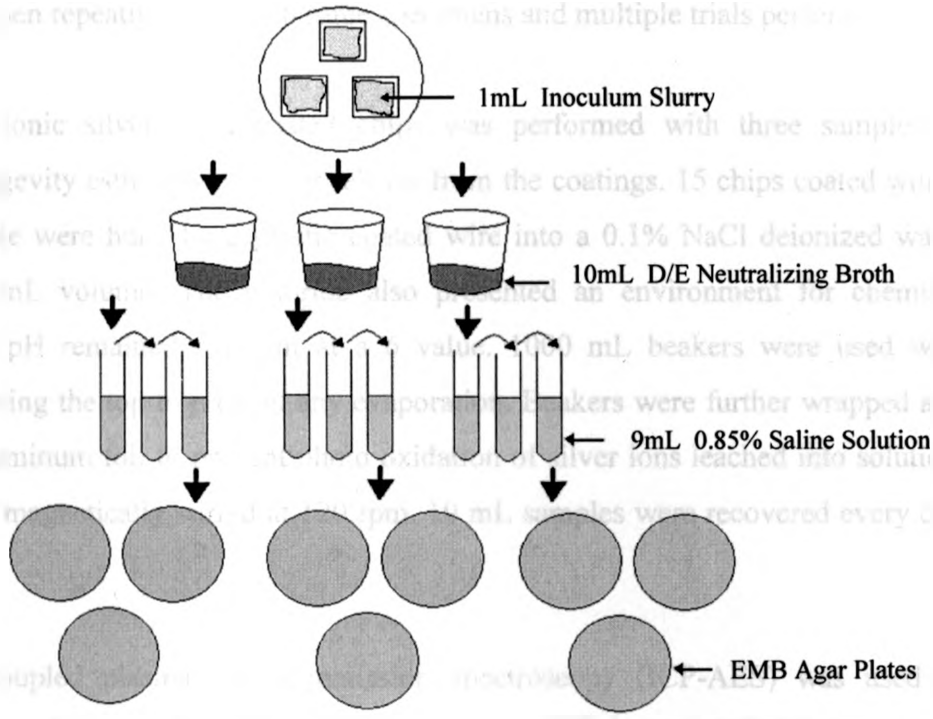

Figure 3.14: Schematic of *E. coli* inactivation procedure for one surface sample and *n*th contact time

Repeatability, Durability, Leaching

Repeatability of the antimicrobial testing procedure was carried forth with certain antimicrobial powders. New aluminum chips were cut and sprayed and a new test of the antimicrobial efficacy of that powder completed. This would result in two sets of data for the same powder under identical conditions.

Durability testing was performed by washing the surfaces of coated specimens with Sunlight Dishwashing Detergent. After conducting the first antimicrobial test, the same chips were washed in soapy deionized water with nitrile laboratory gloves. The chips for that sample would then be wiped dry with a towel. This durability test followed that of the generalized suggestion from ASTM E 2180 and also correlated procedures done in literature. Cowan MM, Abshire KZ, Houk SL, Evans AM., (2003), performed durability tests of antimicrobial surfaces against *E. coli* by washing the surfaces with towels or test tube brushes then repeating tests with same specimens and multiple trials performed.

Leaching of ionic silver from coated chips was performed with three samples to determine longevity estimates of silver release from the coatings. 15 chips coated with a specific sample were hung by a plastic coated wire into a 0.1% NaCl deionized water bath of 800 mL volume. The chloride also presented an environment for chemical damage. The pH remained constant at a 6 value. 1000 mL beakers were used with parafilm covering the top to prevent any evaporation. Beakers were further wrapped and covered in aluminum foil to prevent photo oxidation of silver ions leached into solution. Beakers were magnetically stirred at 120 rpm. 10 mL samples were recovered every day for 168 hours.

Inductively coupled plasma atomic emission spectroscopy (ICP-AES) was used to analyze each sample recovered from the leaching tests. ICP detects trace metals and can find concentrations of elements in a sample. Excited ions emit radiation at wavelengths distinctive of a certain element. The intensity of the wavelength produces the concentration of element in the sample tested. Results were further processed from ICP in order to account for the 10 mL samples recovered from the water baths everyday and replaced with 10 mL 0.1% saline de-ionized water. The following equation accounted for the concentration changes:

$C_n = C_n V_T + V_R (C_{n-1} + C_{n-2} \ldots + C_{n-6})$

Where C = concentration measured by ICP in ppm,

N = the measurement after day 1, 2, 3, 4, 5, 6, or 7,

V_T = total volume in beaker,

V_R = volume recovered from solution.

(Note that the reading taken after 24 hours (C_1) would not change).

4 ANALYSES OF RESULTS

4.1 Characterization of Powder Additives

After performing EDX on all of the antimicrobial additives produced we were able to allocate one reliable value to each sample defined as the percentage of antimicrobial metal contained within each additive powder. These results are very significant to the project as they determine how much additive powder is mixed with the polyester. These results were listed earlier in Table 3.4 and 3.6.

4.1.1 Chabazite

Table 3.5 showed the content of the chabazite before and after treatment with 0.05 and 0.01 M silver nitrate, 0.05 M copper (II) nitrate and 0.05 M zinc (II) nitrate solutions. Sodium ion was completely diminished in all ion exchange experiments. Potassium showed significant declines with the samples possessing most exchange with the antimicrobial salt solutions after sodium. Calcium content did not noticeably change. In addition to sodium and potassium, iron content decreased significantly for higher loadings indicating that Fe may play a role in ion-exchange processes, increasing loading of silver ion.

Selectivity of Ag, Zn and Cu ions in natural zeolite during ion exchange follows that order of listed metals. Silver exchange into natural zeolite is more favorable then zinc or copper (Top A and Ulku S, 2004), and this is precisely what was found in EDX analysis after ion exchange with chabazite at 0.05 M with the corresponding salt solutions. Cations react with water molecules forming clusters (hydrated spheres) and characteristics of these clusters depend on size and charge of the cation. Simply put, the hydrated radius is inversely proportional to cation radius and divalent cations usually have a higher hydrated radius than monovalent cations (Palmer and Gunter, 2001). Furthermore, small cations like Ca^{2+} cannot move out of zeolite channels due to their

higher hydrated radii, while Na^+ and K^+ would have a much easier time (Top A and Ulku S, 2004). Lastly, high Si/Al ratios like chabazite and clinoptilolite natural zeolites create low anionic fields that present good selectivity towards cations of lower charge, monovalent silver, and poor selectivity towards higher charged cations, like divalent copper or zinc (Langella A, Pansini M, Cappelletti P, de Gennaro B, de Gennaro M, Colella, C, 2000).

From the XRPD analysis shown in Appendix D there were only slight changes to the crystallinity of the zeolite when mixed with 0.05 M silver nitrate and copper (II) nitrate compared to the 0.01 M silver nitrate treated zeolite sample. By observing the diffraction patterns (peaks) of all samples, negligible differences may be seen when relating them back to the blank control chabazite or lower loaded samples. Increased loading of chabazite with more concentrated salt solutions may have forced some physical absorption and or adsorption on the surface of the zeolite. A small portion of these loosely bound silver ions may have even changed from monovalent to zerovalent form during the ion exchange process (Inoue and Kanzaki, 1997), but observing XRPD patterns it is difficult to impart significant differences between loadings of zeolites; high and low loadings.

4.1.2 Silica Glass

Sol-Gel Porosity and Surface Area

Sol-gel production includes a critical drying step that directly affects properties of the final solid material. After necessary ageing of the gel, water and alcohol groups are removed from the gel with potential to create solids of extremely high surface area and high porosity; this was the goal of the silica glass samples. Theoretical thermodynamic phase boundary diagrams help to understand the chemistry during the drying stage of the sol-gel.

When considering a simple phase diagram it is known that when a substance evaporates and crosses the boundary from liquid to gas the volume of the substance decreases. As this happens, surface tension at the solid-liquid interface collapses the structure that the liquid is attached to. This means that the delicate structure of the sol-gel before drying may be broken by surface tension if not dried appropriately. This may be resolved by supercritical drying or freeze drying like completed in this research; high temperature and high pressure (supercritical) or low temperature and low pressure (freeze drying) will bring the sample from liquid to gas without crossing the liquid-gas boundary.

Freeze drying is much like supercritical drying. However unlike supercritical drying, freeze drying brings the sample from liquid phase to solid phase to gas phase and this may still cause structure collapse if the sample is too delicate. Potential collapse may still occur by freeze drying because of the transition to solid phase which stresses the structure as water expands and forms a solid. The results listed in Table 3.10 show that heat at normal pressure, normal temperature and low pressure, and freeze drying (low temperature, low pressure) all relate to a collapse of the sol-gel structure. However at normal temperature and pressure and zero aging of the gel, we were able to produce a microporous structure with large surface area. This may be directly related to the aging time of the gel. Since it was forced dried over night by exposing most of the liquid surface area to air it is possible that there was not enough time to create significant siloxane bonds throughout the gel framework and collapse of particles was not possible.

BET characterization for all silica gel additives determined failure for production of microporous structures with high surface area when drying the sol-gel at 200°C and 1013.25mbar, 100°C and 1013.25mbar, 20°C and 215mbar, and even freeze dried at -50°C and 215mbar. Microporous structures with surface area over $300m^2/g$ were observed without extended aging at 20°C and 1013.25mbar drying conditions. These results are summarized in Table 3.10 like previously mentioned; however isotherm plots are shown in Appendix C where contrasts may be made to IUPAC standard isotherm plots. These plots were the basis for determining porosities of the different silica gel samples.

4.2 Inactivation of *Escherichia coli* and Survival Ratios

Survival ratio (N_t / N_0) is plotted with respect to contact time in all figures related to inactivation of *Escherichia coli*. N_t is the number of viable colony forming units of *Escherichia coli* at time t (i.e., after 1, 2, 4, 6 or 24 hours of contact) whereas N_0 is the viable colony count at "0 hour" or time t = 0 hour. The N_0 average value is very significant with all experiments because its accuracy and precision dictates how reliable the survival ratio results will be. This is especially important when comparisons of different experiments are being made. Table 7.1 in Appendix E lists the N_0 data used for all testing and graphing purposes. The standard deviation shown in this table for each coating measures the variability or dispersion of N_0 counts. Low standard deviations indicate reliable averages of N_0 data for that sample and accurate correspondence of survival ratios, since each N_t produced is divided by the same average N_0. Low standard deviations produce stronger survival ratio data. Again, the survival ratios were calculated by normalizing the average N_t colony count by the average N_0.

Vertical error bars produced for each survival ratio represent the standard deviation between colony forming units of that specific N_t. Like previously mentioned each N_t for each sample corresponds to counting and averaging of 9 EMB agar plates. EMB plates showed glistening black/green colonies of *E. coli* as the gram negative bacterium`s cell wall adsorbed the methylene blue dye, thus providing easy identification of gram negative bacteria only.

All related graphs plotted using the survival ratios have a start value of 1 which corresponds to 100% survival of bacteria at hour 0. When a survival ratio of 0 is observed with a zero standard deviation this means that there were 0 CFU counted on all plates for that contact time at a 10^{-7} dilution. When instances like this are observed it means that we can imply a 99% reduction in bacteria population from the initial population. This is because dilutions of 10^{-6}, 10^{-5}, 10^{-4}, etc were not spread plated and so it was possible that there were still decimal bacterial concentrations remaining in those dilutions. This was in

fact confirmed for a few samples in the latter part of research experiments but data will not be presented.

4.3 Repeatability

In this section, repeatability experimentation shows the degree of precision of work conducted in this research, and brings to light the margin of error associated between runs of the procedure ASTM E2180. A silver concentration of 0.5% weight in the powder coatings was chosen to conduct these tests for three of the antimicrobial additives produced, and one of the industrial powders obtained. (A) and (B) found in the legends of the graphs below are both new and completely separate studies using the same powder additive, re-sprayed onto new substrates and re-tested for antimicrobial efficacy. As they are both fresh surfaces, a comparison of their antimicrobial test results can be made and should theoretically be equal; in a perfect world. Figures 4.1 to 4.4 show the survival ratios against time for the repeatability experiments (data not shown for 24 hour contact time where $N_t/N_0 = 0$ and STDEV=0):

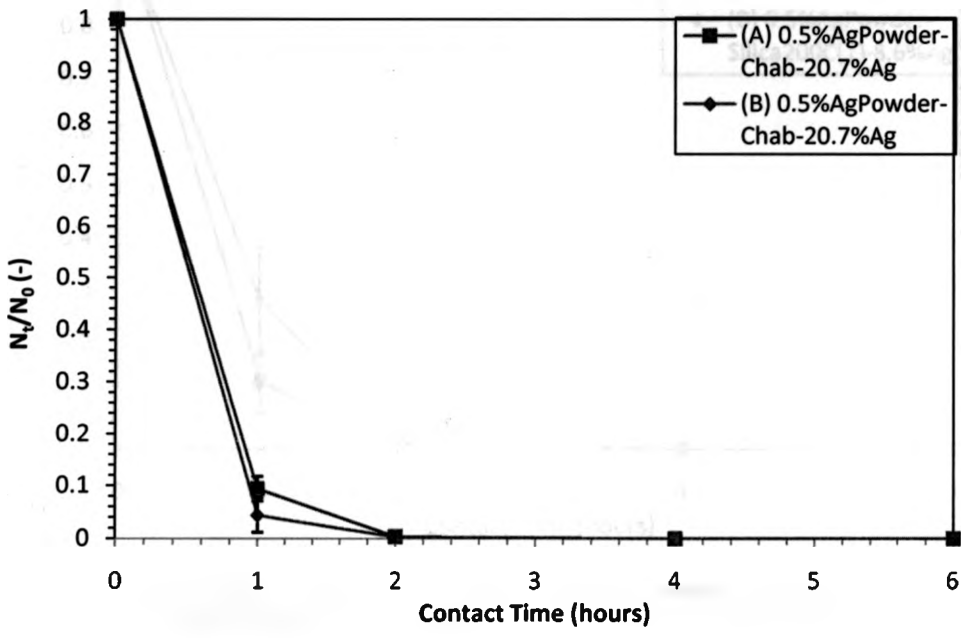

Figure 4.1: Repeatability tests using 0.5%Ag weight in Powder Coatings by chab20.7%Ag additive (24 hr contact time $N_t/N_0 = 0$; STDEV=0)

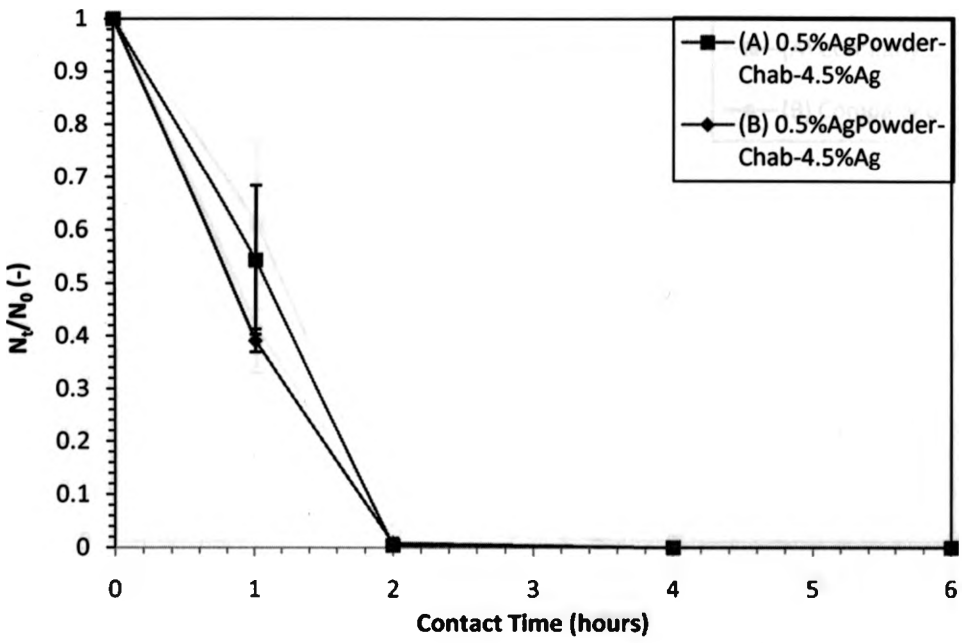

Figure 4.2: Repeatability tests using 0.5%Ag weight in Powder Coatings by chab4.5%Ag additive (24 hr contact time N_t/N_0= 0; STDEV=0)

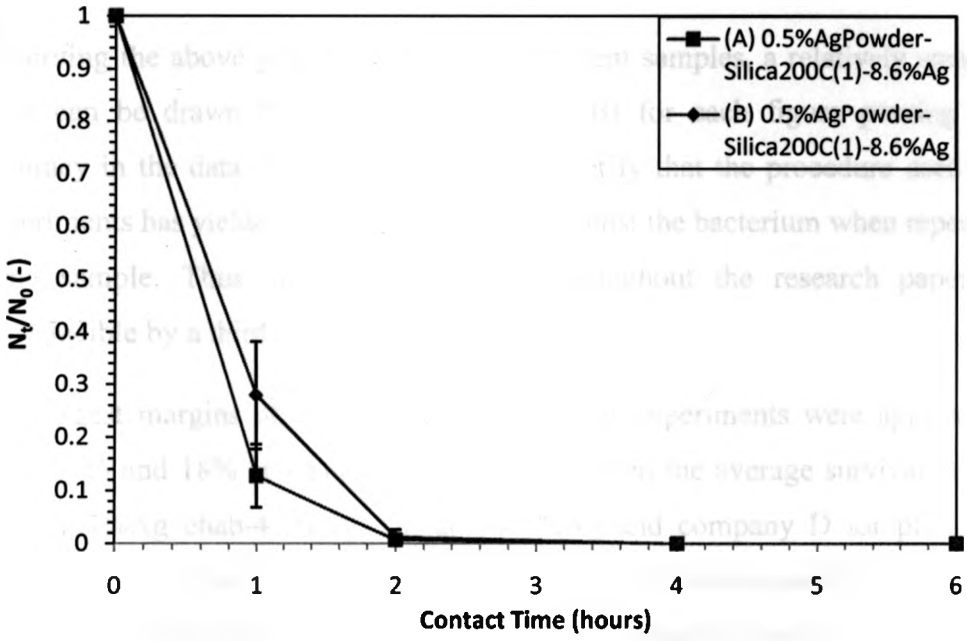

Figure 4.3: Repeatability tests using 0.5%Ag weight in Powder Coatings by Silica200C(1)-8.6%Ag additive (24 hr contact time N_t/N_0= 0; STDEV=0)

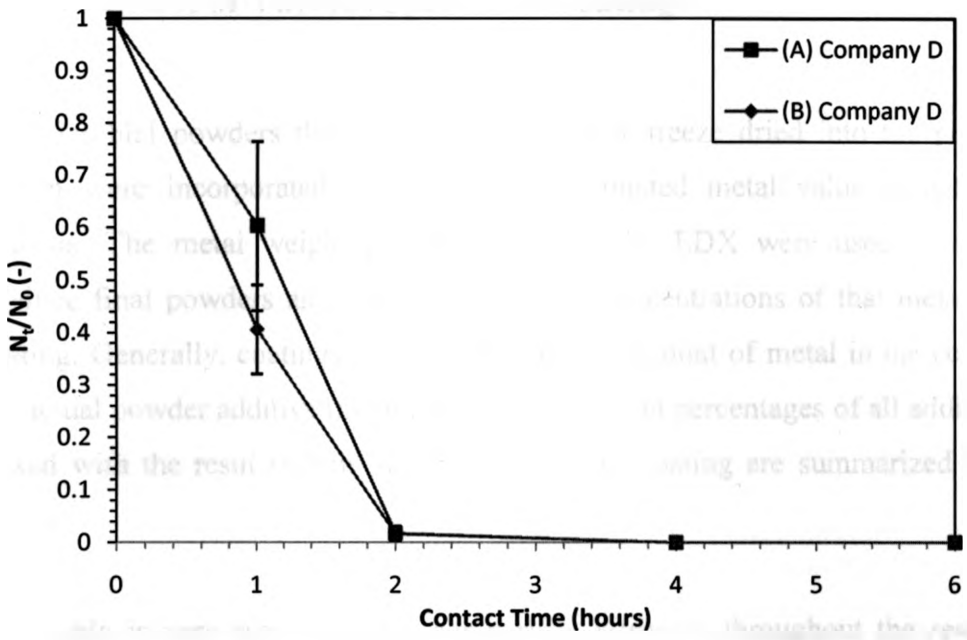

Figure 4.4: Repeatability tests using Powder Coatings by Company D (24 hr contact time N_t/N_0= 0; STDEV=0)

Observing the above graphs, for the four different samples, a relatively small margin of error can be drawn between tests (A) and (B) for each figure proving quality and accuracy in the data. In all cases the results verify that the procedure used for all such experiments has yielded very similar effects against the bacterium when repeated with the same sample. Thus the obtained values throughout the research paper should be reproducible by a third party.

The largest margins of error noticed in the four experiments were approximately 4%, 13%, 12% and 18% at 1 hour contact time between the average survival ratios with the chab-20.7%Ag chab-4.5%Ag, silica(1)-8.6%Ag and company D samples respectively. Hour 2 contact times included negligent decimal error values and hours 6 – 24 produced no error. It should be noted however, that when comparing repeatability runs (A) and (B) for each sample that the standard deviations between average survival ratios at 1 hour contact time overlapped, never falling out of respectable range.

4.4 Effect of Various Species in Coatings

Antimicrobial powders that were dry blended or freeze dried into the polyester resin system were incorporated based on their estimated metal value assigned by EDX analysis. The metal weight percentages found by EDX were used to calculate and produce final powders and coatings at certain concentrations of that metal in the final coating. Generally, coatings were leveled by the amount of metal in the coating, not by the actual powder additive in the coating. The weight percentages of all additive powders mixed with the resin system in the final powder coating are summarized in Table 4.1 below.

This table is very significant for comparison purposes throughout the research paper. Essentially, although the coatings are leveled on fair grounds by the amount of active metal in the coatings by weight percentages, the additive weight percent or volume of a particular additive will be different when compared against a different additive loaded with a different percentage of metal within. For example, at 0.5% active metal in powder coatings, the higher loaded chabazite (loaded at 20.7% Ag) additive is found at 2.4% in the coating while a lower loaded chabazite (loaded at 4.5% Ag) is found at 11.2% weight in the coating. Thus, differences in antimicrobial efficacies may be attributed to the variances of additive powder percentages, and not only to weight percentages of active material.

Table 4.1: Theoretical Antimicrobial Materials and their comparison of active material to additive entirety in the final powder coatings based on EDX analysis

Antimicrobial Additive Sample Description	Active Metal Concentration in final powder (weight %)	Additive Sample Concentration in final powder (weight %)
Chab-20.7% Ag	1	4.8
	0.5	2.416
	0.1	0.483
	0.05	0.2416
	0.03	0.15
	0.005	0.0242
Chab-4.5% Ag	1	22.24
	0.5	11.12
	0.1	2.223
Chab-3.4% Ag	0.05	1.46
	0.005	0.15
	0.0017	0.05
Silica200C(1)- 8.6% Ag	1	11.58
	0.5	5.79
	0.1	1.159
	0.05	0.579
Chab-13.0% Cu	1	7.46
Chab-4.5% Zn	1	25.3
Nanoparticles-31% Ag Metal	0.5	1.61
	0.15	0.5
	0.05	0.161
	0.005	0.0161
SynZ-A- 2.2% Ag	0.1	4.566
No Carrier Ag	0.1	0.1
Tollens Metallic Ag	2	2
	0.1	0.1
CNT- 77.2% Ag	1	0.013
Silica-1013.25mbar- 20C(4)- 3.6% Ag	0.1	2.77
	0.05	1.39
	0.005	0.139
Silica-215mbar- -50C(6)- 2.2% Ag	0.1	4.62
	0.05	2.31
	0.005	0.231
Company P	unknown	unknown
Company D - Ag	0.505	unknown

4.4.1 Control Test Samples

Producing a solid ground for control or blank coatings was one of the first experimental runs performed. Specimen chips were coated with polyester TGIC resin only, producing a smooth clear finish on the surface. Three separate runs were conducted by three separate lines of substrates with coatings including only polyester TGIC. Figure 4.5 displays the control test results.

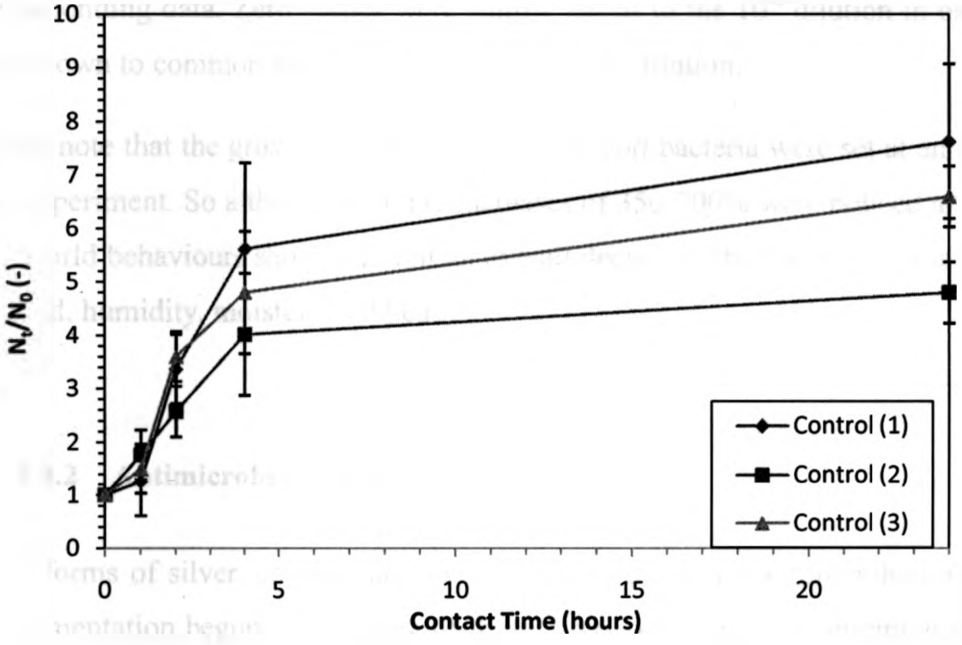

Figure 4.5: Control tests with Blank Polyester TGIC Clear Coating

The above data begins at a ratio of 1 because 100 percent of the bacteria are alive at time 0 hours. Observing Figure 4.5 there is approximately 50%, 200%, 350% and 550% average increases in the *Escherichia coli* population after 1, 2, 4 and 24 hours respectively; with wide ranging standard deviations for each contact time. These large increases for control samples convey zero bactericidal effectiveness against the test microorganism, as what was expected.

In microbiology it is unruly to conduct colony counts from spread plates over 300 CFU. Therefore to help constitute colony counts over 300, counts were conducted using graph paper by dividing the plates into four sections, counting the colonies in each quadrant and adding them together. This was performed for any plates showing over 300 colonies for control sample (1). For control samples (2) and (3) however, extra dilutions of the bacterial solutions was carried out for test times after 4 hours contact and the 10^{-8} dilution would be plated. This dilution was used and counted in control samples (2) and (3) ensuring the counts were within acceptable range, below 300 CFU, when presenting the corresponding data. Zero values were simply added to the 10^{-8} dilution in order to bring them down to common grounds of all counts at 10^{-7} dilution.

Please note that the growth conditions for the *E. coli* bacteria were set at an optimum for this experiment. So although extreme increases of 350-700% were noticed after 24 hours, real world behaviours should exhibit an overall decline in the bacterial concentration with no food, humidity, moisture and heat.

4.4.2 Antimicrobial Agents

Ionic forms of silver, copper and zinc are proven dominant antimicrobial agents. Initial experimentation begun with testing of these three ionic forms to determine which one(s) would prove ideal for the inactivation of the microorganism under study and the testing procedure carried forth. In general, 1% by weight of ionic metal species in the final coating shows a toxicity sequence of $Ag^{+} > Zn^{2+} > Cu^{2+}$ which is displayed in Figure 4.6. 1% weight corresponds to the same concentration of silver, zinc or copper in the coatings, which is dependent on the additive percent into the resin system which was shown prior in Table 4.1.

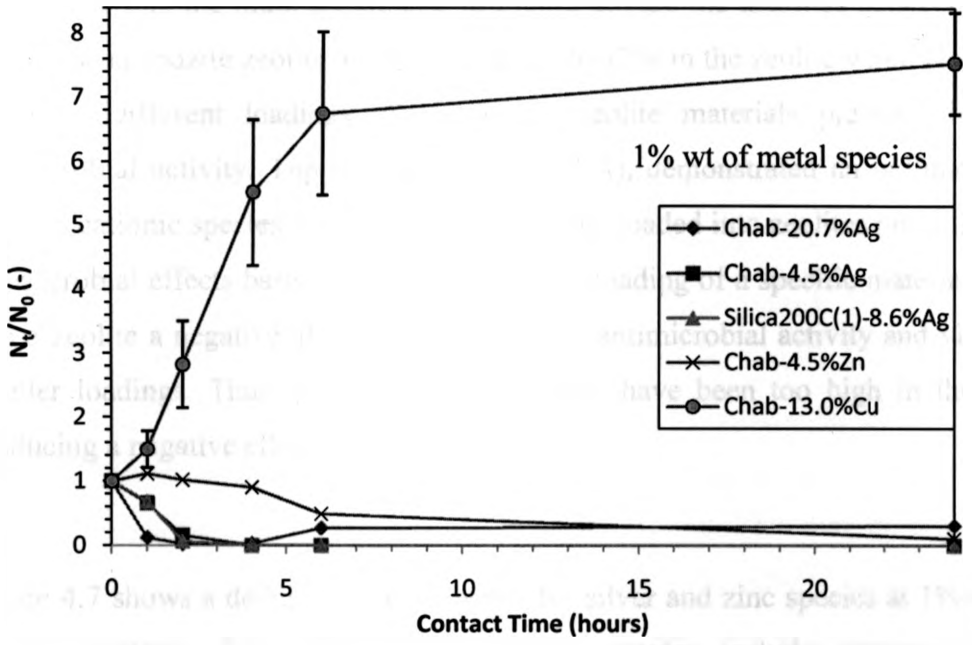

Figure 4.6: *E. coli* inactivation at 1% by weight Ag, Zn or Cu in powder coatings

Copper was the least toxic of the metal species tested in Figure 4.6 above. Tested samples show that when 1% weight of copper is included into the coating, no antibacterial affect against *E. coli* is noticed and result is comparable to the control samples. Copper is a proven antifungal agent and its antibacterial properties are not significant in this experiment. This may be due to the slow release of copper from the zeolite matrix and resulting low concentrations to the bacteria may not be toxic enough for it to create any antibacterial effect. Copper is a constituent of many bacterial enzymes involved in electron transfer, oxygenation and oxidation processes (Bhattacharya PK, 2004) so if the exposed concentration is not high enough to the bacteria then inhibition will not result.

Top A and Ulku S, (2004), reported the superior antibacterial effects of silver loaded clinoptilolite zeolite and relatively equal and weaker antimicrobial efficacies when dealing with copper and zinc loaded zeolite against *E. coli*. Results above do not follow these findings as copper and zinc results are not comparable, however silver does show superiority over both.

Please note that the main differences in Figure 4.6 are the loadings between copper and zinc in the chabazite zeolite. Copper is loaded to 13% in the zeolite while zinc was found at 4.5%. Different loadings of species in zeolite materials present differences in antimicrobial activity. Top A and Ulku S, (2004), demonstrated an optimal loading of biocidal cationic species for silver, copper or zinc loaded into zeolites providing different antimicrobial effects based on the loadings. If a loading of a specific material is too high into a zeolite a negative affect is followed with antimicrobial activity and vice versa for smaller loadings. Thus the copper loading may have been too high in the chabazite, producing a negative effect.

Figure 4.7 shows a detailed view of results for silver and zinc species at 1% weight into powder coatings. It generally shows silver samples include superior antibacterial properties by outperforming the zinc sample:

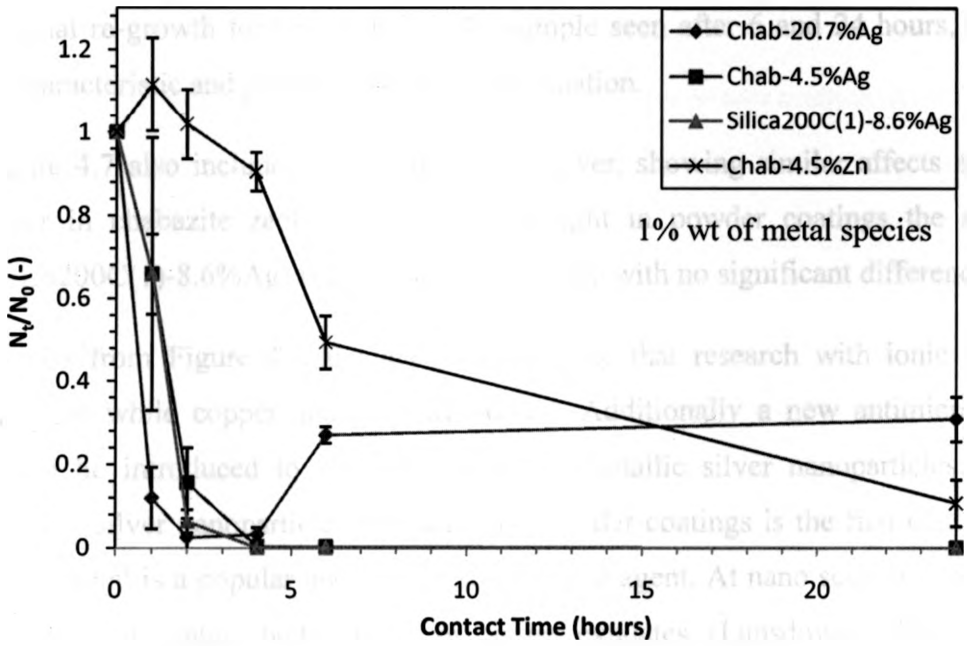

Figure 4.7: *E. coli* inactivation at 1% by weight Ag or Zn in powder coatings

After 1 and 2 hours of contact the zinc species shows increases in survival ratio averages of 10% and 2% respectively from the original inoculums of bacteria. At these times of 1 and 2 hours the silver species show significant reductions of bacterial population almost to 99%. After 4 hours contact the zinc still has not reduced bacterial populations to the point of silver after 1 hour contact.

As a biocidal ingredient against bacteria, Ag^{+} is 1000 time more toxic then a Zn^{2+} (Dong F, Li G, Sun Z, Shen Gang, Feng Q, Dai Q, 2005), and the results from the above figure correlate this. Zinc is an essential element and occurs in several enzymes (Bhattacharya PK, 2005) therefore if the concentration is not high enough at the surface interface with bacteria, similar to copper, the toxicity result is affected. This may be attributed to the slow release from the zeolite matrix and the fact that the loading of zinc species into the zeolite was not at an optimum level.

At 1% Ag in powder coatings, the chabazite zeolite loaded with a high concentration of silver works faster than the lower loaded chabazite of silver. Although, there was some unusual re-growth for the chab-20%Ag sample seen after 6 and 24 hours, this result is uncharacteristic and probably due to contamination.

Figure 4.7 also includes silica vehicle for silver, showing similar affects as those with silver in chabazite zeolite. At 1% Ag weight in powder coatings the silica carrier (silica200C(1)-8.6%Ag) is comparable to zeolite with no significant differences yet.

Results from Figure 4.6 and 4.7 plots indicate that research with ionic silver would continue while copper and zinc would not. Additionally a new antimicrobial species would be introduced to powder coatings – metallic silver nanoparticles. Introducing metallic silver nanoparticles into ultrafine powder coatings is the first of its kind. Nano silver metal is a popular upcoming antimicrobial agent. At nano scale it can ionize in the presence of water, body fluids or tissue exudates (Lansdown, 2006). Due to its antimicrobial potential, and proven success in the next experiment, its use would be continued.

Figure 4.8 shows 0.5% Ag by weight of ionic and metallic silver species in powder coatings and the inactivation effects against *E. coli* (data not shown for 24 hr contact time N_t/N_0= 0 and STDEV=0).

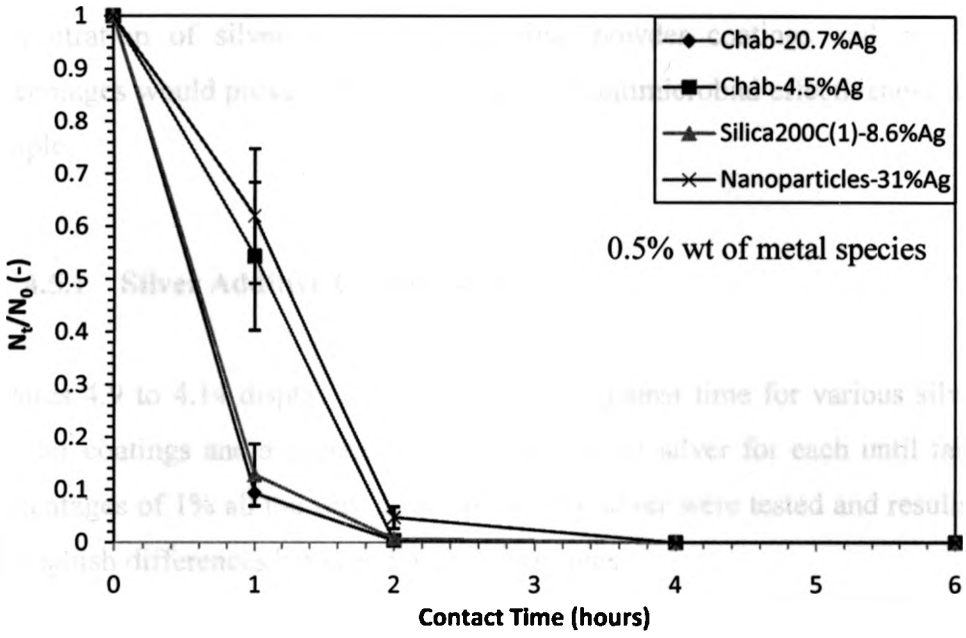

Figure 4.8: *E. coli* inactivation at 0.5% Ag species by weight in powder coatings (24 hr contact time N_t/N_0= 0; STDEV=0)

In Figure 4.8 the silver nanoparticles hold their own against the silver ion powders performing just as well as the lower loaded chabazite sample. However the silica carrier with ionic silver and higher loaded silver chabazite sample outperform the silver nanoparticles at 1 hour contact by approximately 50% improved reduction.

In this section of experimentation it was found that cationic silver and metallic silver nanoparticles are superior antimicrobial species over cationic zinc and copper. The slow release of copper and/or zinc ions from zeolite was due to size and charge of the cation, leading to unsatisfactory affects unto *E. coli*. Cations react with water molecules forming hydrated clusters where the hydrated radius is inversely proportional to cation radius. Since divalent cations have a higher hydrated radius then monovalent cations, the Cu^{2+}, Zn^{2+} have a harder time exchanging in and out of zeolite cages, yielding slow release. Consequently, the working silver species only would be tested further in this paper.

4.5 Effect of Silver Weight Percentages in Coatings

Samples including cationic silver and metallic silver nanoparticles have already been shown to create great antibacterial effects as powder coatings against *E. coli*. The concentration of silver species in the final powder coatings and resultant additive percentages would prove to be a main factor of antimicrobial effectiveness for each silver sample.

4.5.1 Silver Additive Comparisons

Figures 4.9 to 4.14 display the survival ratios against time for various silver species in powder coatings and a decreasing concentration of silver for each until failure. Weight percentages of 1% all the way down to 0.005% silver were tested and results analyzed to distinguish differences between the silver samples.

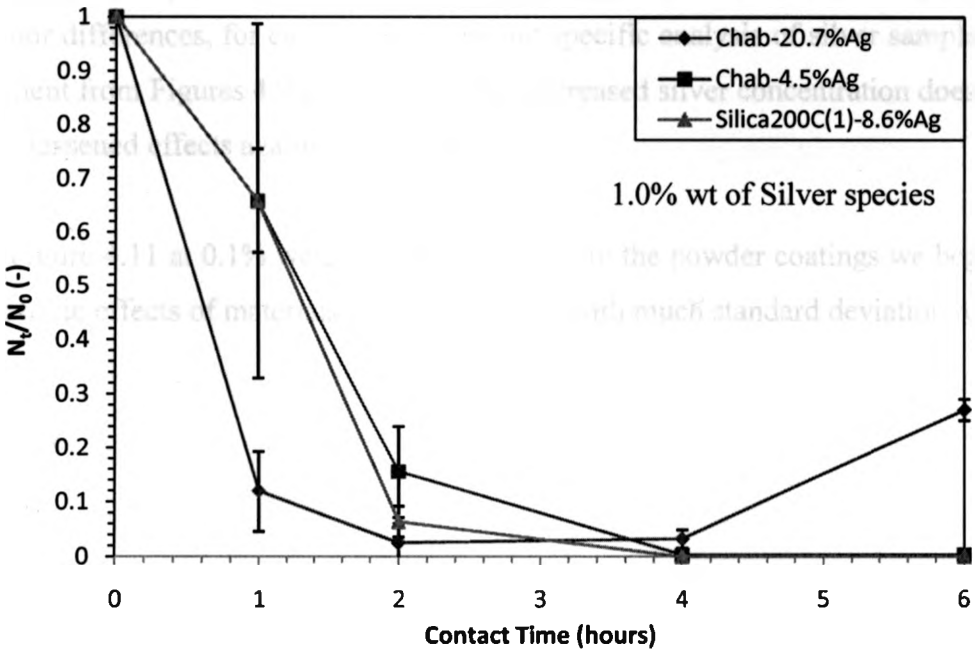

Figure 4.9: *E. coli* inactivation at 1% Ag by weight in powder coatings

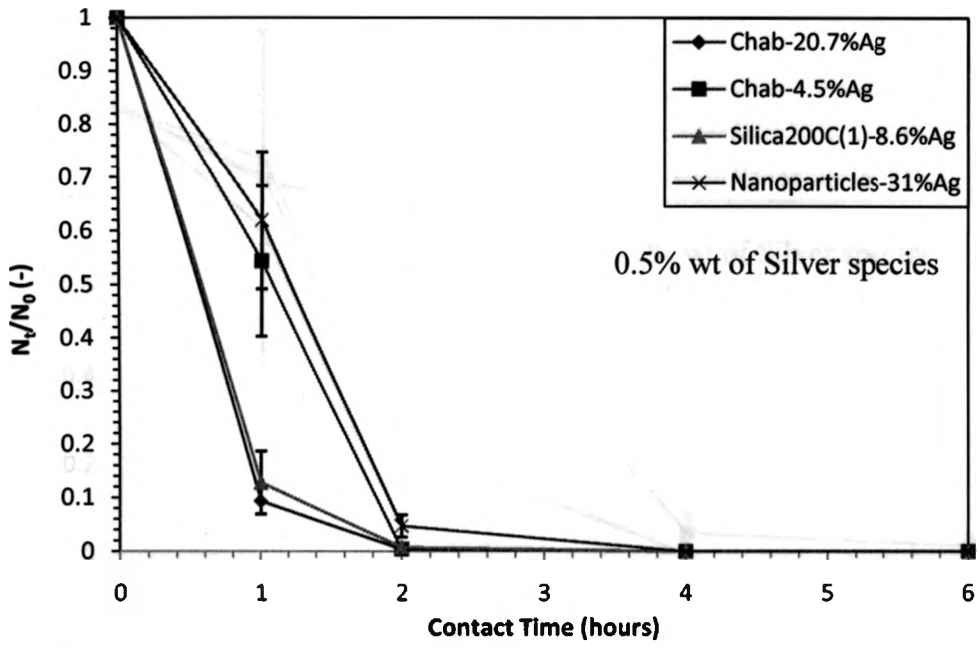

Figure 4.10: *E. coli* inactivation at 0.5% Ag by weight in powder coatings (24 hr contact time N_t/N_0= 0; STDEV=0)

Figures 4.9 and 4.10 are shown again in this section, similar to Figures 4.7 and 4.8 with minor differences, for easy comparison and specific analysis of silver samples only. It is evident from Figures 4.9 and 4.10 that the decreased silver concentration does not present any lessened effects against *E. coli* yet.

In Figure 4.11 at 0.1% weight of silver species in the powder coatings we begin to notice the toxic effects of materials start to alleviate, with much standard deviation resulting.

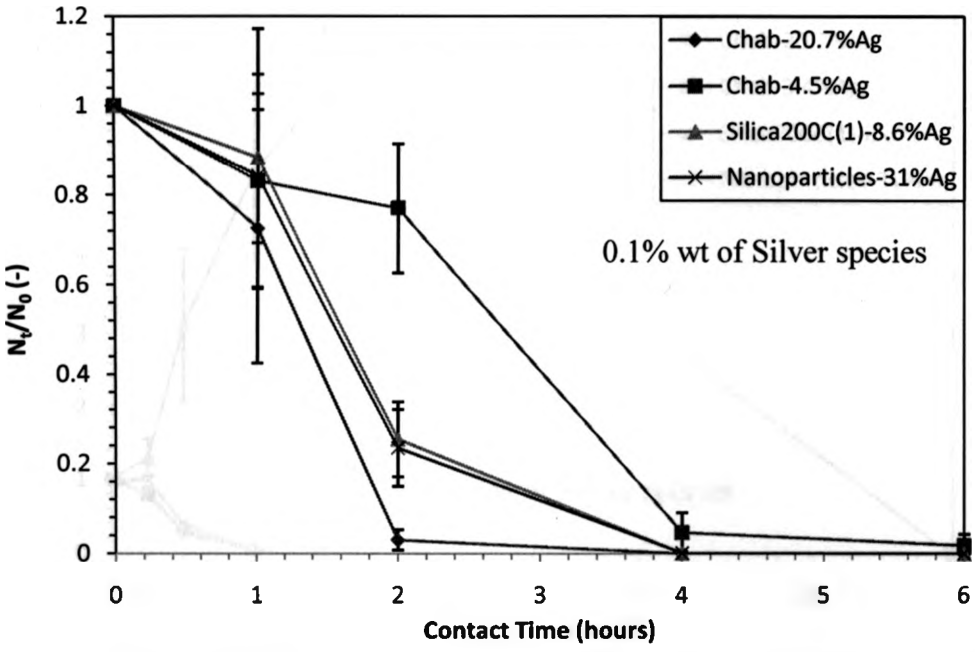

Figure 4.11: *E. coli* inactivation at 0.1% Ag by weight in powder coatings (24 hr contact time N_t/N_0= 0; STDEV=0)

Figure 4.11 above shows an obvious decrease in effectiveness against *E. coli* for all silver samples when compared to Figures 4.9 and 4.10. It is also evident that the lower loaded chabazite sample is the weakest of the silver samples in this case, and it is still being outdone by the chabazite with higher silver loading by significant values. Silver metallic nanoparticles continue to work well against the bacterium, as well as the silica carrier although both have subsided.

Figure 4.12 at 0.05% weight of silver species determines the failure level of the first antimicrobial silver based material shown below.

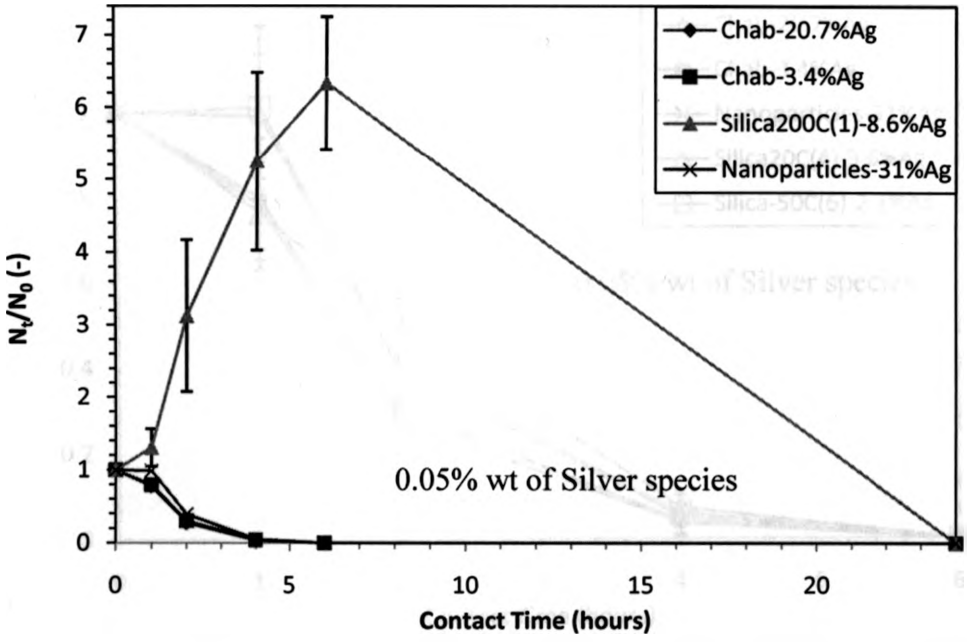

Figure 4.12: *E. coli* inactivation at 0.05% Ag by weight in powder coatings

In Figure 4.12 the silica carrier of 8.6% silver ion shows failure of biocidal effects up to 6 hours contact at 0.05% weight silver in the coating. This result may have risen from the larger particle size (28.8um) in comparison to the other antimicrobial additives; where chabazite particles are found at 3um size and nanoparticles are 1-10nm. Particle size would surely affect the efficacy at this low concentration of silver because the additive weight percent of the antimicrobial powder is very low and larger particle size decreases surface area for the biocidal agent to work. It should also be noted that the silica carrier in Figure 4.12 was dried at 200°C and from earlier characterization results, this sample shows poor surface area and porosity which might attribute to its poor antimicrobial effectiveness at low concentrations in the coating.

Figure 4.13 includes a more detailed display of Figure 4.12 and also includes results from two new silica samples at 0.05% Ag in the powder coatings. Incorporating new significantly smaller silica based carrier materials (over 50% smaller), and at lower loadings of silver ion a result matching the other additives was obtained.

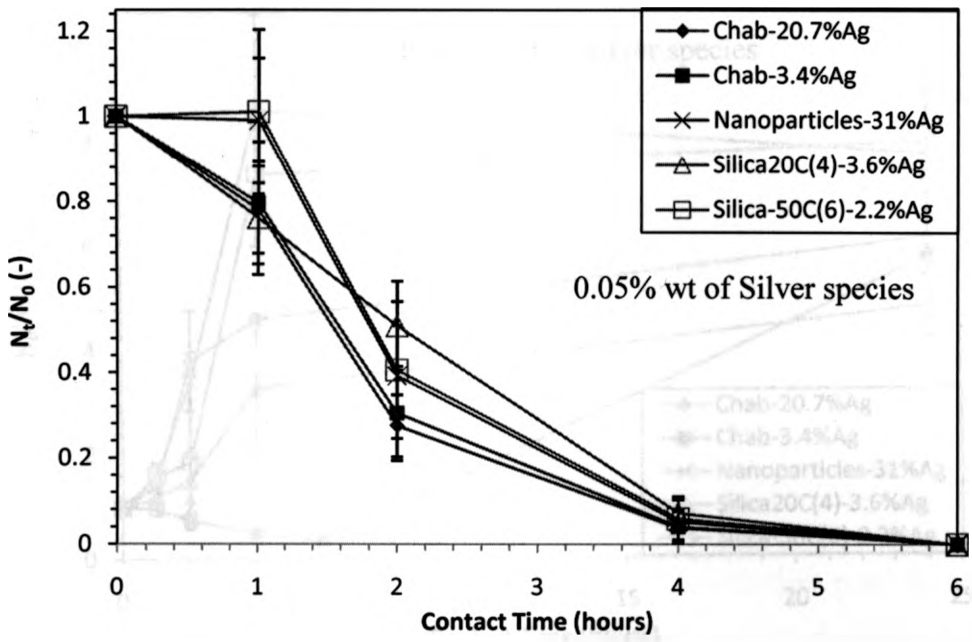

Figure 4.13: *E. coli* inactivation at 0.05% Ag by weight in powder coatings (24 hr contact time N_t/N_0= 0; STDEV=0)

Incorporating new silica samples (Silica20C(4)-3.6%Ag and Silica-50C(6)-2.2%Ag) which were dried differently and included smaller particle size and lower loadings of silver ion produced significantly better results than the previous silica additive. The analysis of silica based materials will be covered later in the paper so detailed discussion and analysis will not be covered here. Also, once again, the chabazite loaded material has outperformed the metallic silver nano particles by only marginal ranges.

Decreasing the silver concentration once again, failure of all or most silver additives was found at 0.005% Ag by weight in powder coatings. These results are shown below in Figure 4.14.

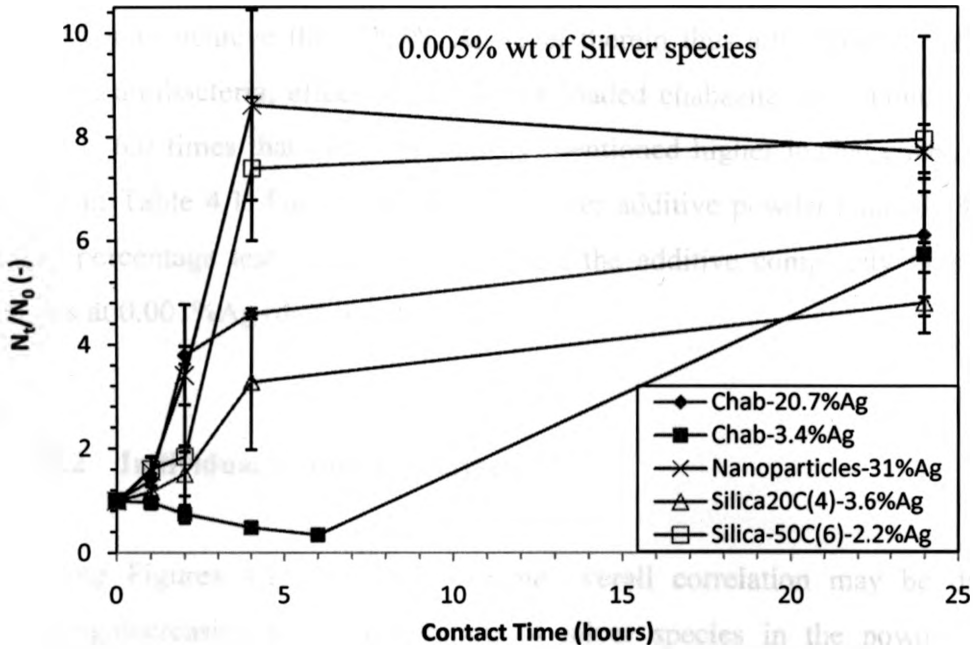

Figure 4.14: *E. coli* inactivation at 0.005% Ag by weight in powder coatings

From Figure 4.14 one may deduce from the findings that after 24 hour contact, silver additives in powder coatings fail within the range 0.05% mass Ag to 0.005% mass of Ag. By further reducing the concentration of silver in the coatings and corresponding additive percentages in the coatings we find the level of failure for all produced samples is 0.005% Ag; except for chabazite loaded at 3.4% Ag which still showed effectiveness against *E. coli* up until 6 hours contact. At some concentration between 0.05-0.005% silver, the other additives lost their efficacy to the point of comparison to the control samples.

The metallic silver nano particles may have failed during the curing process at this low concentration. Company V has stated that the melting temperature of their metallic silver nanoparticles may be as high as 180°C but recent results by the company have shown as early as 100°C melting temperatures, so at low concentrations in powder it may be possible for the material to melt and coalesce more easily then at higher concentrations.

The high loaded chabazite at 20.7%Ag corresponds to a very low additive of powder into the coating to achieve the 0.005% Ag level therein thus attributing to its failure. The continued antibacterial effects of the lower loaded chabazite correspond to an additive percent > 6.0 times that of the previously mentioned higher loaded chabazite sample - evident in Table 4.1. Please note that for silver additive powder Chab-3.4%Ag, further weight percentage tests were performed and the additive completely fails like control samples at 0.001%Ag (data not shown).

4.5.2 Individual Additive Analyses

Observing Figures 4.15 – 4.18 the same overall correlation may be drawn: when increasing/decreasing the concentration of silver species in the powder coating the resulting antimicrobial efficacy respectively increases/decreases. Silver additive powders are simply plotted individually to show individual effects of each sample. This type of comparison simply proves that the concentration of silver in the powder for each additive determines the level of antimicrobial efficacy of the coating. This is predominantly true for all levels of silver in the coatings except at higher concentrations of silver i.e. 1.0% and 0.5%. In some cases 0.5%Ag by weight in coatings presents better *E. coli* inactivation efficacies over 1.0%Ag coatings. The higher the silver concentration, theoretically, the higher the toxicity level to cells and bacteria. However, coatings with a higher concentration of silver, 1.0%Ag by weight, may not work as well due to factors such as: a possible saturation limit of silver, additive agglomeration during processing, and poor film formation after curing as cross linking was compromised due to too much additive volume.

The results of the additives shown below do not include the 24 hour contact time although this point was tested for each. In most cases below, the 24 hour contact time produced a survival ratio of 0 with standard deviation value of 0.

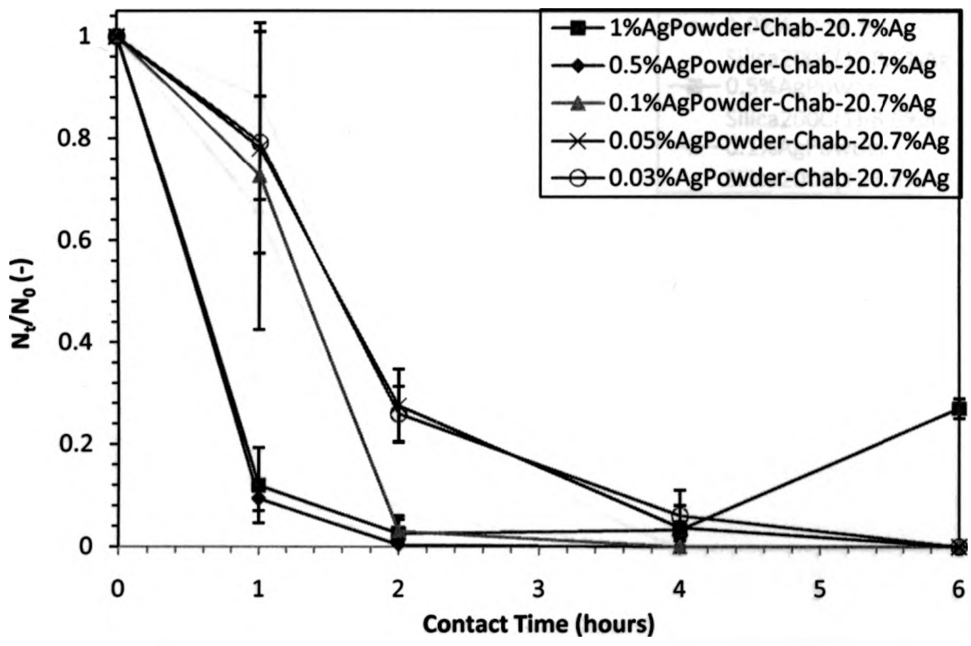

Figure 4.15: Chabazite loaded with 20.7%Ag at different silver concentrations in powder coatings (24 hr contact time N_t/N_0= 0; STDEV=0)

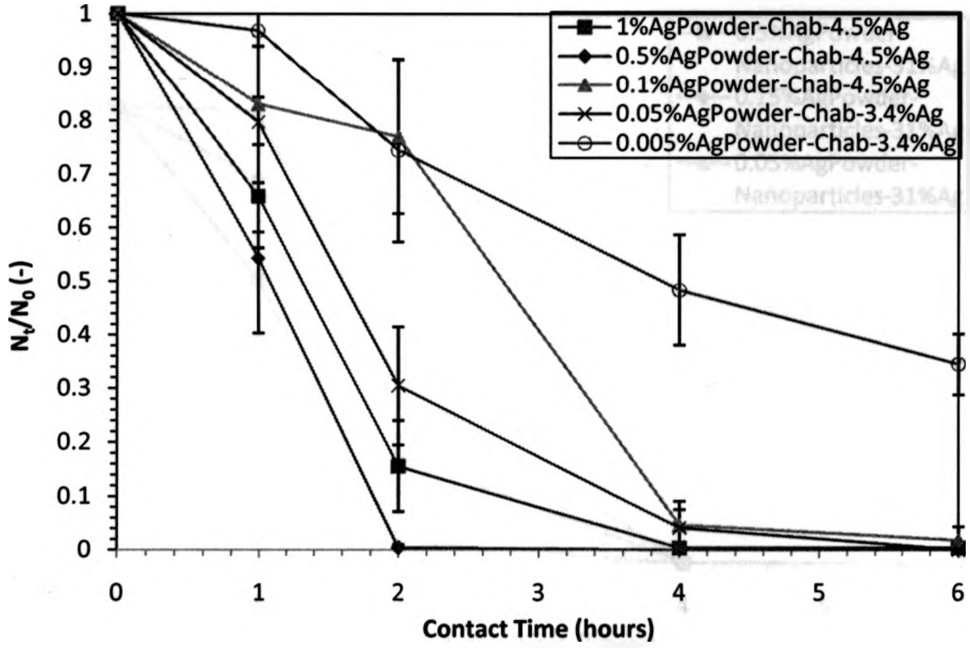

Figure 4.16: Chabazite loaded with 4.5% or 3.4% Ag at different silver concentrations in powder coatings (24 hr contact time N_t/N_0= 0; STDEV=0)

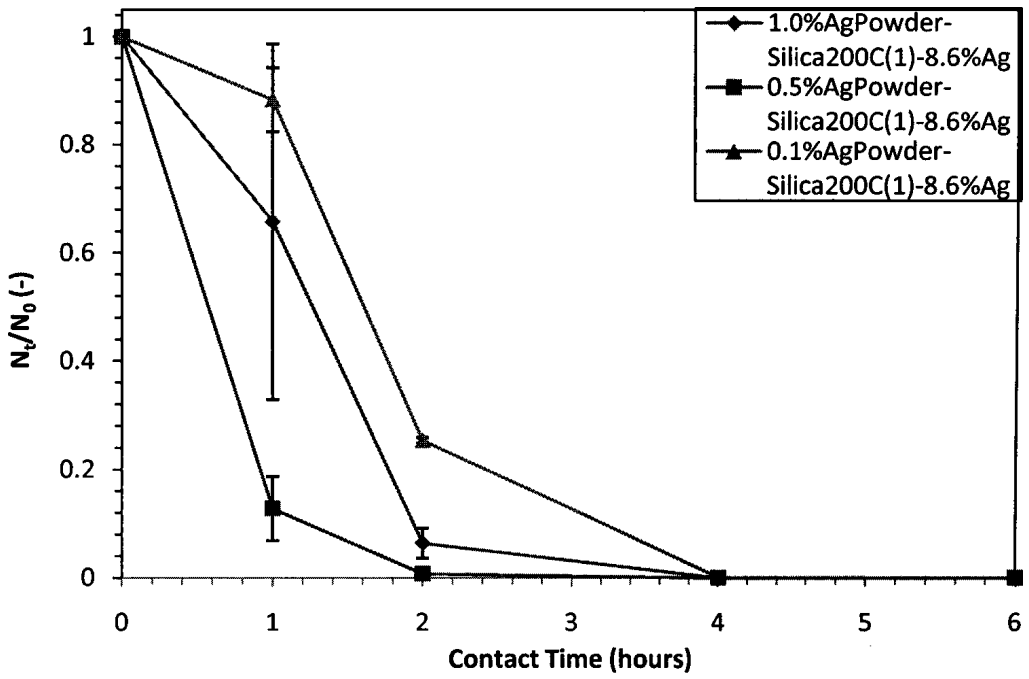

Figure 4.17: Silica glass sample (1) 200C loaded with 8.6%Ag at different silver concentrations in powder coatings (24 hr contact time N_t/N_0= 0; STDEV=0)

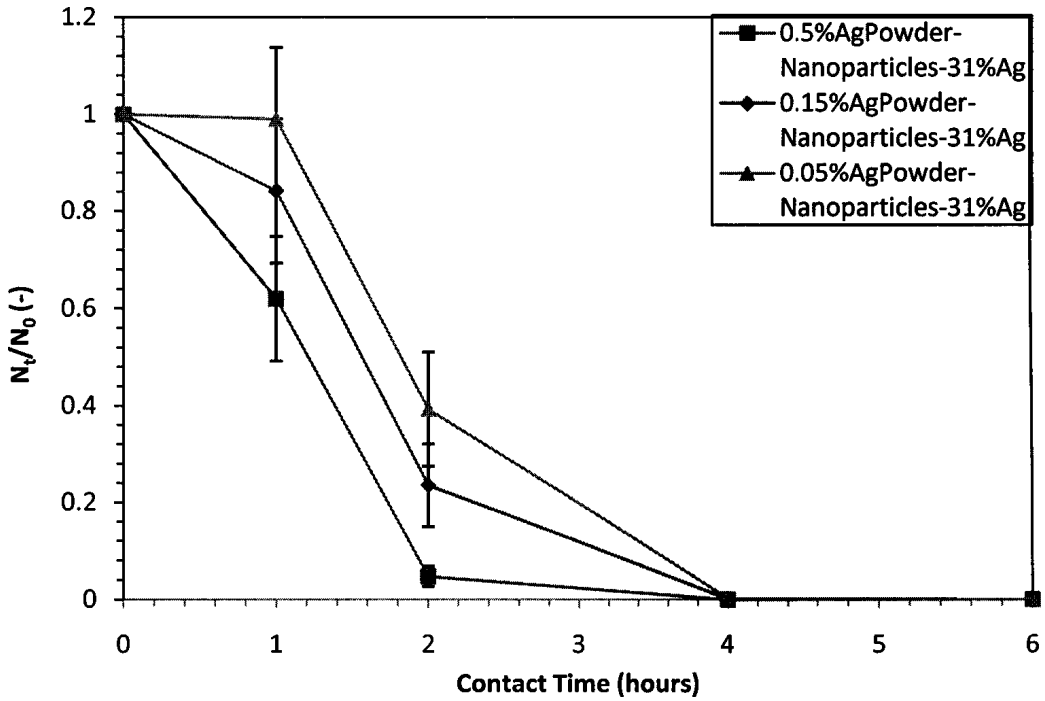

Figure 4.18: Metallic Silver Nano-particles loaded with 31%Ag at different silver concentrations in powder coatings (24 hr contact time N_t/N_0= 0; STDEV=0)

4.6 Morphology of Antimicrobial Agents and Additives

4.6.1 Structure of Silica Gel Carrier

It was initially hypothesized that the porosity and surface area of the silica gel carrier would affect its bactericidal properties based on silver release capabilities. At 0.05% Ag weight of silica200C(1)-8.6%Ag additive the produced coating failed at 1, 2, 4, and 6 hours contact which was shown earlier in Figure 4.12. This may have been due to the significantly larger particle size of this particle in contrast to other additives, reducing surface area, or it may have been due to the porosity of the silica gel carrier holding the ionic silver by physical entrapment. At 24 hours, in Figure 4.12, this coating produced survival ratio of 0 with STDEV of 0. A significantly smaller degree of active particles were probably exposed to the surface at this silver concentration leading to longer time for biocidal concentrations of silver to leach out from deeper levels within the coatings to present an effect.

Four other different silica gel particles were then produced and characterized after silica (1) had failed; differences being the method of drying from the gelation stage, which in turn corresponded to different silver loadings in the final material, different surface areas and different porosities. Silica samples titled Silica20C(4)-3.6%Ag and Silica-50C(6)-2.2%Ag correspond to silica samples (4) and (6) from the materials and methods section where (4) was dried at 20°C and 1013.25mbar and (6) was dried at -50°C and 215mbar. These two were chosen to undergo antimicrobial testing because (4) showed the highest surface area from BET and it was the only micro porous structure produced, while (6) was the freeze dried sample and should have theoretically been the most porous like previously explained. When these three different silica gel carriers were tested against one another at 0.1%Ag weight in coating the following Figure 4.19 was obtained.

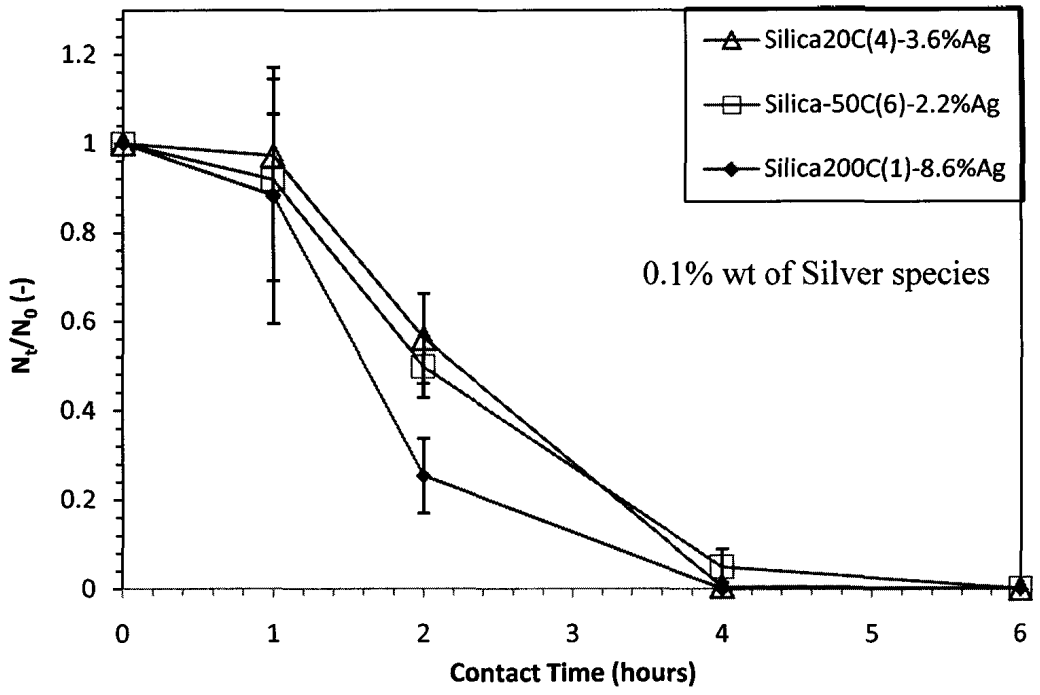

Figure 4.19: Drying effects of silica gel by 0.1% Ag by weight in powder coatings (24 hr contact time N_t/N_0= 0; STDEV=0)

In Figure 4.19 only minor differences of inactivation are noticed. At contact time 1 hour the silica coatings perform relatively equal with large standard deviations where all averages fall within each other's deviation. The only difference is noticed at 2 hours contact time where silica dried at 200°C outperforms others by approximately 9% efficacy, which corresponds to the small separation in standard deviations.

Although there were no significant differences between the three silica carriers at 0.1% Ag weight in powder coatings, when decreased to 0.05% we notice a large discrepancy: silica(1) dried at 200°C fails while silica samples dried at 20°C standard pressure and negative 50°C low pressure (samples (4) and (6)) display excellent results. This was discussed and shown prior in Figures 4.12 and 4.13 where silica dried at 200°C failed up to 6 hours contact and silica samples (4) and (6) show great antibacterial effects. For simple comparison a repeat of these two working silica samples are presented below in Figure 4.20.

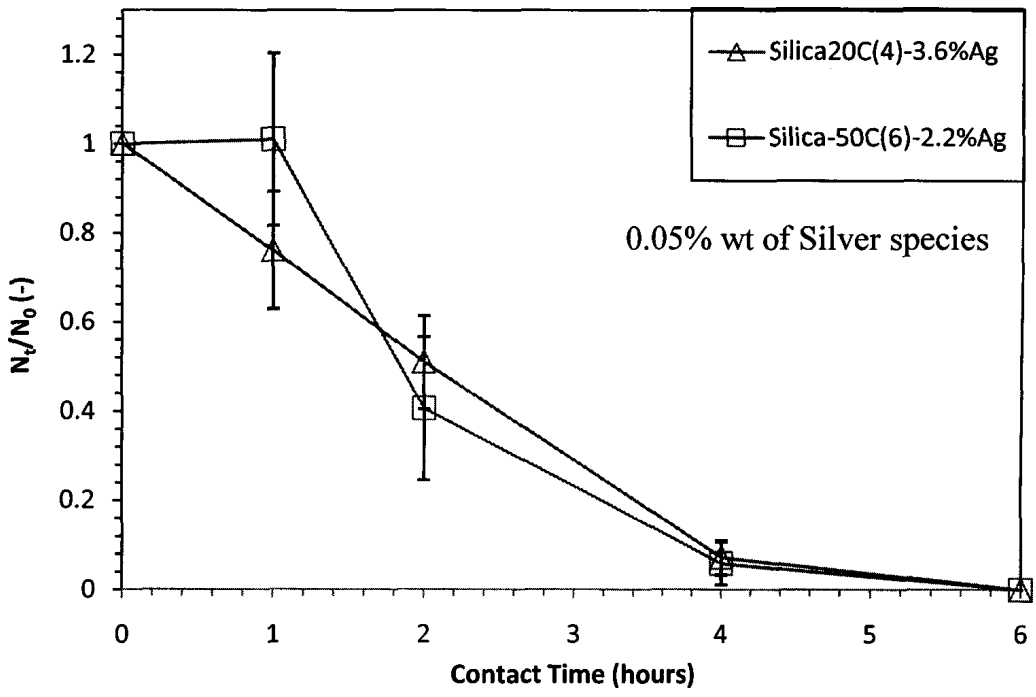

Figure 4.20: Drying effects of silica gel by 0.05% Ag by weight in powder coatings (24 hr contact time N_t/N_0= 0; STDEV=0)

The above silica gel samples, at 0.05% by weight Ag in coatings, may have performed better than the initial silica gel (1) dried at 200°C due to smaller particle sizes – over 50% smaller D(v,0.5) values. Sample (4) dried at standard temperature and pressure was expected to perform better due to its extremely large surface area and micro porosity measured by BET: 341.49m^2/g and 203.63m^2/g. As expected it performed exceptionally well. However, the freeze dried sample (6) worked equally well with negligible surface area or porosity measurements, and standard deviations all falling within range of the micro porous sample in Figure 4.20. However there was a 22% difference in average survival ratios at 1 hour contact in favour of the micro porous sample. Although BET did not show favourable statistics for the freeze dried sample, theoretically it should have been the most micro porous with highest surface area; as previously discussed. The reason for its good result at this low concentration can only be attributed to its 10.3 μm particle size (60% smaller then silica dried at 200°C), and significantly low silver loading (2.2%) yielding high additive volume at the surface. Silica gel samples (4) and (6) present failure together at 0.005% weight silver coatings as previously shown in Figure 4.14.

The sol-gels produced into silica gel/glass, loaded with ionic silver, worked just as well as chabazite zeolite carriers of ionic silver for all silver concentrations outlined in previous Figures 4.9 – 4.14. From various silver weight percentages in powder coatings we may draw the conclusion that silica carrier is no better or worse then chabazite zeolite carrier for ionic silver. However, a different conclusion was drawn from Zeren S, Preuss A, Konig B, (2005), where silica glass carrying ionic silver was more effective then zeolite carrying ionic silver against gram negative and positive bacteria.

4.6.2 Chabazite Loadings

Two chabazite zeolite additives were researched in this paper. One additive was loaded up to 20.7%Ag by ion exchange by 0.05 M silver nitrate and the other was loaded at 3.4%Ag by 0.011 M silver nitrate; (4.5%Ag was also presented but after this additive was depleted in research experiments, 3.4%Ag additive was produced under identical conditions). Throughout experimentation, these two different additives have been compared and contrasted by the percent weight of silver each possessed in their final coating which was equal at all time. Again, however, please note that the amount of particles in each coating from each additive is significantly dissimilar. For example, as shown in Table 4.1, at concentration of 0.05% weight silver in a coating there would only be 0.2416% additive by weight of the higher loaded zeolite (20.7%Ag loaded) in the coating, while 1.46% additive by weight of the lower loaded zeolite (3.4%Ag loaded) would be found; thus creating an equal silver basis but extremely different additive basis. The lower loaded zeolite additive includes 6 times more particles into a coating then its counterpart at a sample concentration of 0.05% weight Ag coating. Therefore, the question of which additive on a singular basis shows most antimicrobial efficacy, needed to be addressed.

Figures 4.21 and 4.22 display the effects of silver loadings into chabazite zeolite particles and their consequential inactivation efficacies at equal additive percents. Coatings produced with 0.15% of each additive powder correspond to silver weight percentages of

0.03% and 0.005% for chab-20.7%Ag and chab-3.4%Ag respectively in the final coatings.

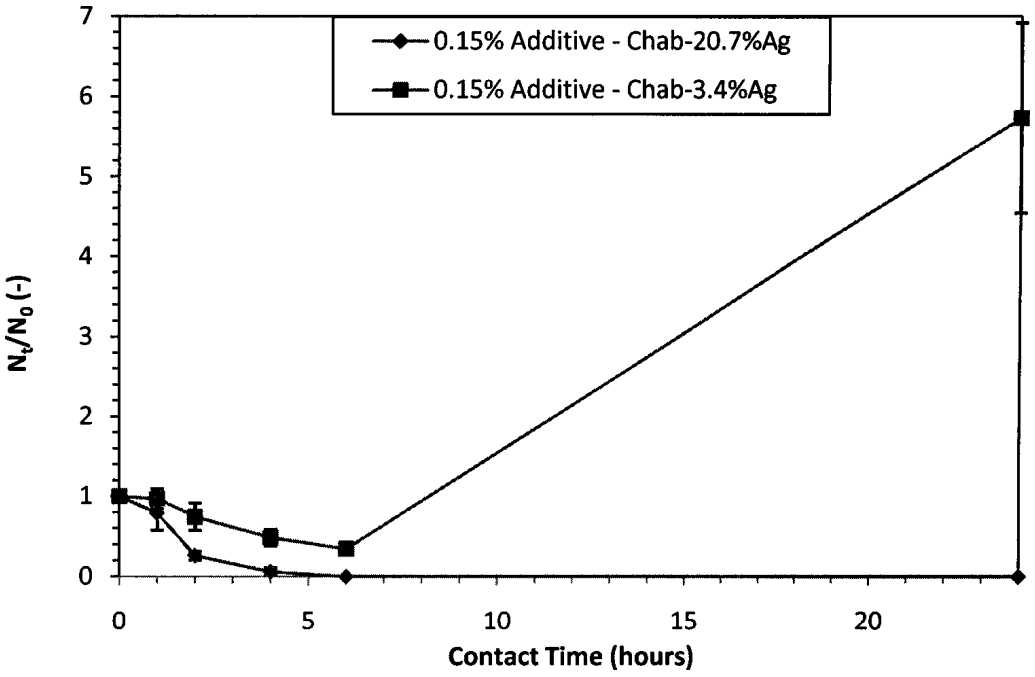

Figure 4.21: Loading effects of Chabazite zeolite - comparing loading percentages of Ag ion in chabazite using 0.15% additive in powder coating formulations

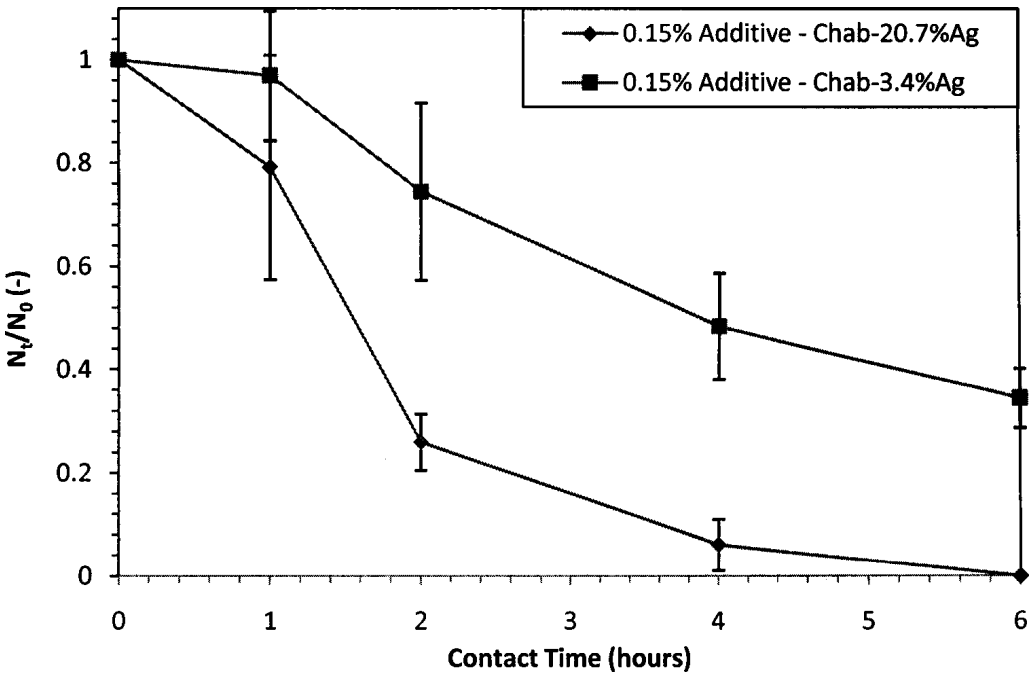

Figure 4.22: Closer view (24 hour contact times excluded) - Loading effects of Chabazite zeolite

Figure 4.21 and 4.22 show the lower loaded zeolite additive failing after 6 hours of contact time while the higher loaded sample shows survival ratios of 0 with standard deviation 0 for 6 hours and times thereafter. Chab-3.4%Ag additive was comparable to controls at 24 hours contact. Even prior to 6 hours contact the higher loaded zeolite sample performs considerably better by reduction differences of 49%, 44% and 34% at 2, 4 and 6 hours contact when comparing survival ratio averages.

From the research conducted above, it is fair to say that a chabazite zeolite particle loaded at a much higher concentration of silver is a better antimicrobial agent then chabazite zeolite loaded at a much smaller concentration on a singular or individual additive basis. This result contradicts some findings in literature but correlates others where comparisons are made between these two types (high loadings vs. low loadings) on the same basis. Top et al. (2004) reported of an optimal silver loading into natural clinoptilolite zeolites against *E. coli.* If the loading of silver was too low, the zeolite would perform poorly, but if the zeolite loading was too high a slightly negative or small decrease in effectiveness against bacteria occurred. Higher loadings may not enhance antibacterial activity due to increase in disordered Ag^+ ions, reducing the porosity of the carrier. All in all there is a certain limit which should be reached for optimal efficacy. Rivera-Garza et al. (2000) reported that reduction of loosely bound Ag^+ in high loaded silver zeolites presents a negative impact on antibacterial properties by preventing ion release due to aggregate formation on the surface. XRPD analysis in Appendix D confirmed differences in crystalline structure pertaining to the 0.05 M silver nitrate loaded zeolite samples compared to control zeolite or zeolite exchanged with a weaker 0.011 M silver nitrate. These findings were apparently not strong enough to negatively impact the chab-20.7%Ag additive against *E. coli* in our experiments, as chab-20.7%Ag is a more toxic additive over lower loaded silver chabazite particles.

4.6.3 Synthetic vs. Natural Zeolite

In this section of experimentation a synthetic sodium zeolite-A was tested. It possesses a perfect cube structure and initially only contained sodium cationic species. After ion exchange with sodium using 0.011 M silver nitrate solution, the loading was determined to be only 2.2%Ag by EDX. The antibacterial results are shown below in Figure 4.23 for 0.1% weight silver powder coatings.

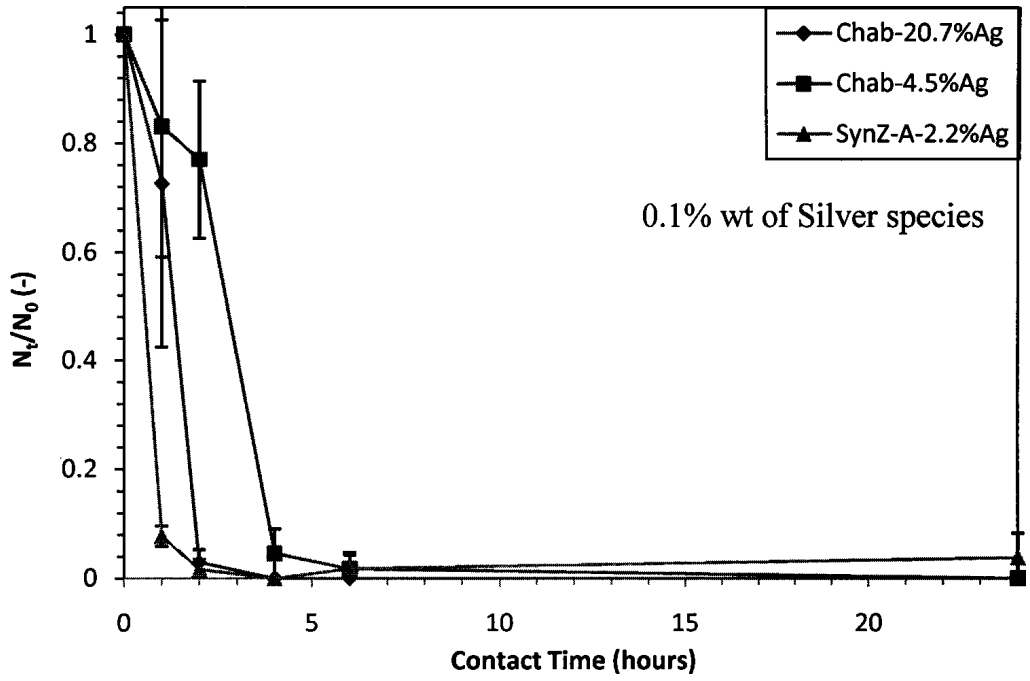

Figure 4.23: *E. coli* inactivation by Synthetic and Natural zeolites at 0.1%Ag by weight in powder coatings

After 1 hour of contact, the synthetic zeolite out performs the natural chabazite zeolites by reductions greater than 66% when observing average survival ratios in Figure 4.23. Thus, synthetic zeolite at this low loading proves to be a more efficient antibacterial agent after 1 hour contact at a base silver concentration of 0.1% in the coating. It should be noted however that this concentration of silver corresponds to additive incorporations of 4.566%, 2.223%, 0.483% in the powder coating for synthetic zeolite-A- 2.2%Ag, chab-4.5%Ag and chab 20.7%Ag respectively from Table 4.1. Keeping in mind the

results from synthetic zeolite here, and observing prior results with Figure 4.10, chab-20.7%Ag performs just as well at 1 and 2 hours contact at 2.416% additive incorporation and accompanied 0.5%Ag coating. Although the two vary in silver loading, it cannot be said from this research that synthetic zeolite-A has better antibacterial effects than natural chabazite when comparing on an individual additive basis. From this research it can be deduced that a synthetic zeolite-A- 2.2%Ag is more efficient at creating antibacterial effects after 1 hour contact versus chab-20.7%Ag and chab-4.5%Ag when the same concentration of silver is coupled into powder coatings. However, on a similar additive leveled basis of coatings, it can be deduced that there is no significant difference of antibacterial activity between synthetic zeolite-A and natural chabazite zeolite both loaded with silver. Yamamoto T, Utida M, Nakata S, and Nakagawa Z, (2002), also observed no differences in anti-bacterial effects regarding synthetic and natural zeolites loaded with silver.

The silica to alumina ratio between synthetic and natural zeolites was found to be 21.31±1.9 : 18.47±3.8 and 38.8±4.4 : 6.9±2.3 respectively. The low Si/Al ratio composing the synthetic zeolite does not give it an advantage for favorable cation ion exchange; as previously mentioned. Also the low Si/Al ratio of synthetic zeolite makes it more susceptible to chemical damage. Finally, it should be noted that although initial contact times showed good results against bacteria for the synthetic zeolite, the synthetic zeolite showed increase of 1% and 3% survival ratios for 6 and 24 hour contact times. This was probably due to contamination as it was uncharacteristic for samples to retain bacterial populations after reaching zero survival ratios.

4.6.4 Silver Ion with/without Carriers

A powder coating including silver ion was produced with silver nitrate alone and no carrier vehicle to house the salt suspension. A 0.1% weight Ag powder coating was produced by a theoretical suspension of silver nitrate in deionized water. This theoretical suspension of silver nitrate was homogeneously mixed with a specific mass of polyester resin in freeze dry vials. After freeze drying the suspension with the polyester resin, the

powder was coated onto the metal substrates. After curing, there was a drastic color change of the coating from perfect clear, to deep, dark yellow. Comparing the inactivation efficacies against *E. coli* of ionic silver with no carrier to loaded carrier materials the following Figure 4.24 was drawn at 0.1% Ag powder coating.

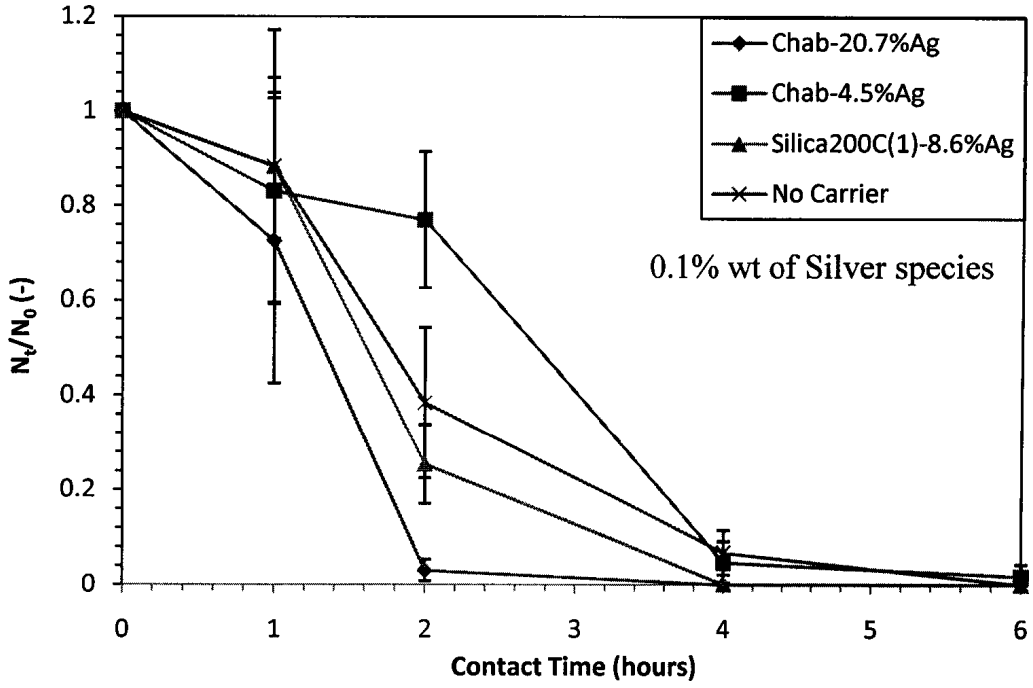

Figure 4.24: *E. coli* inactivation by Ag Ion with and without carrier particles - 0.1% Ag by weight in powder coatings (24 hr contact time N_t/N_0= 0; STDEV=0)

In Figure 4.24 the antibacterial effectiveness of ionic silver powder coating with no carrier material was good, mostly performing in the middle amongst the ionic silver additives with carriers. Chab-20.7%Ag was the only additive at 2 and 4 hours contact to significantly outperform the no carrier additive as other carrier sample comparisons are similar. For this reason, the silver concentration in the powder is presumed to be too high to provide an accurate judgment of the no carrier material, as a lot of the ionic silver must have stayed in ionic form in order to show bactericidal effects. It is proposed then that the longevity of the no carrier material should be far less than all other additives possessing carriers for ionic silver. Evidence to this fact is attributed to the drastic colour change to deep yellow of the coating with silver nitrate and no carrier material. This extreme degree

of color change after curing was never experienced with any other powder coatings in this research indicating that significant changes to ionic silver must have occurred. Hutson NC, Reisner BA, Yang RT, and Toby BH, (2000), report color changes to yellow of silver nitrate upon heat treatment and analysis by X-ray photoemission spectroscopy confirm reduction of Ag^{+} to Ag^{0}.

The proposition of decreased longevity with no carrier is also backed up by literature. Rivera-Garza et al. (2000) reported that the reduction of Ag^{+} has a negative impact on the antibacterial properties of silver. Inoue and Kanzaki, (1997), also investigated oxidation state of silver and antibacterial activity and concluded that after reduction the antibacterial action was troubled.

Another reason for the no carrier material with ionic silver to produce feeble antibacterial effectiveness is due to the inability of the silver ion to stay in ionic form after drying out of liquid suspension in water. Zeolite and silica particles create environments for the silver ion to stay in the cationic form, but without carrier materials, this may not occur. When water is evaporated from a silver colloid suspension silver cations are forced to combine with available anions to form a compound. In water solution for example, the main anions present are hydroxide and carbonate, thus when evaporated silver hydroxide and silver carbonate are formed. Silver hydroxide is unstable and reduces to silver oxide and hydrogen while silver carbonate reduces to silver oxide and carbon dioxide. Silver oxide molecule has no ionic charge so the lack of repulsive force causes attraction by Van der Waals' force leading to aggregation of particles. In solid phase, the average kinetic energy of silver oxide is not strong enough to overcome dipole-dipole interaction of Van der Waals' force. Further, silver oxide contributes limited antibacterial activity, so the effectiveness of ionic silver should be lost.

Chabazite zeolite and silica gel carriers for ionic silver have proven to be worthwhile and durable materials under experimental conditions tested, which will be covered in following chapters. However it should be noted that there was noticeable color changes occurring after curing with these additive as well, especially at high silver concentrations

in the coating. These color changes are credited to formation of silver clusters (Ag^0) in voids and cavities of the carrier framework. They were assumed to form from the ionic species of silver at elevated temperatures by means of automatic reduction where oxygen is released from inside the structure; due to further ensuing H_2O evaporation. However, color change with these materials was never as drastic or to the extreme degree of the no carrier material.

4.6.5 Silver Metals

As described earlier, in Chapter 2, silver cations as their ammonium complex also called Tollen's reagent, can be changed into free metallic form by purposeful reduction. Reducing silver in Tollen's reagent is simply an oxidation-reduction reaction (redox reaction) where an aldehyde is used for the reducing agent. In this research Tollen's reagent was reduced with formaldehyde as described in Chapter 3. Since capping agents were not used to repel the metallic silver particles during formation, the molecules were charge less during the chemical reaction. Thus there was nothing involved in the reaction to prevent or protect the silver from assembling into larger micro metallic structures. Mainly micro structures exist separately or within deposited films when reducing the silver in Tollen's reagent without the use of capping agents to prevent assembly (Buckley F, 2006). This form of metallic silver was produced with carbon nano tubes and polyester particles during the reaction. Comparison of the bactericidal effects of two forms of metallic silver can be made from this research in powder coatings; bulk metallic silver particles vs. nano metallic silver particles. Incorporating the uncapped production of metallic silver into powder coating at 2.0% and 0.1% weight and with CNTs at 1.0% weight the following Figure 4.25 was produced.

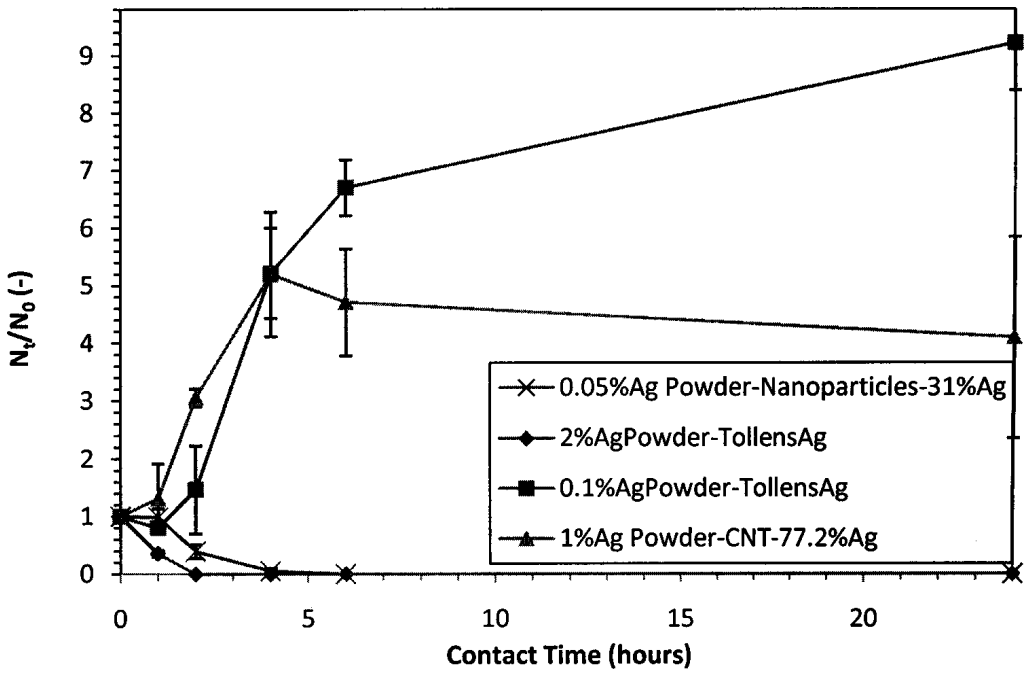

Figure 4.25: *E. coli* inactivation by Metallic Silver from Tollens Reagent (with/without CNTs) and Metallic Silver Nanoparticles

In Figure 4.25 the Nanoparticles-31%Ag additive at 0.05%Ag coating concentration is shown graphically for comparison sake, as this concentration is significantly smaller than other experimental agents in the figure. The above figure demonstrates a well functioning powder coating at 2.0% weight Ag of the presumed micro metallic suspension freeze dried with polyester. However at 0.1% weight into the coating, this metal fails, comparable to control samples. It is presumed that the size and surface area are main determinants for toxicity. Literature states that as the size of metallic silver particles decreases down to nano-scale their antibacterial efficacy increases due to their larger total surface area per unit volume (Kumar A, Vemula PK, Ajayan PM, John G, 2008). The Nanoparticles-31%Ag sample includes metallic silver ranging from 2-10 nm attributing to its functionality at low concentrations in the power coating – As shown prior in Figure 4.18 the Nanoparticles-31%Ag sample shows great effectiveness against *E. coli* down to 0.05%Ag concentration in the coating. Decreasing the concentration of Tollen's produced metallic silver in the powder coating to 0.1%Ag consequently shows failure, attributing to its larger particle size and decreased surface area. Another attribution of failure may

have been the inability of larger metallic silver particles to penetrate inside the bacteria causing further damage to cells.

Nano metal particles, around 5 nm range, present electronic effects which are essentially changes in the local electronic structure of the surface due to size (Morones JR, Elechiguerra JL, Camacho A, Holt K, Kouri JB, Ram´ırez JT, Yacaman MJ, 2005). In turn, these effects are reported to enhance the reactivity of the nano particle surfaces. Further, reactivity of the nano surfaces would force release of silver ions having additional contributions to bactericidal effects. As such, the metallic silver nanoparticles have high sensitivity to oxidation. This experimentation successfully shows the differences in, and particle size dependence of, metallic silver species in powder coatings and their inactivation effects against *E. coli*.

The carbon nano tubes coupled with Tollen's metallic silver showed no antibacterial effect at 1.0% weight of silver into powder coating. The goal was to try and coat the CNTs with metallic silver to decrease their size and increase their antibacterial action, however at the specified concentration, this was not successful. Carbon nano tubes have a tendency to aggregate together due to extremely high surface energy and therefore it is very difficult to uniformly disperse them in solution (Zhang Nanyan, Xie J, Guers M, Varadan K, 2004). This may have been a reason leading to failure during the drying stage.

4.7 Industrial Antimicrobial Powders

4.7.1 Company D and Company P

Industrial antimicrobial claimed powders were obtained from two of the top powder coating companies in North America. For confidentiality issues these two companies will be referred to as company 'P' and company 'D' although their antimicrobial powders have specific names they will not be stated. These two powders presumably represent the

best antimicrobial powder coating systems in the present date. The powder obtained from company P uses a polyester base resin system with white pigment, while the powder obtained from company D uses a polyester base resin system with no pigment. Company D's powder produced a clear coating ideal for comparison to U.W.O. produced powders, both utilizing polyester clear coat resin systems. The industrial powders were applied to specimen chips and tested using the same procedures outlined prior. Figure 4.26 displays the survival ratios plotted with contact time against *E. coli* bacterium for the industrial powder coatings.

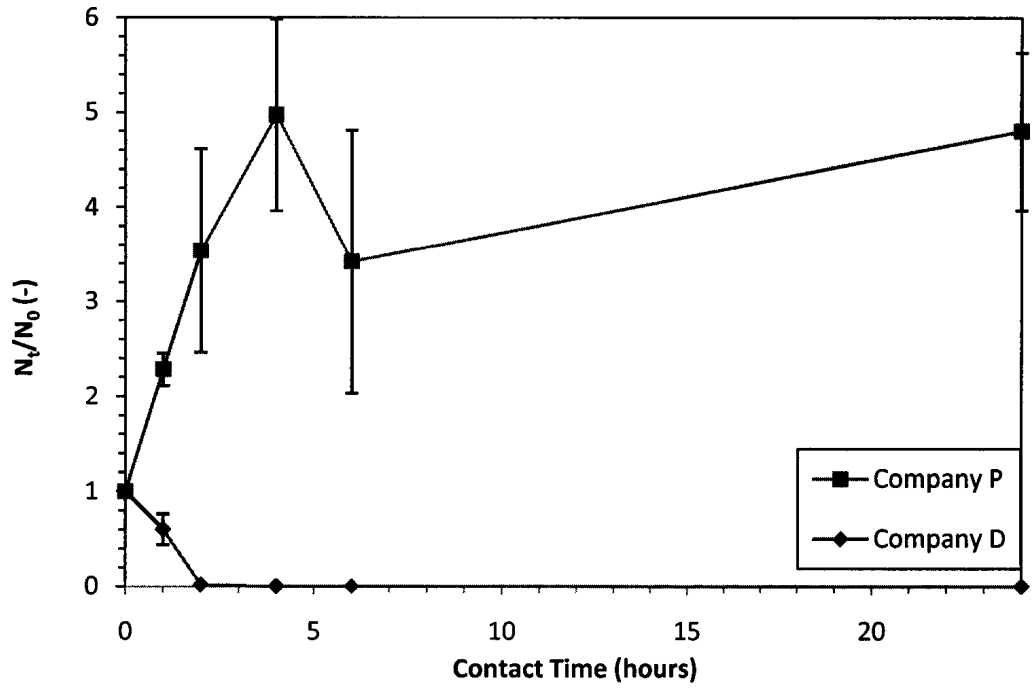

Figure 4.26: *E. coli* inactivation by antimicrobial claimed powders from top Industrial Powder Coating Companies

From Figure 4.26 above it is apparent that through ASTM E2180 company P powder fails while company D powder functions well against *E. coli*. Results for company P powder show no bactericidal effects against *E. coli* as the survival ratios are comparable to control coatings in prior Figure 4.5. Due to failure, Company P's powder is believed to utilize titanium dioxide particles which are commonly found in white pigments. In the case of antimicrobial coatings the TiO_2 serves a double purpose as both a source of

pigment as well as an antimicrobial agent. Titanium dioxide produces bactericidal effects by production of ROS species in the presence of UV light like previously mentioned in Chapter 2. Company P has stated that their powder is bactericidal and did not imply or mention any testing procedures involving UV radiation. Company P is the party whom informed us of their testing procedure which is the same one we utilized for the antimicrobial testing procedure- ASTM E2180. Since company P coating did not show working characteristics and does not threaten the U.W.O. produced powders it`s research was discontinued.

From Figure 4.25, company D`s powder coating initially performed exceptionally well against *E. coli* bacterium. EDX analysis and spectra reveal a 0.505% by weight silver concentration in the coating. Technical information from company D states the use of a silver containing zeolite where process and materials are patented under US6093407(A) and US6432416(B1). Their active antimicrobial compound of silver is registered as a pesticide with the U.S. Environmental Protection agency (EPA 738-F-93-005). Company D`s powder would be researched further in this paper.

4.7.2 Company D vs. U.W.O.

At this point it is clear that company D has initially presented a well functioning antimicrobial powder coating. A comparison of the company D results against inactivation of *E. coli* versus top functioning U.W.O. powder coatings is useful. It should then be vital for these results to be as accurate as possible and fair as possible. Therefore, experimental results obtained from repeatability tests, in Figures 4.1 – 4.4, were combined for chab-20.7%Ag, chab4.5%Ag, silica200C(1)-8.6%Ag, nanoparticles-31%Ag and Company D coatings by averaging all survival ratios and calculating standard deviations with all related counts. Combining test results would produce a most accurate representation of effectiveness for that sample at 0.5% weight of silver in the coating. Please note that 0.5% weight of silver was chosen for U.W.O. powders to compare against Company D because, as stated earlier, Company D powder shows 0.5% weight of silver by averaged EDX values. Figure 4.27 compares the antibacterial

effectiveness of company D's powder with U.W.O.'s best functioning powder formulations.

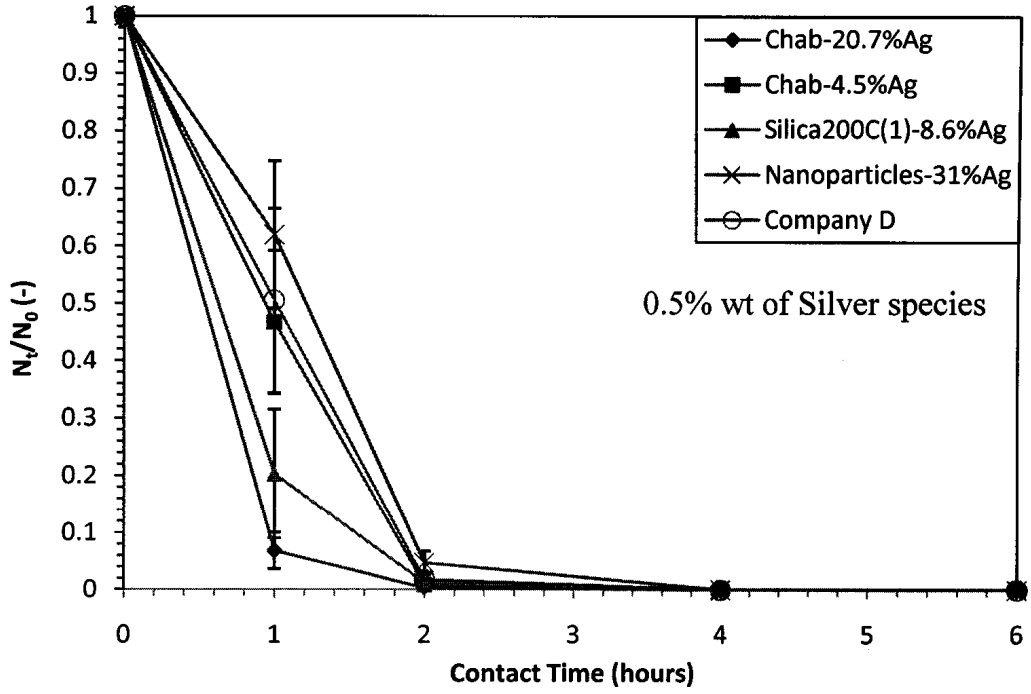

Figure 4.27: *E. coli* inactivation by U.W.O. powder formulations at 0.5%Ag weight in Powder Coatings and by Company D (24 hr contact time N_t/N_0= 0; STDEV=0)

Comparing four of U.W.O.'s best functioning antimicrobial coatings with company D's powder coating, in Figure 4.27, one notices obvious differences of survival ratios amongst the five at 1 hour contact time, but near identical results at 2, 4, 6, and 24 hours contact. At 0.5% weight silver in the powder coating (same as company D by EDX) chab-4.5%Ag additive was very similar at 1 hour contact to the results of company D. Nanoparticles-31%Ag shows a 10% less effective survival ratio at this time but the average falls within the standard deviation of company D and similarly company D's average survival ratio at 1 hour falls within the standard deviation of the silver metal nanoparticle sample. The average survival ratio for silica200C(1)-8.6%Ag at 1 hour outperforms company D by 30% but max standard deviations of the two are only different by approximately 4%. The most significant difference occurs with chab-20.7%

where a 44% difference is observed at 1 hour contact in favour of the U.W.O powder and standard deviation for this sample is very small as well.

From Figure 4.27 it is difficult to pass judgement on whether U.W.O. powder coatings are truly better then the top industrial coating overall. It is understood from this figure that initial results of effectiveness against *E. coli* prove sufficient for both parties, but the idea of an antimicrobial coating is to present longevity and true effectiveness over time under various environmental conditions. This leads to the next experimental section of Durability Testing.

4.8 Durability Tests

In this section of experimentation durability testing, by washing and repeat testing of coatings, was performed. Durability studies were conducted with Company D powder as well as U.W.O. powders at 0.5% weight silver using the following additives: nanoparticles-31%Ag, chab-20.7%Ag, and silica200C(1)-8.6%Ag. The same procedure was used for all samples when durability tests were carried out. Specimen chips were numbered according to contact times after the first testing run by ASTM E2180 and exposed to the same procedure again for a second time. After a first test through ASTM E2180, the same specimen coatings were put through another test after washing with a dilute solution containing household Sunlight Liquid Dish Soap. This type of surfactant was used to simulate real world operating conditions of the coating and to ensure removal of the previous pseudo biofilm formed on the surfaces. Removal of biofilms is achieved through use of concentrated cleaning and sanitizing agents dependent on concentration, exposure time, temperature and mechanical activity. Removal of a real, mature biofilm requires extensive mechanical action accompanied with the use of a cleaning agent. Since we were dealing with a pseudo biofilm, a dilute concentration of surfactant was used in conjunction with light scrubbing with nitrile laboratory gloves, and drying using a towel. Chemical energy and mechanical energy would prove to be sufficient in surface cleansing.

4.8.1 Issues of Durability

Industrial Coatings

Durability testing was conducted for company D's coating using the procedure outlined above and detailed in Chapter 3. Run #1 corresponds to initial tests while Run #2 corresponds to secondary testing with the same specimen coated chips after the washing method. Two durability test runs under the same conditions were completed for company D powder coating to ensure certainty in the results (Run #2a and #2b). Figure 4.28 presents the durability results for secondary testing after washing for company D's coating.

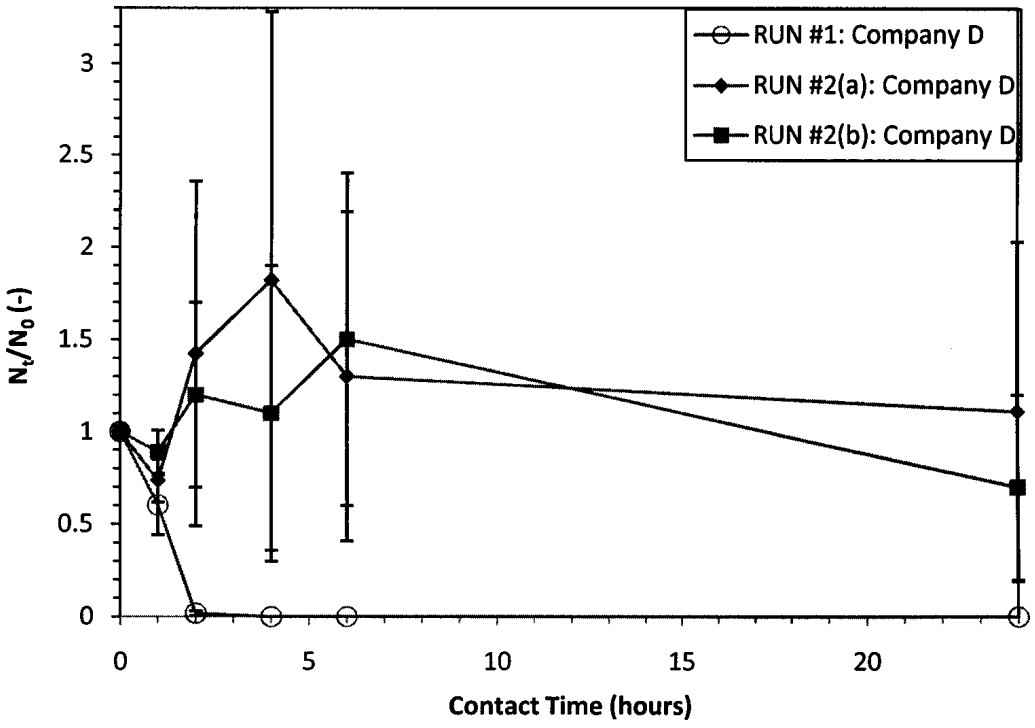

Figure 4.28: Durability tests using Company D Powder Coatings

Results from Figure 4.28 show that company D's coating is very unstable and does not hold up after chemical and mechanical energy induced cleansing and repeated use. Average survival ratios for secondary runs after washing (Run #2a and Run #2b) show large increases in *E. coli* bacteria populations after 2, 4, and 6 hours contact. The standard

deviations are extremely high for all data points signifying a very sensitive surface; as counts for different chips were wide ranging at the same contact times. Some chips showed complete inactivation of bacteria at times when others showed over 100% and 200% increases at the same time.

Company D's failure of this durability testing may be directly linked to their powder manufacturing procedure. It is stated in their patents that their antimicrobial additives were to be blended with the resin system pre-extrusion. This method essentially melts all components together into one homogeneous mixture. However, U.W.O. produced powders have their additives blended post extrusion, dry – blended, to the resin system. By use of dry-blending method, the additives essentially coat each resin particle and will not be buried consequently by extruded resin. Thus, U.W.O. coatings will include a higher concentration of additives at the surface than the industrially produced powders. Further, with a higher concentration of additives at the surface, the coatings will be more durable and utilize the volume of additives better, additionally yielding a cheaper coating as fewer additive particles are required. This proposition indicates the main difference between industrial and U.W.O. produced coatings and the reasons why U.W.O. coatings should present superior durability and effectiveness.

4.8.2 Durability of U.W.O. Powders

Figures 4.29 – 4.31 present the *E. coli* inactivation efficacies of the U.W.O. powder coating durability experiments.

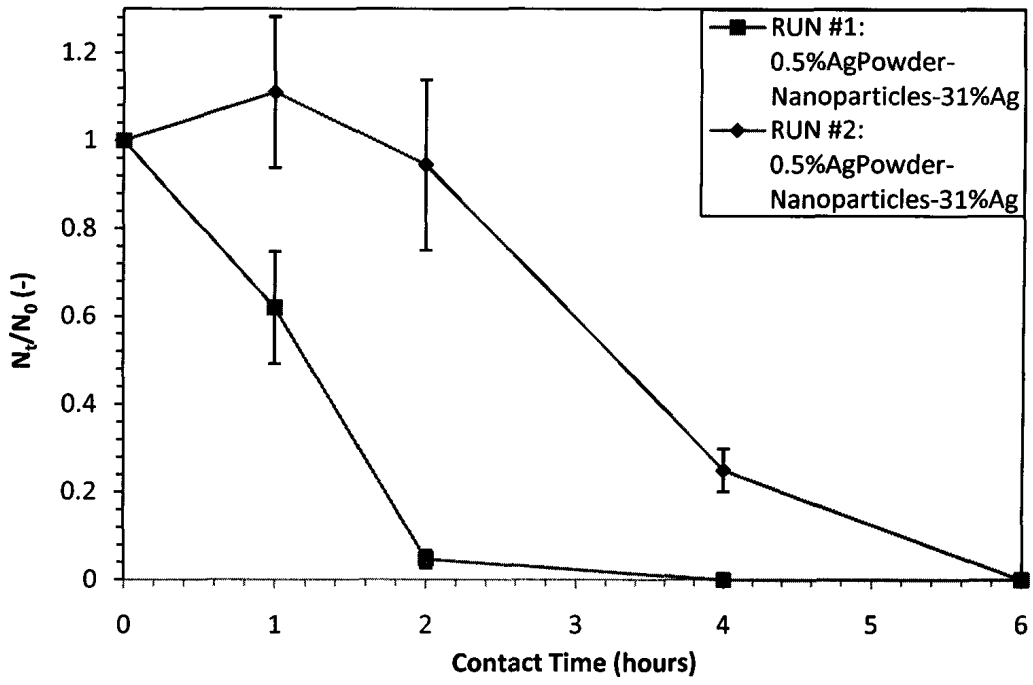

Figure 4.29: Durability tests using 0.5%Ag Powder Coatings by Nanoparticles-31%Ag additive (24 hr contact time N_t/N_0= 0; STDEV=0)

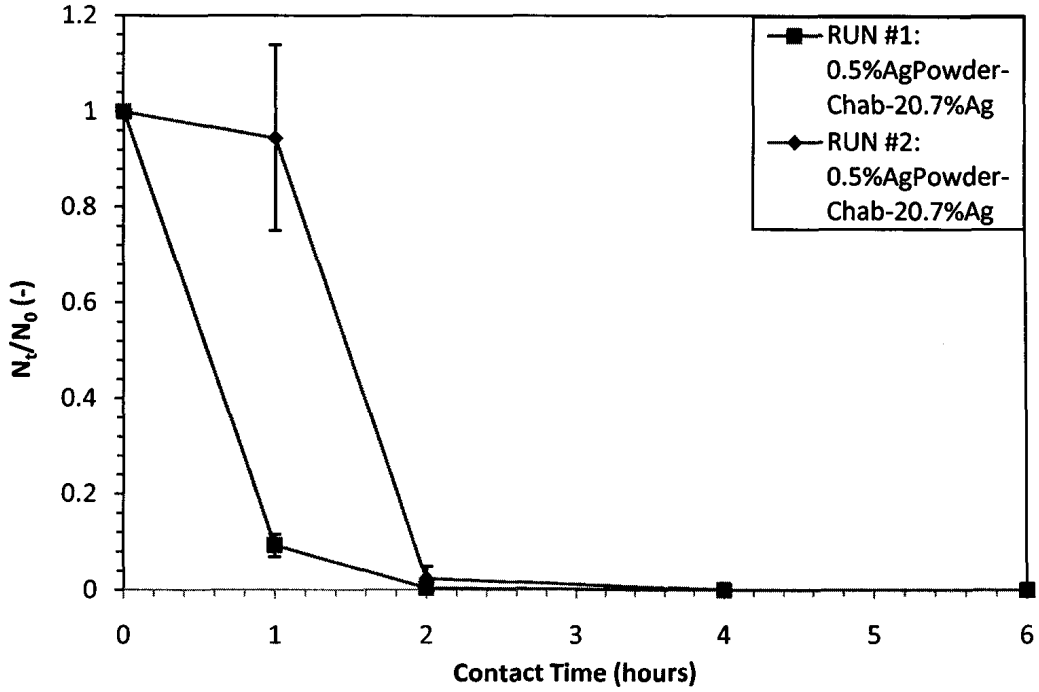

Figure 4.30: Durability tests using 0.5%Ag Powder Coatings by Chab-20.7%Ag additive (24 hr contact time N_t/N_0= 0; STDEV=0)

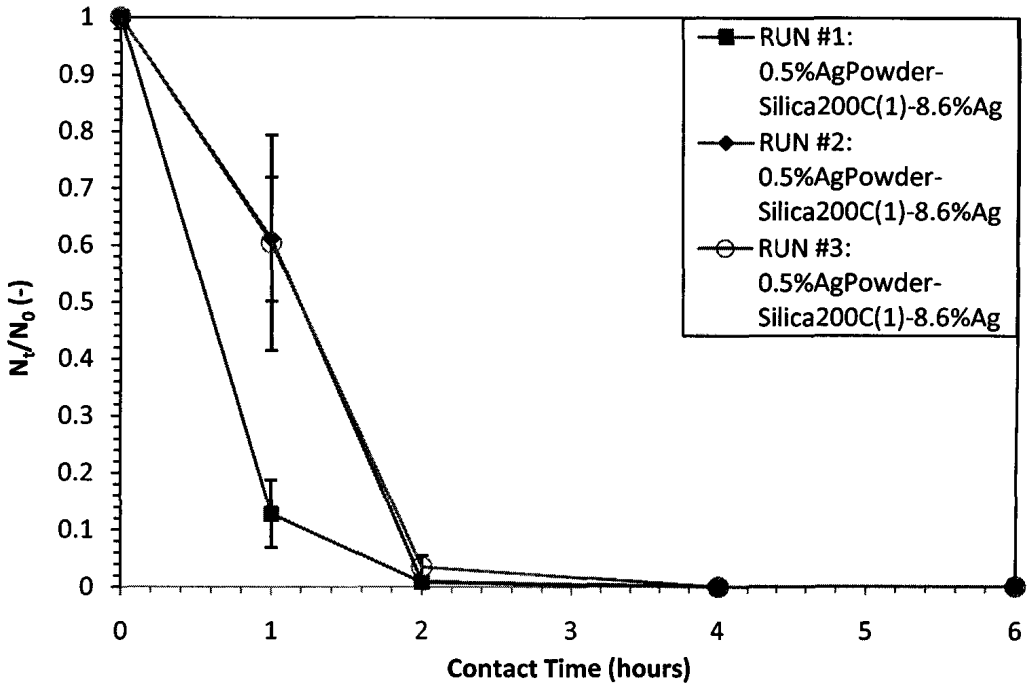

Figure 4.31: Durability tests using 0.5%Ag Powder Coatings by Silica200C(1)-8.6%Ag additive (24 hr contact time N_t/N_0= 0; STDEV=0)

Observing the above figures it is clear that the silica gel additive, after multiple runs through the antimicrobial testing procedure, out performs the chabazite carrier and the silver nanoparticles. A 47% and 85% increase in survival ratios from initial test results is shown with the silica and chabazite additives respectively at 1 hour contact times for durability test runs. Also, at 2 hours contact, survival ratios increase marginally for these two samples and finally survival ratios of 0 are noticed for remaining times. Regardless of weakened efficacies, in all cases, the U.W.O. coatings still hold up relatively well after the durability testing - may be relating to significant longevity for each coating.

In Figure 4.29, the silver nanoparticle additives in coatings were shown to be the least durable coating under washing conditions by 48%, 90% and 26% increases in survival ratios, compared to initial test results, for 1, 2, and 4 hour contact times respectively; 6 and 24 hour times presented survival ratios of 0 value. The silver metal nanoparticles create bactericidal effects by their size through attaching and penetrating *E. coli* cell walls and/or releasing silver ions. Literature does not present any research on silver

nanoparticles dispersed and freeze dried in a resin system and electrostatically sprayed to form a powder coating so as far as we know this is the first data of its kind. Although this coating did not totally lose its antibacterial effectiveness, it did show the most pronounced weakened activity after washing. This may be due to the rigidity of the metallic silver particles in the coating and their incapability to penetrate and attach to bacteria not on the surface. Thus the release of silver ion may be the only mechanism of action against bacteria not directly on the surface, unless the nano metal species can detach from the coating and move into the pseudo biofilm. Silver ion is immediately released from the nano metal in solution but as time passes silver ion decreases in solution due to reduction processes to form Ag^0 containing clusters or re-association with the original nanoparticles (Morones JR, Elechiguerra JL, Camacho A, Holt K, Kouri JB, Ramirez JT, Yacaman MJ, 2005). Thus after washing, the reduction of silver ion and the ability to release silver ion from the nanoparticles may be compromised.

4.8.3 Periodical Cleansing

The use of a surfactant for durability washing was re-assured in this section of testing, where a reclaimed stronger antibacterial surface was shown. This result presents some evidence for the need to appropriately wash antimicrobial surfaces after they have succumbed to an extreme soil load like with ASTM E 2180. The same procedure as the above durability testing was used with a couple exceptions. Rather than using chemical energy by washing with a dilute surfactant, only mechanical energy was used to conduct trial 2 by scrubbing the surface with only deionized water. Trial 3 was conducted after washing conditions using chemical energy with dilute surfactant solution – same as the above durability testing. Figure 4.32 presents the effects of periodical cleansing against *E. coli* for one of U.W.O. `s powder coatings.

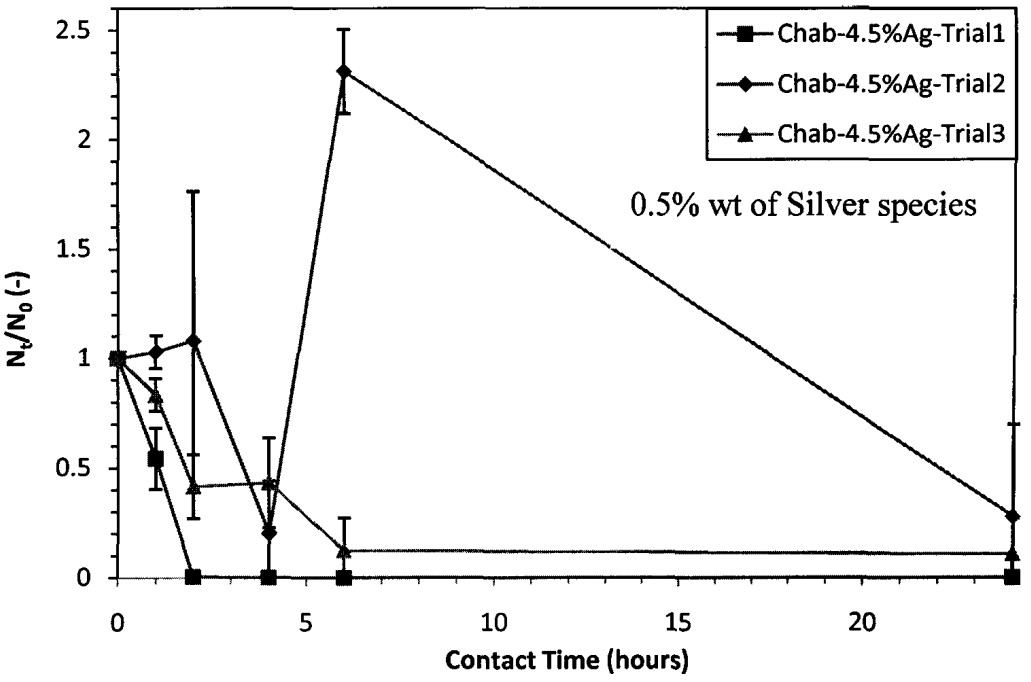

Figure 4.32: Periodical Cleansing test using 0.5%Ag Powder Coating by chab-4.5%Ag additive

Firstly, it should be noted that extremely high surface tension was noticed when applying the inoculum agar slurry with trial 2, which decreased significantly when proceeding with trial 3. This may have been caused by a thin film of dead cells still on the surface of the coating after the attempt of washing with water only. In Figure 4.32, Trial 3 showed reclaimed survival ratio averages of 19%, 67%, -21%, 220% and 17% for contact times of 1, 2, 4, 6 and 24 hours respectively when comparing to trial 2. These results may signify that periodical cleansing of an antimicrobial surface can be worthwhile under certain conditions for best results of the surface.

4.8.4 Disposed Chemical Damage and Leaching Tests

A different type of durability study was carried forth in this section providing *E. coli* inactivation results after freshly coated specimens were subjected to saline solution for 168 hours. Chab-20.7%Ag, chab4.5%Ag, and silica200°C(1)-8.6%Ag were hung from a plastic coated wire into a 0.1% saline solution with mechanical agitation for 168 hours or

7 days. Averaged from major North American cities, there is 35±41 Na^+ and 91±67 Na^+ in tap water from surface and ground sources respectively (Azoulay A, Garzon P, Eisenberg MJ, 2001). Thus 0.1% saline bath was chosen because it represents 312mg Na^+ and 488mg Cl^- being significantly stronger (50% - 300% higher) ionic solution than average North American tap water, promoting degradation, exchange and leaching of silver from the samples. The 488 mg of Cl^- present in each water bath represents a strong corrosion presence and likeliness to initiate chemical damage to the coatings. Samples recovered from the three water baths were measured by ICP and plotted against soaking time, shown in Figure 4.33.

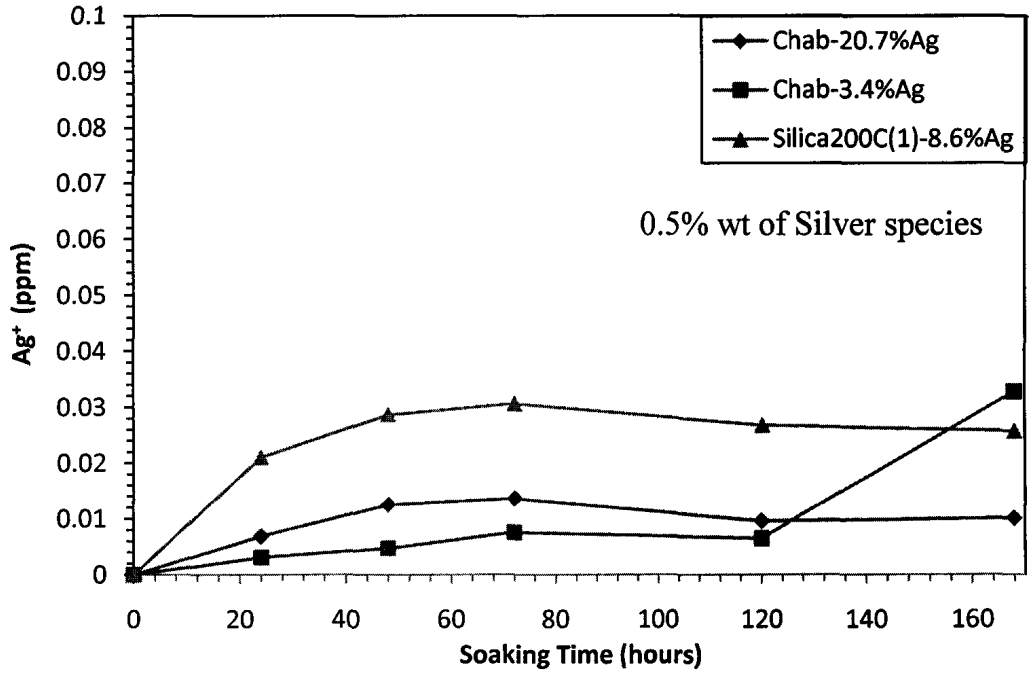

Figure 4.33: Silver Ion Release Profiles after 168 hours soaking in 0.1% saline solution by 0.5%Ag powder coatings

From Figure 4.33 the amount of silver released in ppm from the coatings occurs in the sequence: Silica200C(1)-8.6%Ag > Chab-20.7%Ag > Chab-3.4%Ag. Trace amounts of silver were measured for all three samples indicating that under the influence of relatively strong ionic solutions, leaching from the coatings occurs but may not be a major concern. The sequence of silver release followed the order that was hypothesized which will be

explained. Silica particles hold ionic silver in the structure by a physical nature only. Whether silver is adsorbed and found on the surface of silica particles or inside the framework, easy release due to leaching is a result. Rapid release of silver ions after 24 hours soaking by silica glass particles was also observed by Kawashita M, Tsuneyama S, Miyaji F, Kokubo T, Kozuka H, and Yamamoto K, (2000), and accompanied slower release profile thereafter. Kawashita et al, (2000), also explain silver colloids from reduction of silver ion attributing to fast release from silica gel particles.

The highest concentration of silver was released after 24 hours for the chabazite additives, as a slow release was observed thereafter; with the exception of chab-3.4%Ag after 120 hours – which cannot be explained and was probably an error in sample acquisition. The slow release mechanism and property of zeolite is well known and verified in a lot of literature. Only in the presence of like cations will the ionic silver exchange from the chemisorbed zeolite structure. If the chabazite particles were exposed to a de-ionized water bath solution, there would be 0 ppm silver measured by ICP theoretically; as ionic silver is supposed to be chemically bonded only in the zeolite framework. O'Neill C, et al. (2006), showed that there was no detectable silver leaching from zeolite matrix after testing by extensive soaking in de-ionized water bath for 8 weeks.

The powder coated specimen chips also showed degradation and blistering or bubbling of the coating, after soaking in the electrolyte solution for the 168 hours. Chemical damage was obviously evident to most metal specimen chips, some more than others; most damage occurring and proceeding from the edges of the coatings. Damage to paint coatings caused by immersion in electrolyte solutions was also observed by Souto RM, Gonzalez-Garcia Y, Gonzalez S, and Burstein GT, (2004), where the degradation was observed as a swelling of the polyester coating as a function of time of immersion in chloride solution. They noticed an aggressive effect of chloride ions towards coating degradation, after short exposure times, where in contrast blistering was not noticed with chloride- free solutions thus attributing the damage to chloride. Surface topographies of the U.W.O. antimicrobial polyester coated metal samples succumbed to similar degradation effects in our research as ones stated in literature.

After conducting the above tests with U.W.O powder coated samples, the same samples were then subjected to the antimicrobial testing procedure. This would identify changes in antimicrobial efficacies that may have occurred from soaking in the saline water bath; specifically leaching/ion exchange of silver from coatings and chemical damage to the coatings. Figure 4.34 displays inactivation efficacies against *E. coli* before and after chemical damage testing.

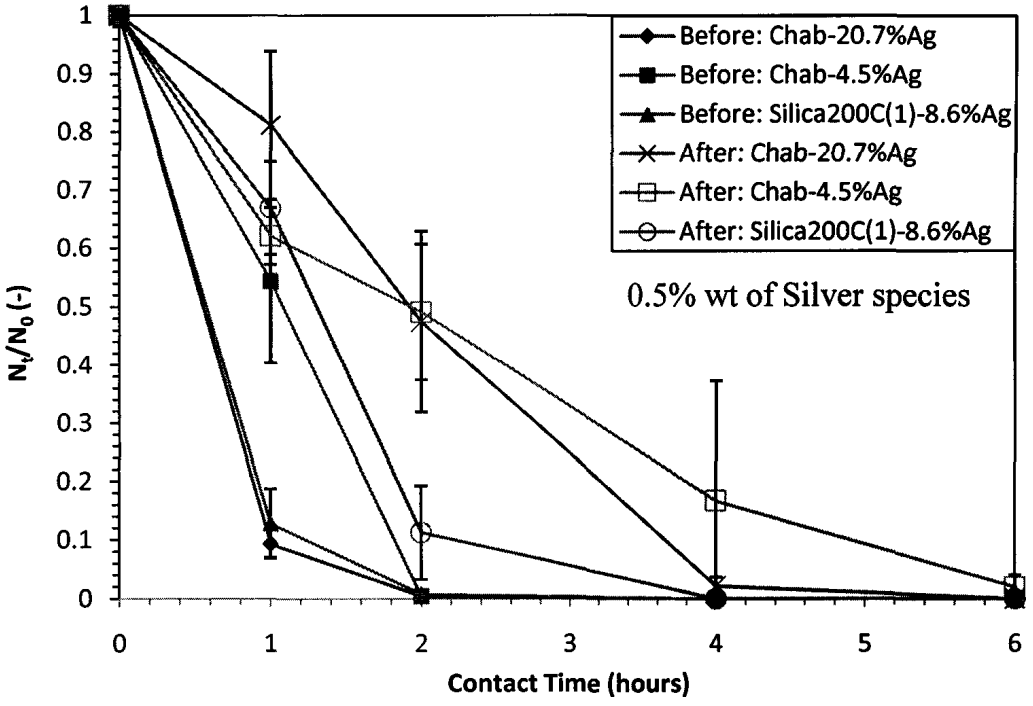

Figure 4.34: *E. coli* inactivation before and after 168 hour soaking in 0.1% saline solution by 0.5%Ag powder coatings (24 hr contact time N_t/N_0= 0; STDEV=0)

In Figure 4.34, with all three U.W.O. samples, it was observed that antibacterial efficacies against *E. coli* worsened due to soaking in the electrolyte water bath. Although efficacies were worsened, they did not fail, as chab-20.7%Ag and silica200C(1)-8.6%Ag showed survival ratios of nearly 0 after 4 hours contact, while chab-4.5%Ag made it to this value after 6 hours contact; 24 hour data showed N_t/N_o=0 with *STDEV*=0 for all samples tested after exposure.

The alleviated toxicity effects shown in Figure 4.34 were caused by two factors previously mentioned: leaching of silver from the coatings and/or chemical damage due

to chloride. The effects due to leaching may have slowed the release of silver from the coatings taking a longer time for the survival ratios to reach 0 values, as the silver concentrations are lower at initial contact times. Surface damage effects may have also negatively impacted the coatings. Degradation of the coatings by means of bubbling and blistering may represent a changed functional ability at the bacteria-surface interface.

Company D's powder coating was subjected to a similar soaking test, but since it failed after gentle washing as previously proven and discussed, it was now predisposed to a very gentle soaking experiment, trying little as possible to negatively detriment the coated surface. With Company D's powder, specimen coated chips were hung, similarly as described prior for U.W.O. samples, in a de-ionized water bath with no mechanical agitation and without the addition of sodium chloride. The time period was also reduced 7 fold as this test only ran for 24 hours rather than 168 hours. Figure 4.35 shows the bactericidal results of company D's powder coating before and after 24 hour soaking period in de-ionized water.

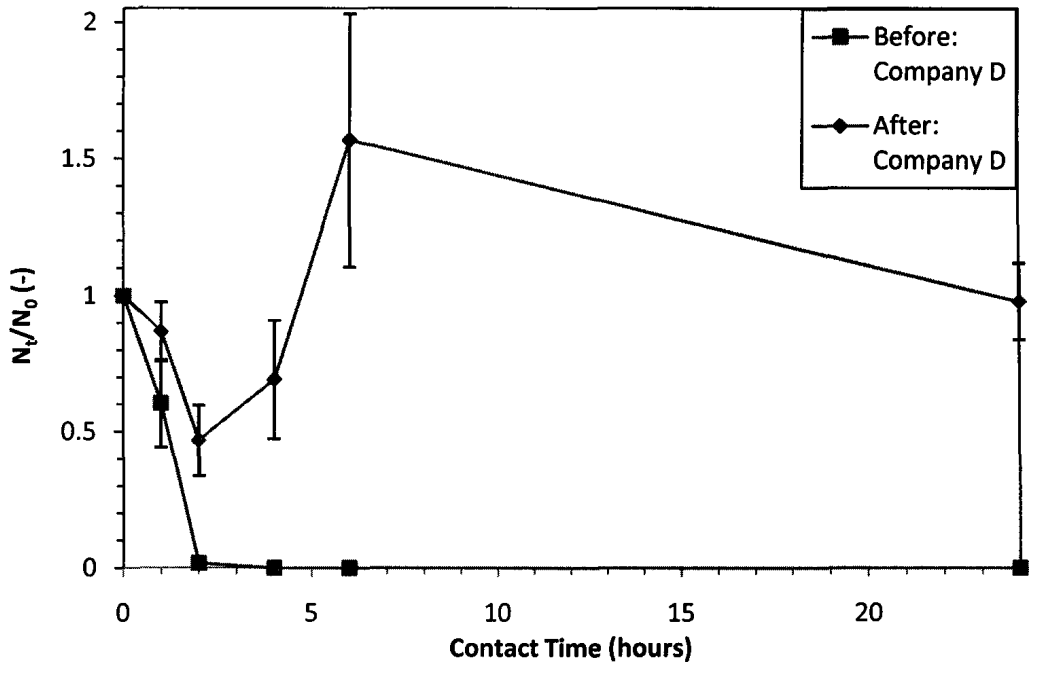

Figure 4.35: *E. coli* inactivation before and after 24 hour soaking in de-ionized water bath by Company D Powder Coating

In Figure 4.35 Company D`s powder coating failed against *E. coli* after gentle soaking in de-ionized water. Although the wear and tear of durability testing procedures was reduced drastically for company D`s coating compared to U.W.O. coatings, Company D`s coating still fails after antimicrobial testing. Company D's coating showed bacterial reductions of 50% after 2 hours contact, but significant increases in population were noticed for almost every time thereafter. The antimicrobial surface coating by company D is simply too sensitive for any kind of environmental stress, as proven in the durability chapter of research.

4.9 Bacterial Kinetics

Inactivation efficiencies of *Escherichia coli* were assumed to follow first order rate kinetics expressed as:

$$\ln\left(\frac{N_t}{N_0}\right) = -kt$$

Where N_t is the average count of CFUs after t hours contact time,

N_0 is the average CFUs at t=0,

k is the inactivation rate constant,

N_t/N_0 is the survival ratio.

The magnitude of the *k* ($hour^{-1}$) constant represents the velocity at which a coated surface can inactivate bacteria. They were calculated from the slope of the survival curves following the first order kinetic analysis or Log_{10} survival ratio plot. There is no present literature that models bacterial inactivation rates based on contact with silver loaded powder coating surfaces. However, literature presents *E. coli* to follow first order inactivation kinetics by inactivation with high carbon dioxide pressure, and TiO_2 photocatalysis (Karaman H, Erkme O, 2001; Pal A, Yu LE, Pehkonen SO, Ray MB, 2007).

The first 4 – 6 hours were examined and *k* constants determined for each main U.W.O. antimicrobial powder produced. Control samples and additives not showing antibacterial action could not be analyzed by this method. Figures 4.36 – 4.39 display the Log_{10} survival ratio plots for the following additives chab-20.7%Ag, chab-3.4(4.5)%Ag, silica200C(1)-8.6%Ag, silica20C(4)-3.6%Ag, silica-50C(6)-2.2%Ag and nanoparticles-31%Ag:

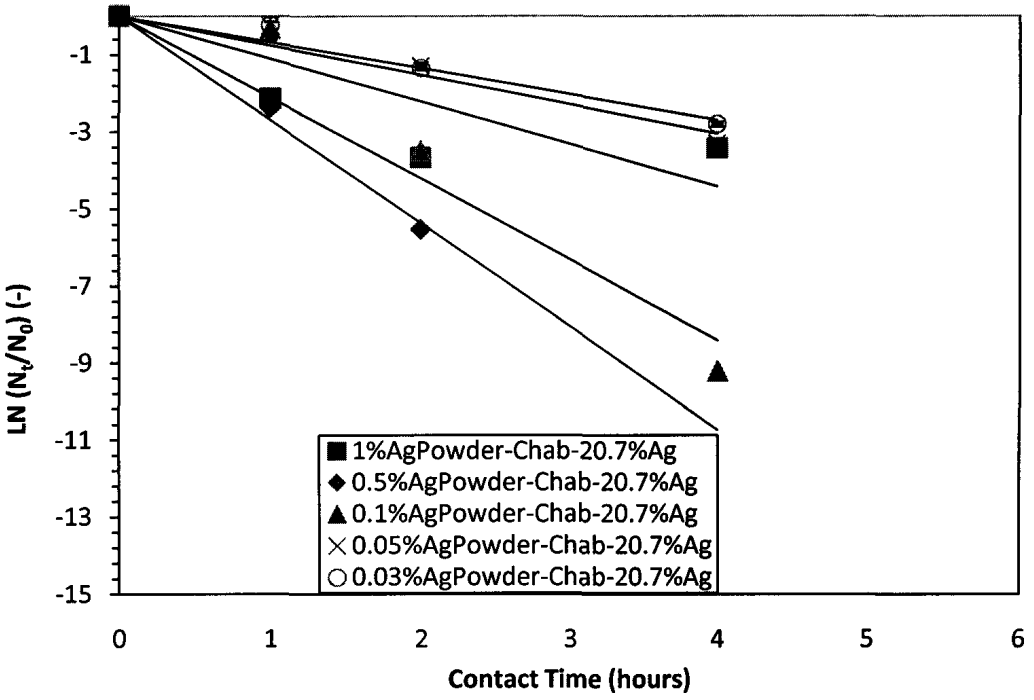

Figure 4.36: Determination of first order rate constant from log_{10} survival ratios with Chab-20.7%Ag additive and varying concentrations in powder coating

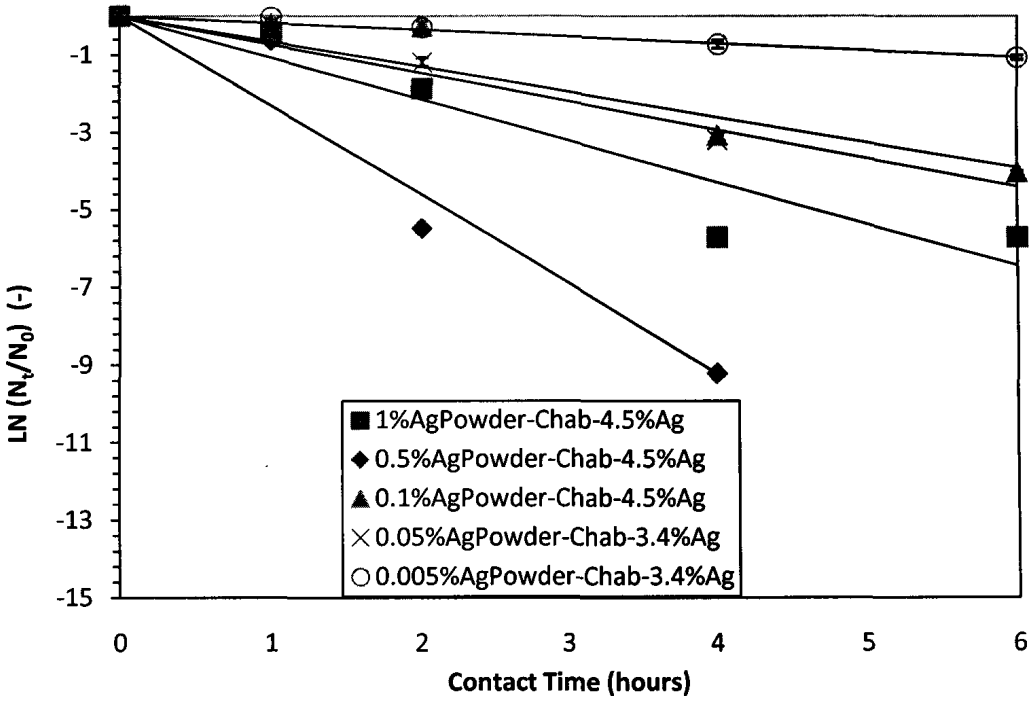

Figure 4.37: Determination of first order rate constant from log_{10} survival ratios with Chab-4.5% or 3.4%Ag additive and varying concentrations in powder coating

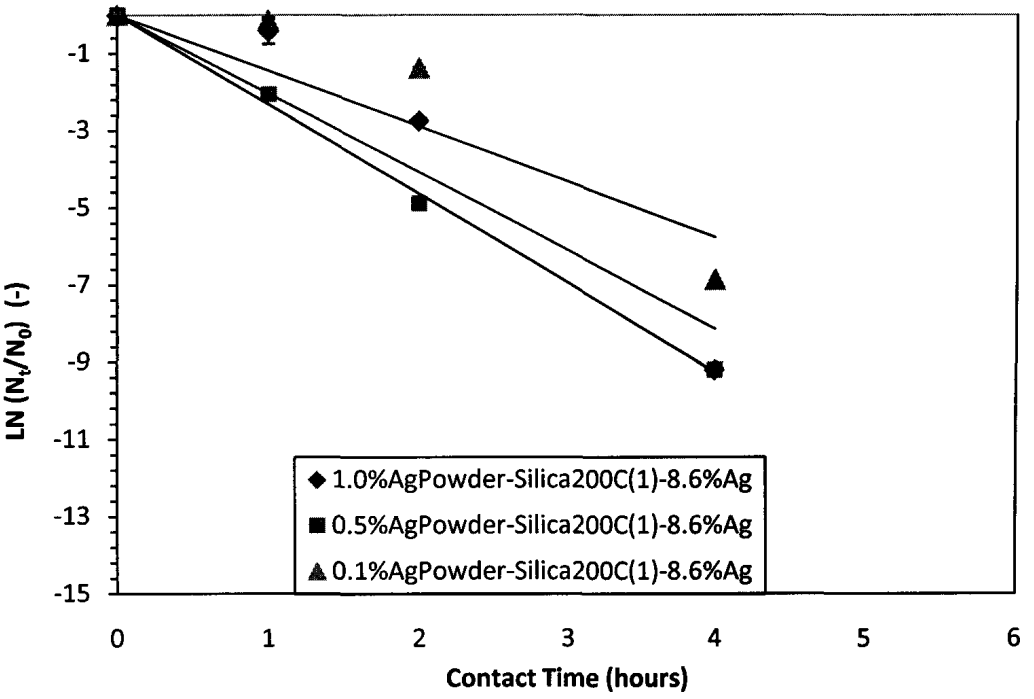

Figure 4.38: Determination of first order rate constant from log_{10} survival ratios with Silica200C(1)-8.6%Ag additive and varying concentrations in powder coating

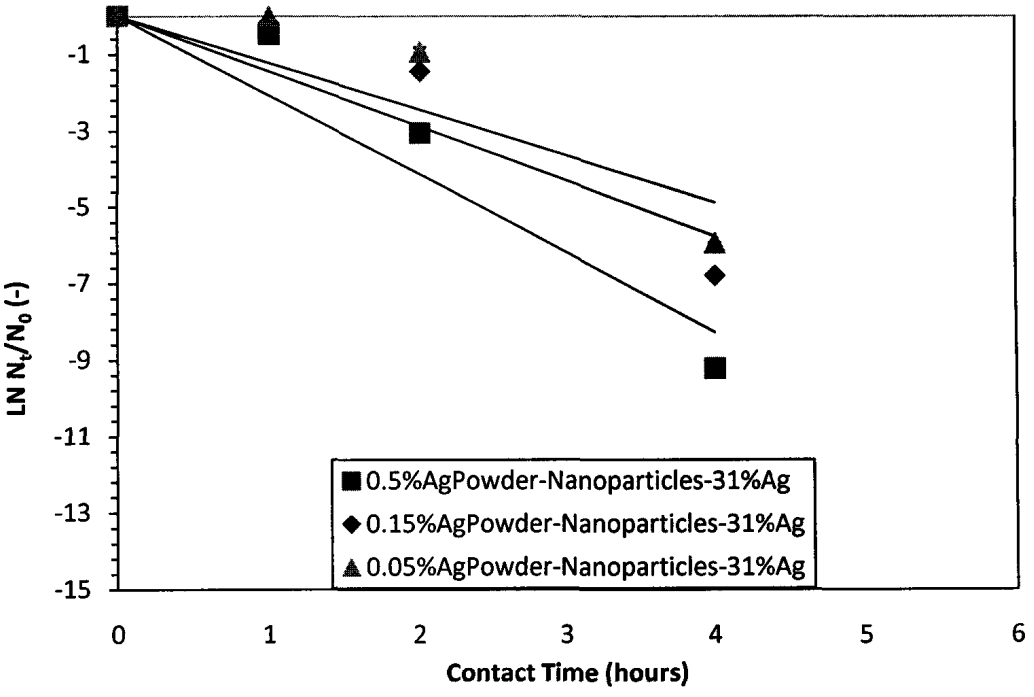

Figure 4.39: Determination of first order rate constant from log_{10} survival ratios with Nanoparticles-31%Ag metal additive and varying concentrations in powder coating

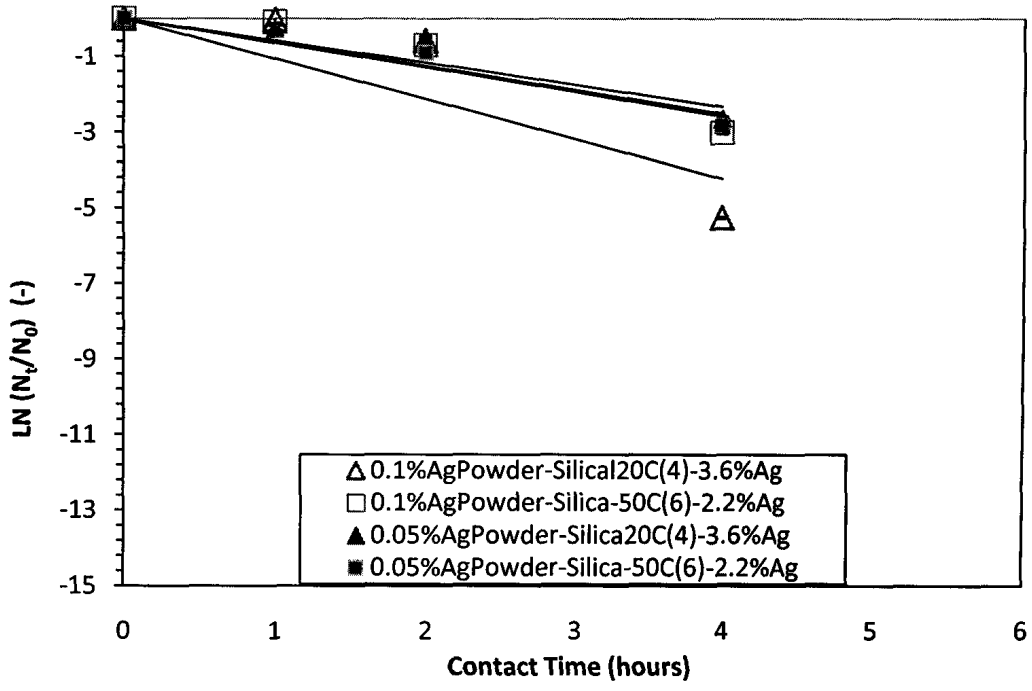

Figure 4.40: Determination of first order rate constant from $\log_{10}$ survival ratios with Silica20C(4)-3.6%Ag and Silica-50C(6)-2.2%Ag additives and varying concentrations in powder coating

From the above plots the first order inactivation rate constants were calculated for all powders at their varying silver weight percentages in the powder coating. Again, only powders tested with varying silver loadings showing bactericidal effects were calculated. k values from each sample can be compared to evaluate the effect of silver loadings for different additives. The Pearson Correlation Co-efficient R^2 was also calculated to verify the first order kinetic models produced and the accuracy of resultant k (hour^{-1}) constants. Table 4.2 summarizes the first order rate constants k and pearson correlation co-efficient R^2 for each sample.

Table 4.2: First order rate constants (k hour^{-1}) and pearson correlation coefficients (R^2) from log_{10} survival ratio plots

Sample Description	Concentration Ag in Coating (weight %)	k (hour^{-1})	R^2
Chab-20.7%Ag	1	1.1035	0.5088
	0.5	2.6828	0.992
	0.1	2.1025	0.9211
	0.05	0.7614	0.9438
	0.03	0.6734	0.9582
Chab-4.5%Ag	1	1.0737	0.9026
	0.5	2.3061	0.9358
	0.1	0.6516	0.8933
Chab-3.4%Ag	0.05	0.7329	0.9367
	0.005	0.174	0.9714
Silica200C(1)-8.6%Ag	1	2.0362	0.8986
	0.5	2.3181	0.9971
	0.1	1.4427	0.8342
Silica20C(4)-3.6%Ag	0.1	1.0567	0.7689
	0.05	0.5781	0.8995
Silica -50C(6)-8.6%Ag	0.1	0.6418	0.8578
	0.05	0.6244	0.88
Nanoparticles-31%Ag Metal	0.5	2.0676	0.9147
	0.15	1.4386	0.8456
	0.05	1.219	0.8006

The correlation coefficient shown for each inactivation constant, provided in the above table, correspond to the validity of the first order kinetic model prescribed to that set of data representing inactivation of bacteria by ionic or metallic silver. It is simply the strength of the relationships between $\log_{10}(N_t/N_0)$ and contact time for each set of data. Results indicate strong relationships in Table 4.2, so previous conclusions may be solidified by the data of inactivation rate constants (k $hour^{-1}$):

- In all or most experiments the same correlation may be drawn for each antibacterial additive: Increased ionic or nano metallic silver weight percentages in the powder coatings equals higher k ($hour^{-1}$) constants thus faster *E. coli* inactivation efficacies, and vice versa,
- Depending on the powder coating system, silver concentrations of atleast 0.05 – 0.03% are required to achieve effectiveness against E. coli after 24 hours contact. Powders failed somewhere in the range below 0.05 – 0.005% silver after 24 hours contact,
- Metallic silver particles in the nanometer range (2-10 nm) present similar inactivation efficiencies when compared with ionic silver additives in ultrafine powder coatings,
- Chabazite zeolite loaded at higher ionic silver loading of 20.7%Ag performs better on an overall basis than loaded at lower level of 4.5%Ag or 3.4%Ag.
- As an inorganic carrier material for ionic silver, Silica Gel is comparable to Chabazite zeolite for most silver concentrations tested,
- Characterization results verifying differences of drying effects between sol – gels were made however bactericidal comparisons present indecisive conclusions as to which sample is superior, as analogous results were obtained for silica samples (4) and (6) possessing microporous and non microporous structures respectively.

5 CONCLUSIONS AND RECOMMENDATIONS

5.1 Summary

Characterization of biocidal powder additives presented properties to help base judgment on accompanied *E. coli* inactivation efficacies:

- For chabazite zeolite, when determining exchange capacities of Ag, Cu, and Zn cations, silver was most susceptible to ion exchange followed by copper and zinc.
- The sequence of ion exchange for cations found naturally in the chabazite followed Na^+, $K^+ > Fe^{2+}$, Ca^{2+}.
- XRPD of chabazite showed slight alterations to crystal structure with higher loaded samples compared to lower loaded samples thus indicating possible surface adsorption of exchanged ionic species; small portion of loosely exchanged silver may have changed from monovalent to zerovalent form.
- BET of silica gel showed failure in microporous structures when drying the sol-gel at 200°C, 1013.25mbar; 100°C, 1013.25mbar; 20°C, 215mbar; and even freeze dried at -50°C, 215mbar. Micro porous structure was obtained without extended aging at 20°C, 1013.25mbar.

Under ASTM E2180 antimicrobial test procedure, different powder coating systems were studied and analyzed against *Escherichia coli* (ATCC 10798) inactivation:

- For all chabazite and silica carriers of ionic silver and freeze dried nano metallic silver, the same general correlation was observed: the higher the silver concentration in the powder coatings, the higher k ($hour^{-1}$) constants thus faster *E. coli* inactivation efficiencies; the lower the silver the less the coating performed. This was observed through testing silver weight percents of 1%, 0.5%, 0.1%, 0.05% and 0.005% for almost all additives.
- Depending on the powder coating system, silver concentrations of atleast 0.05 – 0.03% are required to achieve effectiveness against *E. coli* after 24 hours contact.

Powders failed somewhere in the range below 0.05 – 0.005% silver after 24 hours contact.

- Metallic silver particles in the nanometer range (2-10 nm) from Company V presented similar inactivation efficiencies when contrasted to chabazite and silica carriers of ionic silver in ultrafine powder coatings. At all the specified concentrations tested zero-valent silver worked well as did ionic silver, however the ionic silver samples showed better durability.
- Chabazite zeolite loaded at higher ionic silver loading of 20.7%Ag performs better on an overall basis then loaded at lower level of 4.5%Ag or 3.4%Ag.
- As an inorganic carrier material for ionic silver, Silica Gel is comparable to Chabazite zeolite on all fronts including durability testing. Which one is a superior carrier, cannot be drawn from this research.
- Although characterization results verifying differences of drying effects between sol – gels were made, their bactericidal comparisons present indecisive conclusions, thus the differences in effectiveness are attributed to particle sizes, microporous structures, and/or lower silver loadings yielding higher additive volume.
- Repeatability for certain powders tested at 0.5%Ag concentration presents small error between average survival ratios ranging from 4 – 14% at 1 hour contact times and none or negligible differences for other times.
- Durability testing of chabazite, silica and nanoparticle additives presents only small increases from original trials of survival ratios at 1 – 4 hours contact after light washing with surfactant solution and repeat testing.
- Leaching or ion release sequence obtained after ICP analysis follows silica200C(1)-8.6%Ag > chab-20.7%Ag > chab-3.4%Ag. After the 168 hours in 0.1% saline solution the additives showed excellent *E. coli* inactivation efficacies with small increases in survival ratios from 1 – 6 hours contact. However coatings showed chemical damaging and degradation due to chloride.
- Of the two industrial antimicrobial powder coating systems tested only one, company D, showed any worthwhile effectiveness. Although comparable to

U.W.O. additives for initial trials, durability testing by light washing and soft abrasion, and exposure to deionized water for 24 hours caused the coating to fail.

- Synthetic zeolite-A carrier of ionic silver showed comparable *E. coli* inactivation vs. natural chabazite zeolite at 0.1%Ag concentration, with 1 hour contact outperforming natural zeolite by 66% survival ratio, not including STDEV or repeatability errors. However there are no differences when the zeolites themselves are found in the powder at the same concentrations, regardless of silver loading.
- When ionic silver is incorporated into powder coating by its lonesome without a carrier the curing process causes extreme color changes to the film from clear to deep yellow indicating reduction of Ag^{+} to Ag^{0}, silver oxide, which literature has proven to be less effective against bacteria. Although initial testing works comparatively at 0.1%Ag weight in the coating, it is presumed that the longevity of this coating is feeble.
- Reduction of ionic silver to silver metal through chemical process by Tollen's Reagent, assuming complete reaction, presents excellent initial antibacterial effectiveness at high concentrations in powder coatings. These micro metallic silver species do not hold up at lower concentrations where nano silver particles do, verifying the size of metallic silver particles; as they decrease down to nano-scale their antibacterial efficacy increases due to their size, larger total surface area per unit volume in the coating, and sensitivity thereby releasing silver ions.
    - Carbon nano tubes were shown to be ineffective for inactivation of bacteria when tollen's reagent was reduced in their presence.
- By applying the obtained growth curve results from research to a first order bacterial kinetic model, R^2 values verified that the *E. coli* inactivation by powder coatings followed first order kinetics. This allowed determination of inactivation k ($hour^{-1}$) constants to further support and justify previous findings.

5.2 Conclusion

Antimicrobial activity due to inorganic silver agents shows promising results in the area of ultrafine powder coatings. In this research, simple clear coloured surfaces were produced through essential use of a clear polyester TGIC resin system with no fillers or pigments. Inorganic antimicrobial additives were dry blended or freeze dried with the ultrafine resin powder, post extrusion, becoming the first antimicrobial powder coating system of its kind. The unique coatings produced, on aluminum substrates, possessed the ability to inactivate *Escherichia coli* populations, of average 100×10^7 CFU, to proven reductions of over 99% within only couple hours of contact under ideal bacterial growth conditions. The most functional additives in the coatings included ionic silver species housed in natural chabazite zeolite or silica glass particles, as well as silver metallic nanoparticles. These coatings proved to be equal to or outperform the best industrial antimicrobial coatings under first trial conditions. Moreover, after durability washing and leaching/chemical damaging experiments it was proven that U.W.O. antimicrobial coatings revealed superior longevity and impressive functionality over industrial coatings even under worsened environmental conditions.

The goal to develop simple, highly durable, antimicrobial ultrafine powder coatings was achieved in this research project.

5.3 Recommendations

There are many aspects that may be considered for future work:

- Evaluate the effectiveness of other inorganic functional carriers for ionic and/or nano metallic silver.
- Conduct studies with photocatalytic agents into powder coatings at minimal UV exposure similar to normal room conditions to justly compare against silver species.
- Doped TiO_2 is a suggested material for future work as it exhibits high reactivity as a photocatalyst under visible light ($\lambda \leq 400$ nm) allowing the main part of the solar spectrum, even under poor illumination of interior lighting, to be used.
- Work with powder coating manufacturers of antimicrobial additives to standardize a procedure for durability testing of antimicrobial surfaces.
    - Continue with durability testing of UWO antimicrobial powder coatings and determine an accurate time frame for the longevity of the coatings and the accompanied effectiveness over time.
- Conduct similar studies with dry blended nano additives (Zhu J and Zhang H, 2004; U.S. Patent 6,833,185) to increase surface area and effectiveness of antimicrobial additives by enhancing fluidization of powder.
- Incorporate antimicrobial additives pre-extrusion and conduct similar testing to evaluate the advantages/disadvantages of dry blending additives post extrusion in antimicrobial ultrafine powder coatings (Zhu J, Zhang H, 2006; U.S. Patent Application 11/601,846).
- Direct research into the biomedical engineering field and initialize *in vitro* testing of functional antimicrobial surfaces by ultrafine powder coatings mimicking *in vivo* conditions and present results for applications of biomaterials and accompanied cytotoxicity.
- Evaluate the antimicrobial effectiveness of U.W.O. powder coatings against other strains of bacteria including *Staphylococcus aureus* as this type is gram positive and most popular for nosocomial infections.

6 REFERENCES

Anandan S, Vinu A, Venkatachalam N, Arabindoo B, Murugesan V. (2006). Photocatalytic activity of ZnO impregnated Hβ and mechanical mix of ZnO/Hβ in the degradation of monocrotophos in aqueous solution. *Journal of Molecular Catalysis A: Chemical*, (256), 312-320.

Azoulay A, Garzon P, Eisenberg MJ. (2001). Comparison of the Mineral Content of Tap Water and Bottled waters. *JGIM.* 16, 168-175.

Bansal RC, Goyal M. (2005). *Activated carbon adsorption.* CRC Press: 103-107

Baranoski S, Ayello E. (2007). *Wound Care Essentials: Practice Principles.* Lippincott Williams & Wilkins, (2), 358.

Bayston R, Ashraf W, Bhundia C. (2004). Mode of action of an antimicrobial biomaterial for use in hydrocephalus shunts. *Journal of Antimicrobial Chemotherapy.* (53), 778–782.

Bayston R, Allison D. (2000). *Community Structure and Co-operation in Biofilms: Biofilms and prosthetic devices.* Nottingham: Cambridge University Press, 295 – 300.

Bennett JV, Brachman PS. (1992). *Hospital infections.* Boston: Little, Brown, and Company, 577-596.

Berins ML. (1991). SPI plastics engineering handbook of the Society of the Plastics Industry. Springer Inc. (5), 497-503.

Bhattacharya, P.K. Metal ions in biochemistry. Edition: illustrated. Published by Alpha Science Int'l Ltd., 2005

Bonilla HF, Zervos MJ, Kauffman CA. (1996). Long-term survival of vancomycin-resistant Enterococcus faecium on a contaminated surface. *Infect. Control Hosp. Epidemiol.* (17), 770–771.

Bouvy C, Marine B, Sporken R, Su BL. (2007). Nanosized ZnO confined inside a Faujasite X zeolite matrix: Characterization and optical properties. *Colloids and Surfaces A: Physicochemical and Engineering Aspects,* 300 (1-2), 145-149.

Brinker CJ, Scherer GW. (1990). *Sol-Gel Science: The Physics and Chemistry of Sol-Gel Processing.* New York: Academic Press Inc.

Buckley F, Hope G. (2006). Electroless Deposition of Ag Thin Films. *ICONN Nanoscience and Nanotechnology.* (1-2), 528-531.

Centers for Disease Control and Prevention. (2002). Evaluation of Bacillus anthracis contamination inside the Brentwood mail processing and distribution center. *JAMA.* 287(4), 445-446.

Chung RJ, Hsieh M, Huang CW, Perng LH, Wen HW, Chin TS. (2005). Antimicrobial Effects and Human Gingival Biocompatibility of Hydroxyapatite Sol–Gel Coatings. *Journal of Biomedical Materials Research. Part B. Applied Biomaterials*, 76(1), 169-178.

Cohen HA, Amir J, Matalon A, Mayan R, Beni S, Barzilai A. (1997). Stethoscopes and otoscopes--a potential vector of infection? *Fam Pract.*14(6), 446-9.

Conly JM, Johnston LB. (2000). Antibiotic resistance in Canada at the dawn of the new millennium – A model for the developed world? *Can Journal Infect Dis.,* 11, 232-236.

Cowan M, Abshire KZ, Houk SL, Evans SM. (2003). Antimicrobial efficacy of a silver-zeolite matrix coating on stainless steel. *Journal of Industrial Microbial Biotechnology*, (30), 102-106.

Cytec Product Guide. (2006). *Binder Resins, Hardeners and Additives Americas*. Cytec Surface Specialties Inc: UV Links

Dong F, Li G, Sun Z, Shen Gang, Feng Q, Dai Q. (2005). Preparation and antimicrobial ability of natural proous antibacterial materials. *Journal of central South University of Technology*. 12(4), 370-375.

Dorcheh AS, Abbasi MH. (2008). Silica aerogel; synthesis, properties and characterization. *Journal of materials processing technology,* 199, 10–26.

Dutronc H, Dupon M, Cipriano G, Lafarie S, Lafon ME, Fleury HJ, Bocquentin F, Neau D, Ragnaud JM. (2004). Severe acute respiratory syndrome: one case of indirect transmission by Coronavirus. *Rev Med Interne*. (8), 607-609.

Ewald A, Gluckermann SK, Thull R, Gbureck U. (2006). Antimicrobial titanium/silver PVD coatings on titanium. *BioMedical Engineering OnLine.*(5), 22.

Fang M, Chen JH, Xu XL, Yang PH, Hildebrand H. (2006). Antibacterial activities of inorganic agents on six bacteria associated with oral infections by two susceptibility tests. *International Journal of Antimicrobial Agents*. 27, 513-517.

Feied, Craig. (2004). Novel Antimicrobial Surface Coatings and the Potential for Reduced Fomite Transmission of SARS and Other Pathogens. *MD*. (1), 1-22.

Feng QL, Cui FZ. (1999). Ag-substituted hydroxyapatite coatings with both antimicrobial effects and biocompatibility. *Journal of Materials Science Letters*. 18, 559-561.

Feng QL, Wu J, Chen GQ, Cui FZ, Kim TN, Kim JQ. (2000). A Mechanistic Study of the Antibacterial effect of Silver Ions on Escherichia coli and Staphylococcus aureus. *Journal Biomed Mater Res*, 52(4), 662-668.

Folgar C, Folz D, Suchicital D, Clark D. (2007). Microstructural evolution in silica aerogel. *Journal of Non-Crystalline Solids,* 353, 1483–1490.

Furno F, Morley K, Wong B, Sharp B, Arnold P, Howdle S, Bayston R, Brown P, Winship P, Reid H. (2004). Silver nanoparticles and polymeric medical devices: a new approach to prevention of infection? *Journal of Antimicrobial Chemotherapy.* 54, 1019–1024.

Ghosh SK. (2006*). Functional coatings: by polymer microencapsulation.* Wiley-VCH. 357: 1-25

Gollwitzer H, Ibrahim K, Meyer H, Mettelmeier W, Busch R, Stemberger A. (2003). Antibacterial poly(D,L-lactic acid) coating of medical implants using a biodegradable drug delivery technology. *Journal of Antimicrobial Chemotherapy.* 51, 585–591.

Gottenbos B, Grijpma DW, van der Mei HC, Feijen J, Busscher HJ. (2001). Antimicrobial effects of positively charged surfaces on adhering Gram-positive and Gram negative bacteria. *Journal of Antimicrobial Chemotherapy.* 48, 7-13.

Gottenbos B, Klatter F, van der Mei HC, Busscher HJ, Nieuwenhuis P. (2001) Late Hematogenous Infection of Subcutaneous Implants in Rats. *Clinical and Diagnostic Laboratory Immunology.* 8, 980-983.

Gottenbos B, van der Mei HC, Busscher HJ. (1999). Models for studying initial adhesion and surface growth in biofilm formation on surfaces. *Methods in Enzymology*, 310, 523-33.

Haile T, Nakhla G. (2008). Inhibition of bacterial 504 concrete corrosion by Acidithiobacillus thiooxidans with functionalized zeolite-A coating, *Biofouling,* 12, 1–12.

Hardy SP. (2002). *Human microbiology.* Illustrated Edition. CRC Press. pg 191.

Hitti M. (2007). *Top Spots for Bacteria at home.* Survey Source: The Hygiene Council. MDMedical News: Chang, Louise MD.

Howell D. (2000). *Powder Coatings: The Technology, Formulation and Application of Powder Coatings.* Volume 1. West Sussex, England: John Wiley and Sons Ltd.

Huang Z, Maness PC, Blake DM, Edward J, Wolfrum EJ, Smolinski SL, and Jacoby WA. (2000). Bactericidal mode of titanium dioxide photocatalysis. *Journal of Photochemistry and Photobiology A: Chemistry*, 130, 163–170.

Hughes WT, Williams B, Pearson T. (1986). The nosocomial colonization of T. Bear. *Infect Control.* (10), 495-500.

Hu CH, Xu ZR, Xia MS. (2005). Antibacterial effect of Cu2+-exchanged montmorillonite on Aeromonas hydrophila and discussion on its mechanism.*Veterinary Microbiology,* 109, 83–88.

Hutson NC, Reisner BA, Yang RT, Toby BH. (2000). Silver Ion-Exchanged Zeolites Y, X, and Low-Silica X: Observations of Thermally Induced Cation/Cluster Migration and the Resulting Effects on the Equilibrium Adsorption of Nitrogen. *Chem. Mater.*, 12 (10), 3020–3031.

Inabo, HI. (2006). The significance of Candida infections of medical Implants. *Academic Journals*. 1 (1), 8-10.

Inoue Y, Kanzaki Y. (1997). The mechanism of antibacterial activity of silver loaded zeolite. *Journal of Inorganic Biochemistry*. 67 (1– 4), 377.

Ijaz MK, Brunner AH, Sattar SA, Nair RC, Johnson-Lussenburg CM. (1985). Survival characteristics of airborne human coronavirus 229E. *Journal of Gen. Virol.*, 66, 2743-8.

IUPAC. (1994). *Recommendations*. Pure Applied Chemistry. 66, 1739.

Johnson WA. (1998). *Invitation to Organic Chemistry*. Jones and Bartlett Publishers. Illustrated edition. 456- 457.

Karaman H, Erkme O. (2001). High carbon dioxide pressure inactivation kinetics of Escherichia coli in broth. *Food Microbiology*. 18, 11-16.

Kawashita M, Tsuneyama S, Miyaji F, Kokubo T, Kozuka H, and Yamamoto K, (2000). Antibacterial silver containing silica glass prepared by sol gel method. *Biomaterials*. 21, 393-398.

Kourai H, Manabe Y, Yamada Y. (1994). Mode of bactericidal action of zirconium phosphate ceramics containing silver ions in the crystal structure. *Journal of Antibacterial Antifungal Agents*, 22, 595-601.

Kuhn KP, Chaberny IF, Massholder K. (2003). Disinfection of Surfaces by photocatalytic oxidation with titanium dioxide and UVA light. *Chemospherel*. 53, 71-77.

Kumar A, Vemula PK, Ajayan PM and John G. (2008). Silver-nanoparticle-embedded antimicrobial paints based on vegetable oil nature materials. *Nature Materials*, 7, 236-241.

Langella A, Pansini M, Cappelletti P, de Gennaro B, de Gennaro M, Colella C. (2000). NH4+, Cu2 +, Zn2 +, Cd2 +, and Pb2 +exchange for Na+ in a sedimentary clinoptilolite, North Sardinia, Italy. *Microporous and Mesoporous Materials,* 37, 337–343.

Lansdown A. (2006). Silver in Health Care: Antimicrobial Effects and Safety in use. *Karger Journals - Biofunctional Textiles and the Skin*. 33, 17–34.

Lee L. (2004). *100 Most Dangerous things in everyday life and what you can do about them*. Broadway. 60-61.

Lehr W. (1991). *Powder Coating Systems*. New York, USA: McGraw-Hill Inc.

Li Z, Flytzani-Stephanopoulos M. (1997). Selective catalytic reduction of nitric oxide by methane over cerium and silver ion-exchanged ZSM-5 zeolites. *Applied Catalysis A: General.* 165 (1-2), 15-34.

Liberto N. (2003). *User's Guide to Powder Coating.* 4th Edition, Michigan, USA: Association
for Finishing Processes and Society of Manufacturing Engineers.

Maness PC, Smolinski S, Blake DM, Huang Z, Wolfrum EJ and Jacoby WA. (1999). Bactericidal activity of photocatalytic TiO_2 reaction: toward an understanding of its killing mechanism. *App. and Envi. Microbiology.* 65, 4094–4098.

Mawatari M, Hamazaki C, Furuyama T. *Antibacterial Resin Composition.* USPTO Full text and Image Database. United States Patent 5614568: March 25, 1997.

Matsumura Y, Yoshikata K, Kunisaki S, Tsuchido T. (2003). Mode of Bactericidal Action of Silver Zeolite and Its Comparison with That of Silver Nitrate. *Appl Environ Microbiol.* 69(7), 4278–4281.

McDonnell AMP, Beving D, Wang A, Chen W, Yan Y. (2005). Hydrophilic and antibacterial zeolites coatings for gravity-independent water separation. *Advanced Functional Materials,* 15, 336-340.

Merriam-Webster's Medical Desk Dictionary. (2005). Merriam-Webster Incorporated.

Modak SM. (1973). Binding of silver sulfadiazine to the cellular components of Pseudomonas aeruginosa, *Biochemical Pharmacology*, 22, 2391-2404.

Moore CM, Sheldon BW, Jaykus LA. (2003). Transfer of Salmonella and Campylobacter from stainless steel to romaine lettuce. *Journal Food Prot.*, 66(12), 2231- 2236.

Morones JR, Elechiguerral JL, Camacho A, Holt K, Kouri JB, Ram´ırez JT, Yacaman MJ. (2005). The bactericidal effect of silver nanoparticles. *Nanotechnology*, 16, 2346–2353.

Neuta D, van de Belt H, Stokroos I, van Horn JR, van der Mei HC, Busscher HJ. (2001). Biomaterial-associated infection of gentamicin-loaded PMMA beads in orthopaedic revision surgery. *Journal of Antimicrobial Chemotherapy.* 47, 885–891.

Niira R, Niira Y, Yamamato T, Uchida M. *Antibiotic Resin Composition.* USPTO Full text and Image Database. United States Patent 4938955 July 3, 1990.

Noskin GA, Stosor V, Cooper I, Peterson LR. (1995). Recovery of vancomycin-resistant enterococci on fingertims and environmental surfaces. *Infect Control Hosp Epidemiol.*(16), 577-581.

Novak KD, Kowalski RP, Karenchak LM, Gordon YJ. (1995). Chlamydia trachomatis can be transmitted by a nonporous plastic surface in vitro. *Cornea.* 14(5), 523-526.

O'Neill C, Beving DE, Chen W, Yan Y. (2006). Durability of Hydrophilic and Antimicrobial Zeolite Coatings under Water Immersion. *AIChE Journal.* 52 (3), 1157-1161.

Pal A, Min X, Yu LE, Pehkonen SO, Ray MB. (2005). Photocatalytic inactivation of bioaerosols by TiO_2 coated membranes. *International Journal of Chemical reactor Engineering.* 3 (A45), 1-11.

Pal A, Yu LE, Pehkonen SO, Ray MB. (2007). Photocatalytic inactivation of Gram – positive and Gram-negative bacteria by fluorescent light. Journal *of Photochemistry and Photobiology A: Chemistry,* 186 (2-3), 335-341.

Palmer JL, Gunter ME. (2001). The effects of time, temperature, and concentration on Sr2 + exchange in clinoptilolite in aqueous solutions. *American Mineralogist*, 86, 431–437.

Pinnel SR, Fairhurst D, Gilles R. (2000). Microfine Zinc oxide is a Superior Sunscreen Ingredient to microfine Titanium dioxide. *Dermatol Surg.* 26(4), 309-314.

Preston, Richard. (1994). *The Hot Zone.* New York: Random House.

Radheshkumar C, and Munstedt H. (2007). Antimicrobial Polymers from Polypropylene/Silver Composites-Ag+ Release Measured by Anode Stripping Voltammetry. *Reactive and Functional Polymers.* 66, 780-788.

Ratner BD, Hoffman AS, Schoen FJ, Lemons JE (2004). Biofilms, biomaterials, and device-related infections. *Biomaterials science: An introducion to materials in medicine.* San Francisco, CA: Elsevier Academic Press; (2) 345-354.

Rimondini L, Fini M, Giardino R. (2005). The microbial infection of biomaterials: A challenge for clinicians and researchers. *Journal of Applied Biomaterials & Biomechanics.* 3 (1), 1-10.

Rodrigues L, Banat IM, Teixeira J, Oliveira R. (2006). Biosurfactants: potential applications in medicine. *Journal of Antimicrobial Chemotherapy.* 57(4), 609–618.

Rossi S, Azghani AO, Abdelwahab O. (2004). Antimicrobial efficacy of a new antibiotic-loaded poly(hydroxybutyric-co-hydroxyvaleric acid) controlled release system. *Journal of Antimicrobial Chemotherapy.* 54, 1013–1018.

Sakaoka H, Saheki Y, Uzuki K, Nakakita T, Saito H, Sekine K, Fujinaga K. (1986). Two outbreaks of herpes simplex virus type 1 nosocomial infection among newborns. *Journal Clinical Microbiology.* 24(1), 36-40.

Schachter B. (2003). Slimy Business – the biotechnology of bioflms. *Nature Biotechnology.* 21, 361- 365.

Schram PJ, Earley MW. (1997). *Electrical Installations in Hazardous Locations.* Jones & Bartlett Publishers, (2), 91 – 98.

Shen B, Scaiano JC, English AM. Zeolite Excapsulation Decreases TiO2 photosensitized ROS Generation in Cultured Human Skin Fibroblasts. *Photochemistry and Photobiology.* 82 (1), 5-12.

Shen Z, Ning F, Zhou W, He X, Lin C, Chin DP, Zhu Z, Schuchat A. (2004). Superspreading SARS events, Beijing, 2003. *Emerg Infect Dis.* 10(2), 256-60.

Souto RM, Gonzalez-Garcia Y, Gonzalez S, Burstein GT. (2004). Damage to paint coatings caused by electrolyte immersion as observed in situ by scanning electrochemical microscopy. *Corrosion Science.* 46(11), 2621-2628.

Sun Y, Yin Y, Mayers B, Herricks T, Xia Y. (2002). Uniform Silver Nanowires Synthesis by Reducing AgNO3 with Ethylene Glycol in the presence of Seeds and Poly (Vinyl Pyrrolidone). *Chem. Mater.* 14, 4736-4745.

Sundkvist T, Hamilton GR, Hourihan BM, Hart IJ. (2000). Outbreak of hepatitis A spread by contaminated drinking glasses in a public house. *Commun Dis Public Health.* (1), 60-62.

Suratwala T.I. (2003). Surface Chemistry and Trimethylsilyl functionalization of stober silica sols. *Journal of Non-crystalline Solids.* 316, 349-363.

Starfield B. (2000). Is US Health Really the Best in the World? *JAMA*, 284(4), 483-5.

Top A, Ulku S. (2004). Silver, zinc, and copper exchange in a Na-clinoptilolite and resulting effect on antibacterial activity. *Applied Clay Science,* 27, 13– 19.

Vohre A, Goswami DY, Deshpande DA, Block SS. (2005). Enhanced Photo-catalytic Inactivation of Bacterial Spores on Surfaces in Air. *Journal of Industrial Microbial Biotechnology*, 32, 364-370.

Von Recum AF, and LaBerge M. (1995). Educational Goals for Biomaterials Science and Engineering: Perspective View. *Journal of Applied Biomaterials*, 6, 137-144.

Wagener M, Steinruecke P, Bechert T. (2004). Antimicrobial Coatings by Using Nanosilver Particles. Orlando, FL: Published Papers from the Second Global Conference Dedicated to *Hygienic Coatings and Surface.*

Watterson RS, Hanrahan WD. (2002). *Antimicrobial Acrylic Material.* USPTO Full text and Image Database. U.S. Patent 6448305.

Wendt C, Wiesenthal B, Dietz E, Ru-den H. (1998). Survival of Vancomycin-Resistant and Vancomycin-Susceptible Enterococci on Dry Surfaces. *Journal of Clin Microbiol.* (12), 3734–3736.

Wenzel RP. (1995). The Economics of Nosocomial Infection. *Journal of Hospital Infections.* 31, 79-87.

Wenzel RP, Edmond MB. (2001). Emerging Infectious Diseases. *Centers for Disease Control*, 7, 1-2.

Whitman WB, Coleman DC, Wiebe WJ. (1998). Prokaryotes: the unseen majority. *Proc Natl Acad Sci*, 95(12), 6578-83.

Williams RL, Doherty PJ, Vince DG, Grashoff GJ and Williams DF. (1989). The biocompatibility of silver. *Critical Reviews in Biocompatibility*, 5, 221.

Wilson AD, Nicholson JW, Prosser HJ. (1987). *Surface Coatings-1*. London: Elsevier Science & Technology, (1), Chapter 1.

Wright JD, Johnson AN, Moldover MR. (2003). Design and Uncertainty Analysis for a PVTt Gas Flow Standard. *Journal of Research of the National Institute of Standards and Technology*. 108, 21-47.

Xie Y, Liu H, Hu N. (2007). Layer-by-layer films of hemoglobin or myoglobin assembled with zeolite particles: Electrochemistry and electrocatalysis. *Bioelectrochemistry*. 70(2), 311- 319.

Yamamoto T, Utida M, Nakata S, Nakagawa Z. Preparation of anti-bacterial zeolites and their anti-bacterial effects. *Journal of Food Chem*, 9(3).

Zeren S, Preuss A, Konig B. (2005). *Checkmate for Microbes: Biocides based on silver ions.* BNP Publication. Paint and Coatings Industry Magazine – European Coatings Show Issue: 38-44.

Zhang L, Jiang Y, Ding Y, Povey M, York D. (2007). Investigation into the antibacterial behaviour of suspensions of ZnO nanoparticles. *Journal of Nanoparticle Research*, 9, 479-489.

Zhang N, Xie J, Guers M, Varadan K. (2004). Chemical bonding of multiwalled carbon nanotubes to polydimethylsiloxanes and modification of the photoinitiator system for microstereolithography processing. *Smart Material Structure*. 13, N1–N4.

Zhu J, Zhang H. *Fluidization Additives to Fine Powders*. USPTO Full text and Image Database. U.S. Patent 6,833,185. 2004.

Zhu J, Zhang H. *Method and Apparatus for Uniformly Dispensing Additive Particles in Fine Powders.* USPTO Full text and Image database. U.S. Patent Application 11/601,846. 2006.

7 APPENDIX

7.1 Appendix A: Equipment Images

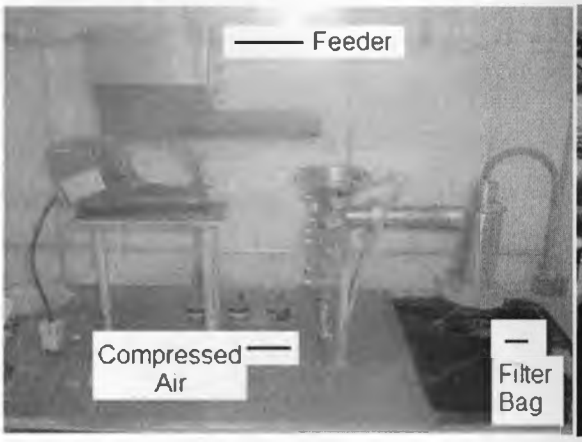

Figure 7.1: Opposed Nozzle Jet Milling System

Figure 7.2: Ball Milling Equipment

Figure 7.3: Freeze Dryer Equipment

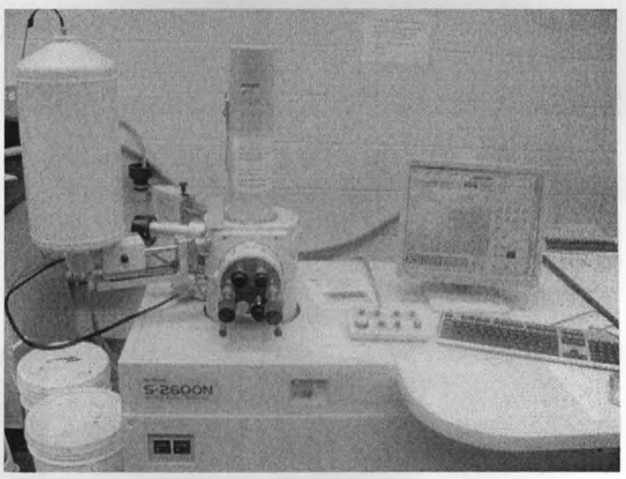

Figure 7.4: Scanning Electron Microscope

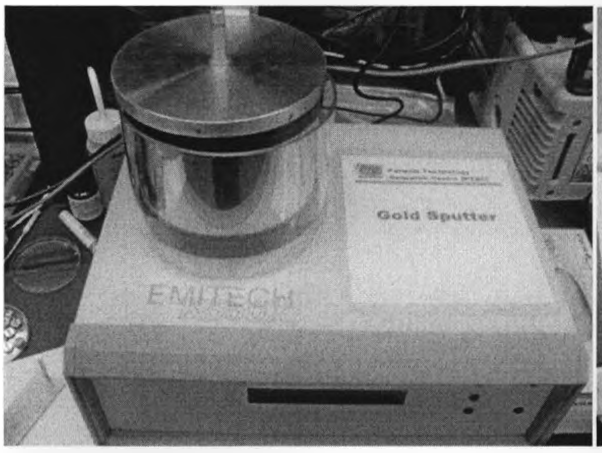

Figure 7.5: Gold Sputter Device

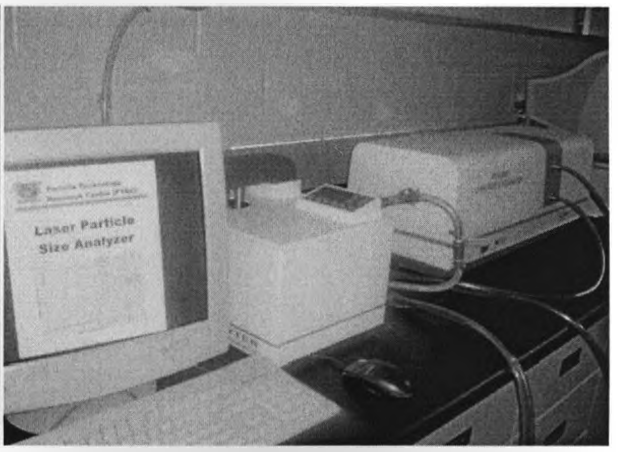

Figure 7.6: BT-9300 Laser Particle Size Analyzer

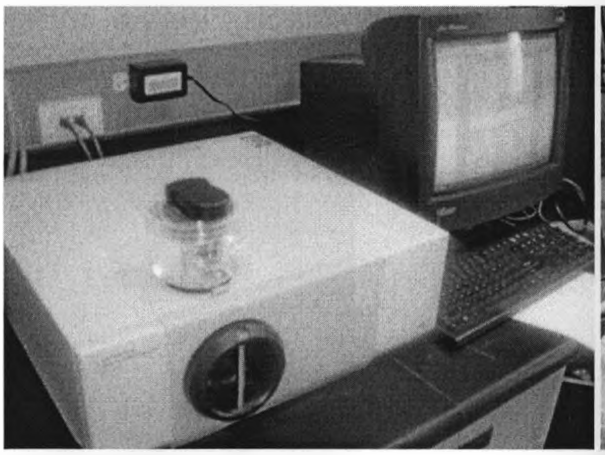

Figure 7.7: TSI 3603 Particle Size analyzer

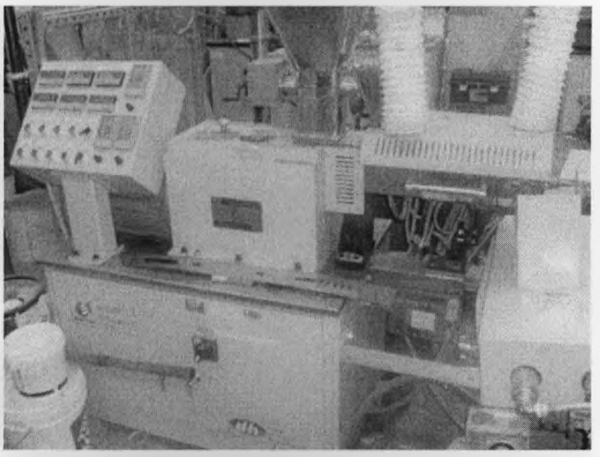

Figure 7.8: Twin screw extruder with cooling belt

Figure 7.9: High Shear Grinder

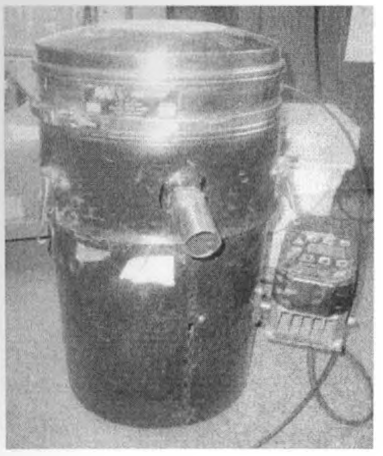

Figure 7.10: Vorti-Siv Screening Equipment

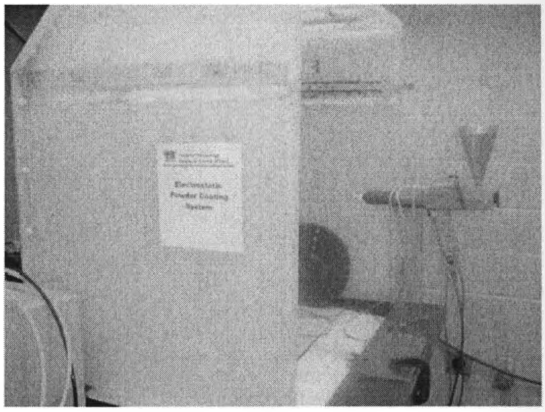

Figure 7.11: Coating booth and Spray gun

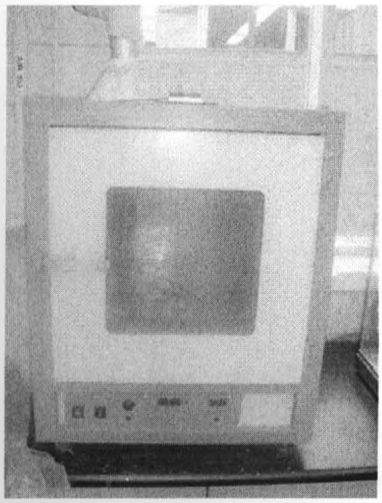

Figure 7.12: Convection oven for curing

Figure 7.13: Autoclave for sterilization purposes

Figure 7.14: Biological Safety Cabinet

Figure 7.15: Orbital Incubator

7.2 Appendix B: Sample EDX Spectrums

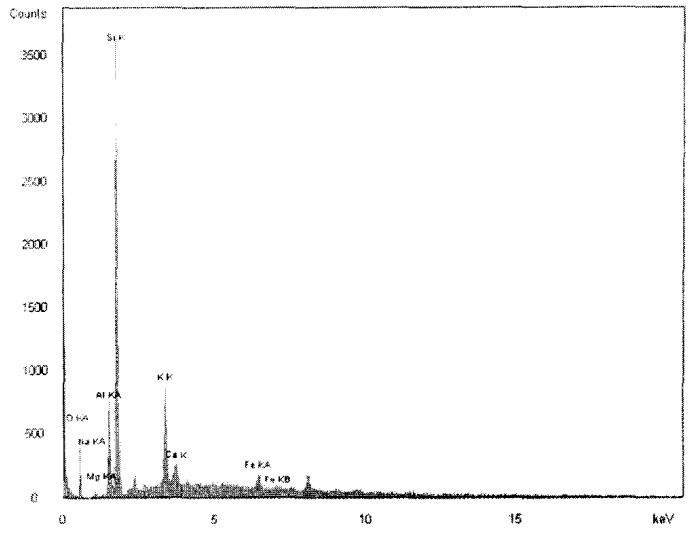

EDX	Oxygen (O)	Aluminum (Al)	Silica (Si)	Sodium (Na)	Potassium (K)	Calcium (Ca)	Iron (Fe)
Concentration Weight %	38.63	5.84	35.77	1.7	10.72	1.24	6.1

Figure 7.16: EDX Spectrum Blank Chabazite Zeolite

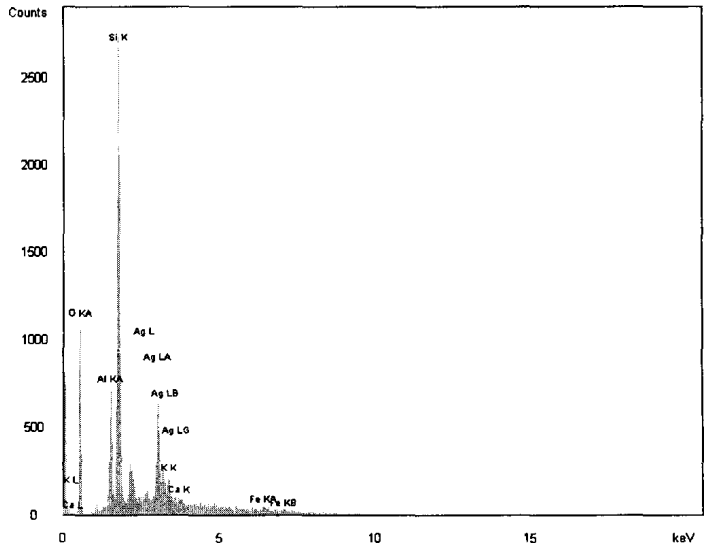

EDX	Oxygen (O)	Aluminum (Al)	Silica (Si)	Potassium (K)	Calcium (Ca)	Iron (Fe)	Silver (Ag)
Concentration Weight %	33.87	4.63	34.52	1.7	0.68	4.12	20.48

Figure 7.17: EDX spectrum Chabazite Zeolite after ion exchange with 0.05 M silver nitrate

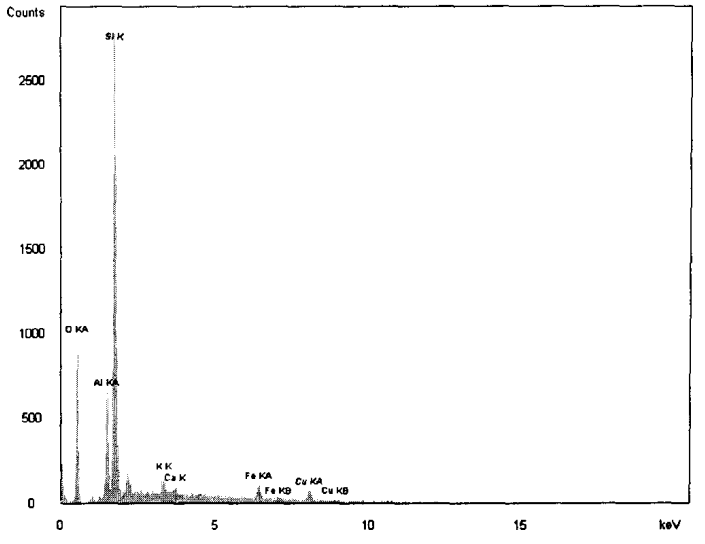

EDX	Oxygen (O)	Aluminum (Al)	Silica (Si)	Potassium (K)	Calcium (Ca)	Iron (Fe)	Copper (Cu)
Concentration Weight %	40.44	6.36	34.33	1.73	0.72	5.14	11.28

Figure 7.18: EDX spectrum Chabazite Zeolite after ion exchange with 0.05 M copper (II) nitrate

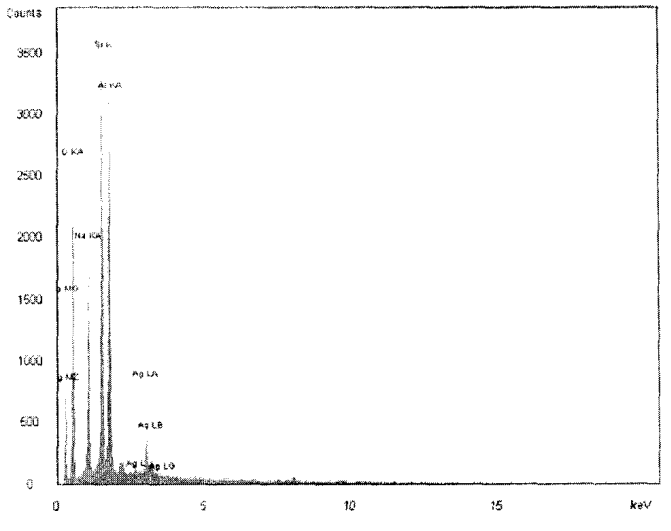

EDX	Oxygen (O)	Sodium (Na)	Aluminum (Al)	Silica (Si)	Silver (Ag)
Concentration Weight %	42.20	16.56	17.67	21.46	2.10

Figure 7.19: EDX spectrum Synthetic Zeolite A after ion exchange with 0.011 M silver nitrate

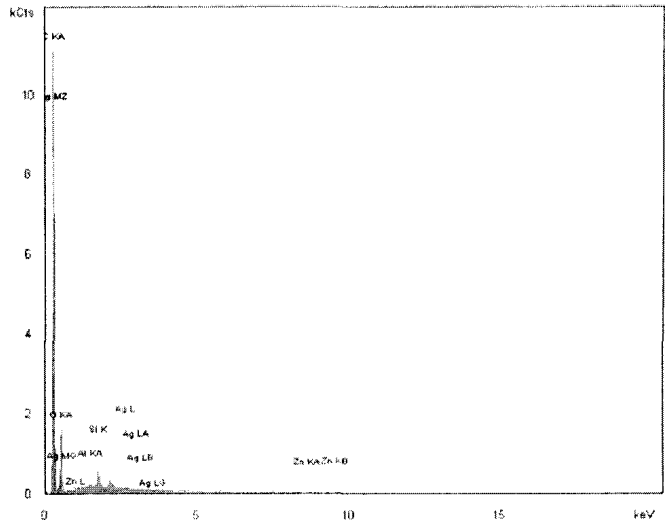

EDX	Carbon (C)	Oxygen (O)	Aluminum (Al)	Silica (Si)	Zinc (Zn)	Silver (Ag)
Concentration Weight %	80.60	18.04	0.11	0.35	0.00	0.90

Figure 7.20: EDX spectrum Antimicrobial powder from Company D

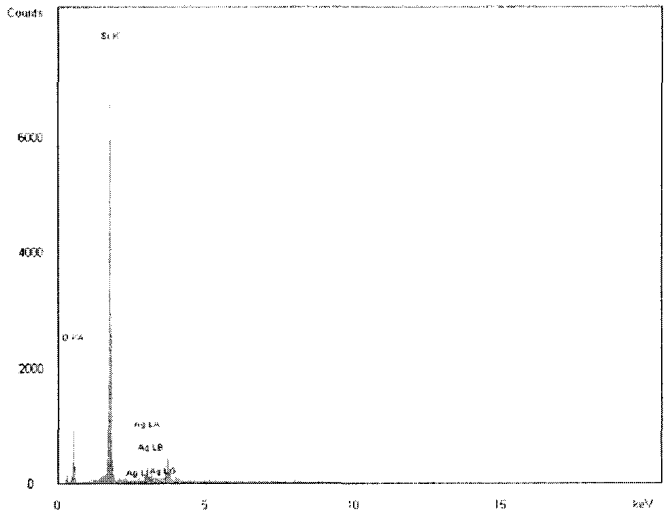

EDX	Oxygen (O)	Silica (Si)	Silver (Ag)
Concentration Weight %	44.20	48.45	7.35

Figure 7.21: EDX spectrum Silica Glass 200C (1)

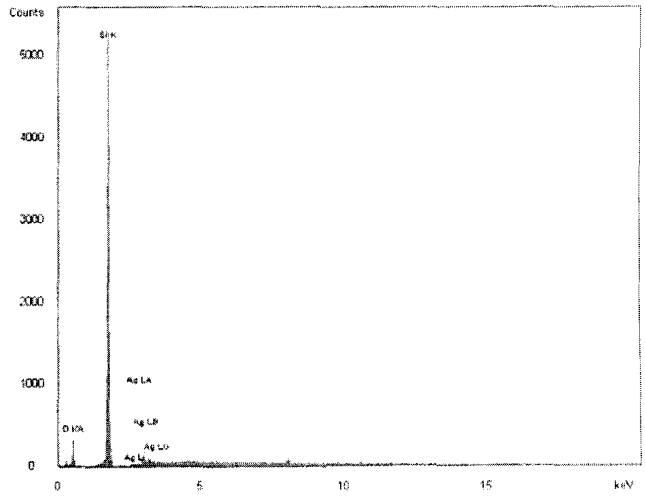

EDX	Oxygen (O)	Silica (Si)	Silver (Ag)
Concentration Weight %	34.62	62.33	3.05

Figure 7.22: EDX spectrum Silica Glass 200C (2)

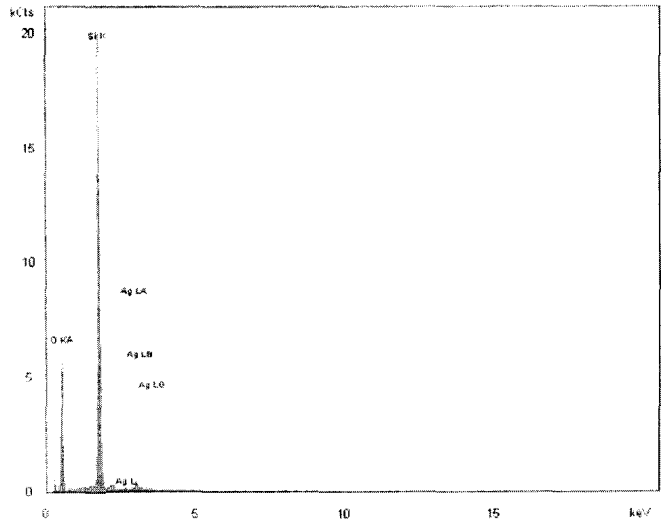

EDX	Oxygen (O)	Silica (Si)	Silver (Ag)
Concentration Weight %	60.02	38.59	1.38

Figure 7.23: EDX spectrum Silica Glass freeze dried (6)

7.3 Appendix C: Sample BET Isotherms

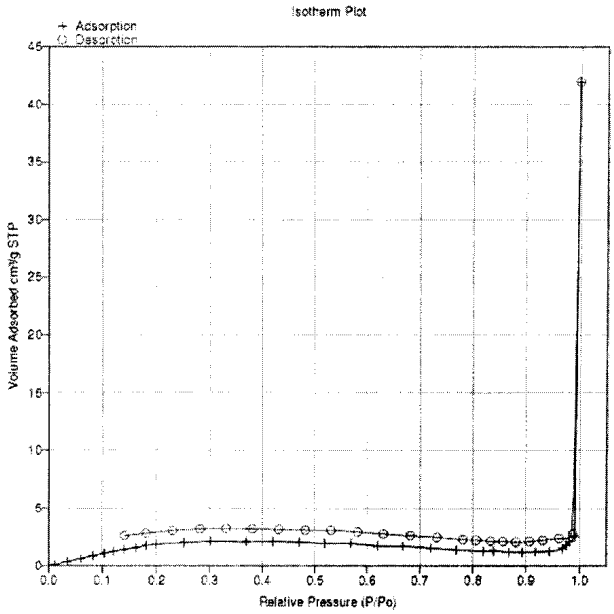

Figure 7.24: BET isotherm Silica Glass (1) dried 200C and 101.325kPa

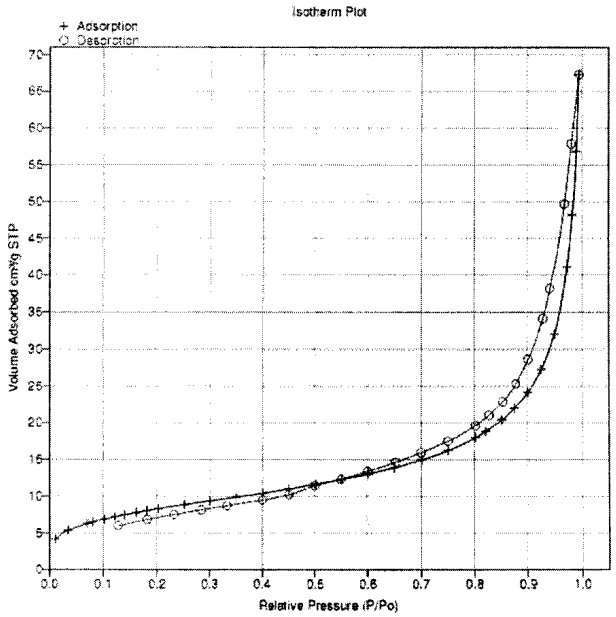

Figure 7.25: BET isotherm Silica Glass (2) dried 200C and 101.325kPa

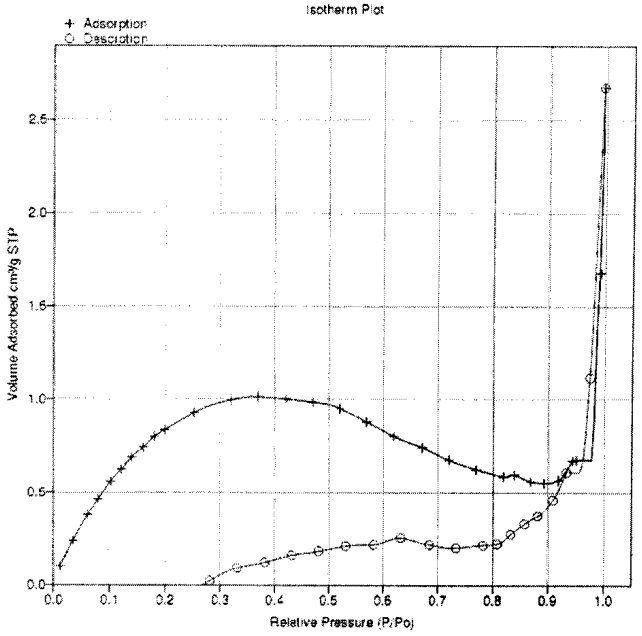

Figure 7.26: BET isotherm Silica Glass (3) dried 100C and 101.325kPa

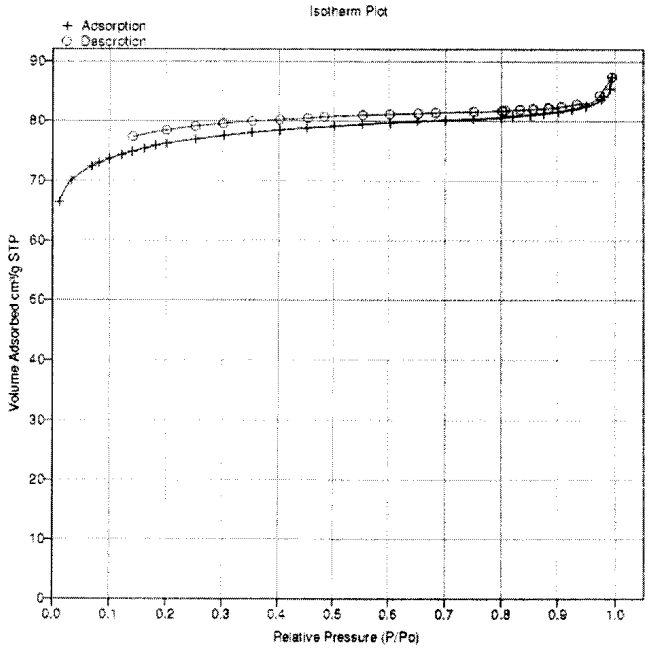

Figure 7.27: BET isotherm Silica Glass (4) dried 20C and 101.325kPa

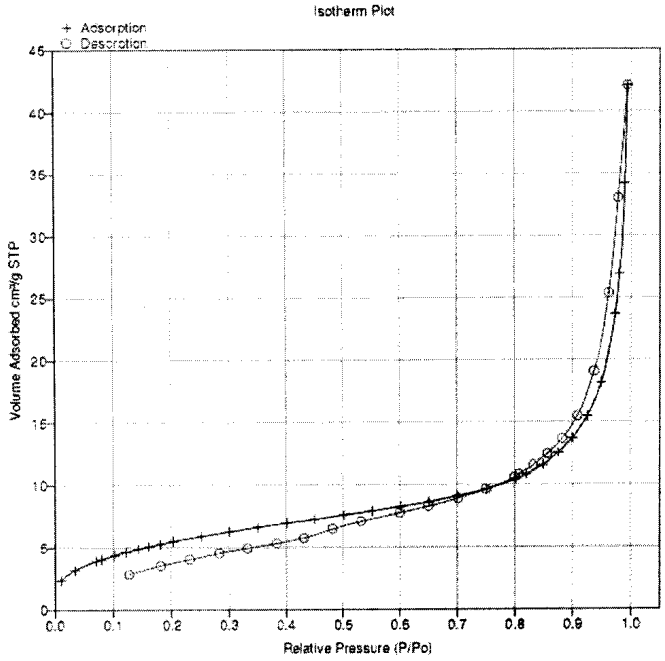

Figure 7.28: BET isotherm Silica Glass (5) dried 20C and 21.5kPa

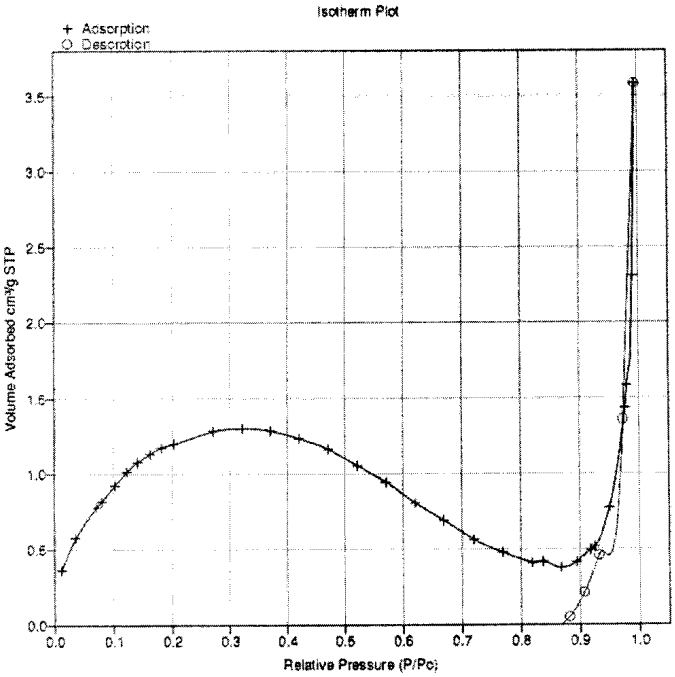

Figure 7.29: BET isotherm Silica Glass (6) dried -50C and 21.5kPa

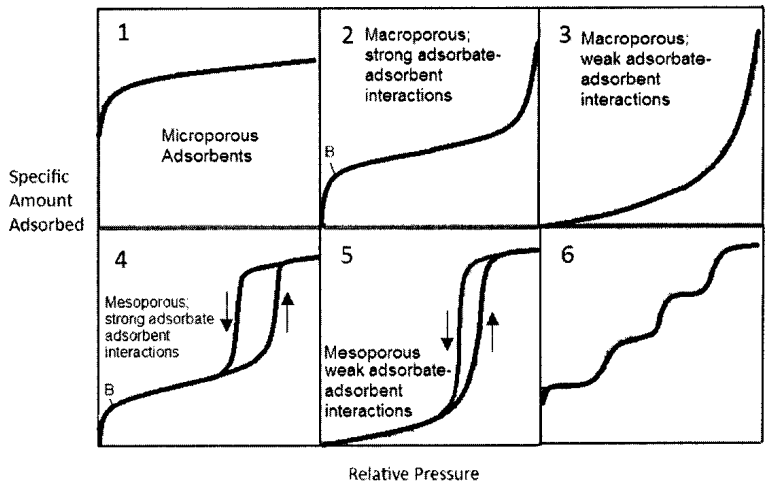

Figure 7.30: Classification for Adsorption Isotherms (re-drawn from IUPAC, 1994)

BET Adsorption and Desorption

Adsorption is the concentration of gas molecules near the surface of a solid material. The phenomena are physical phenomena therefore it may also be called physisorption. Adsorption occurs due to intrinsic surface energy. The result of the forces acting between the exposed surface and gas molecules is characterized as physical adsorption due to Van der Waals forces. Thus due to these weak physical bonds, adsorption is a reversible phenomena shown in the above isotherm plots.

Gas physisorption experiments by BET allow measurement of surface area of the material, because the amount of gas adsorbed is proportional to the entire surface area. The IUPAC standard isotherm plots differ because the systems present different gas/solid interactions. Genrally, type 1 is microporous while others are usually non-porous. Type II and III isotherms are generally obtained in cases of nonporous or highly macroporous adsorbents (Bansal RC, Goyal M, 2005).

The total sum of void volume in a solid is the porosity of that solid. Porosity can determine durability, strength, permeability and adsorption properties of a solid. Pore structure characteristics are important for analyzing behaviour of solid materials. Pores of material are classified as three main types: micropores (less than 2nm diameter), mesopores (between 2 and 50nm diameter) and macropores (larger then 50nm diameter). Surface area of a solid is directly related to pore size and pore volume; the larger the pore

volume the larger the surface area and the smaller the pore size the higher the surface area.

7.4 Appendix D: Sample XRPD Peaks

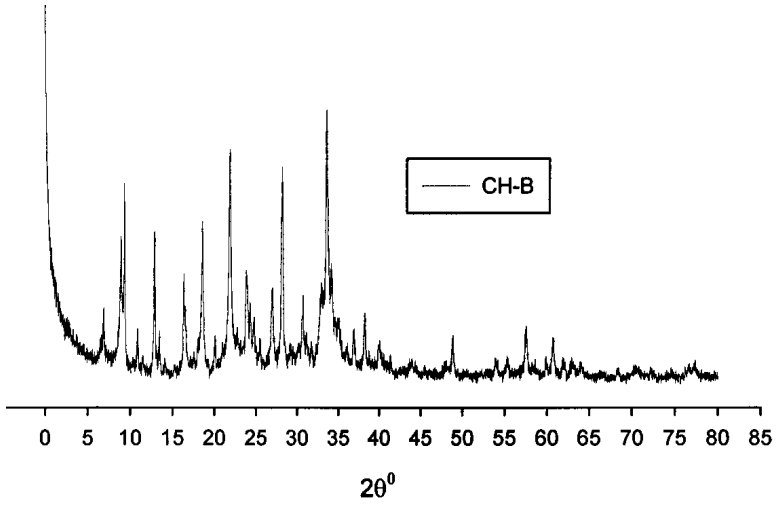

Figure 7.31: XRPD Blank Chabazite

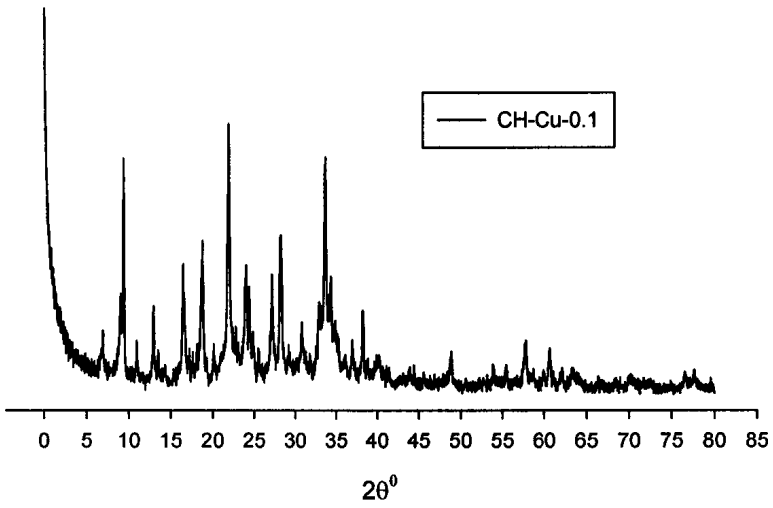

Figure 7.32: XRPD Chabazite after ion exchange with 0.011 M copper (II) nitrate

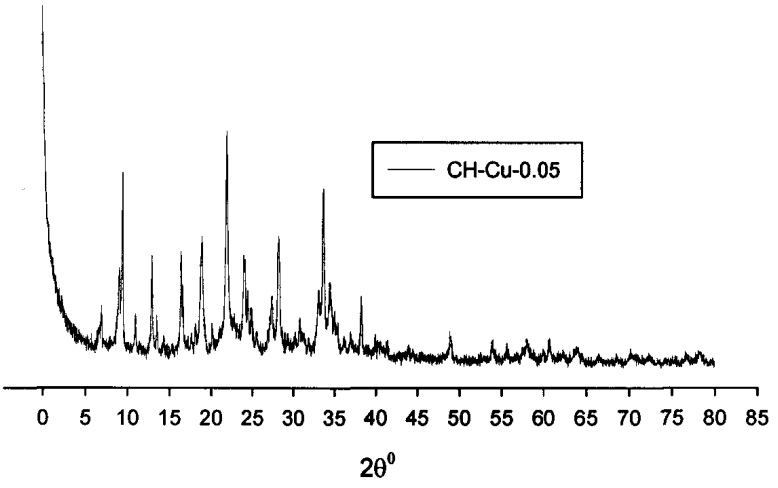

Figure 7.33: XRPD Chabazite after ion exchange with 0.05 M copper (II) nitrate

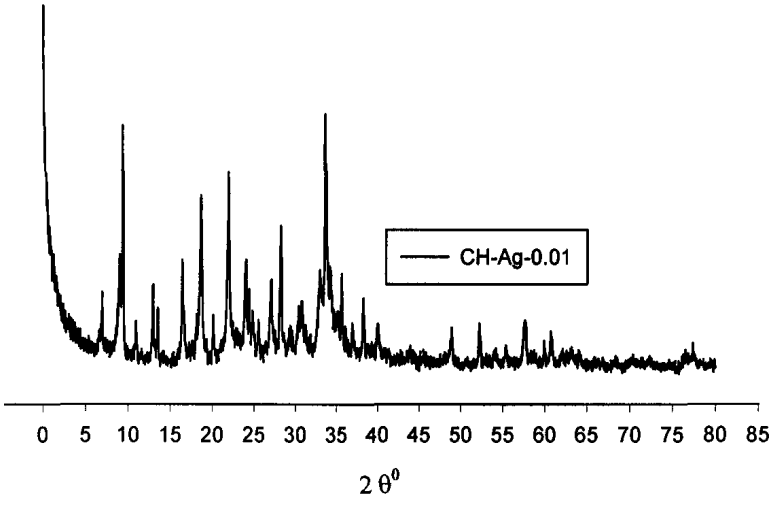

Figure 7.34: XRPD Chabazite after ion exchange with 0.011 M silver nitrate

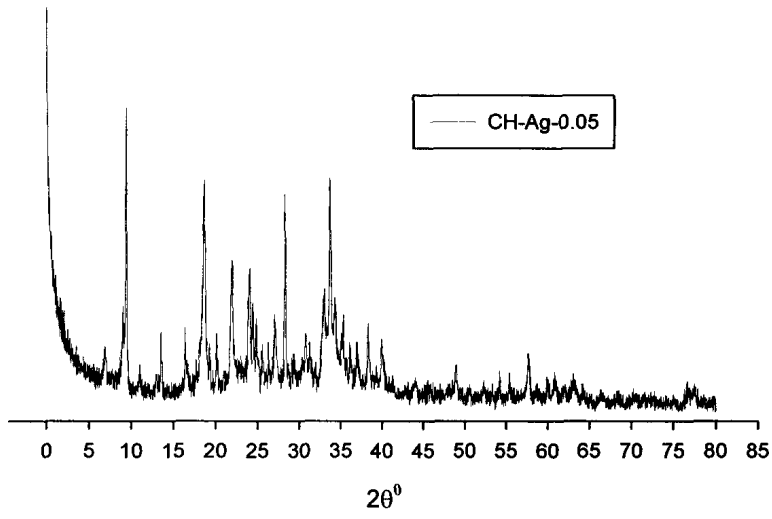

Figure 7.35: XRPD Chabazite after ion exchange (at 60°C) with 0.05 M silver nitrate

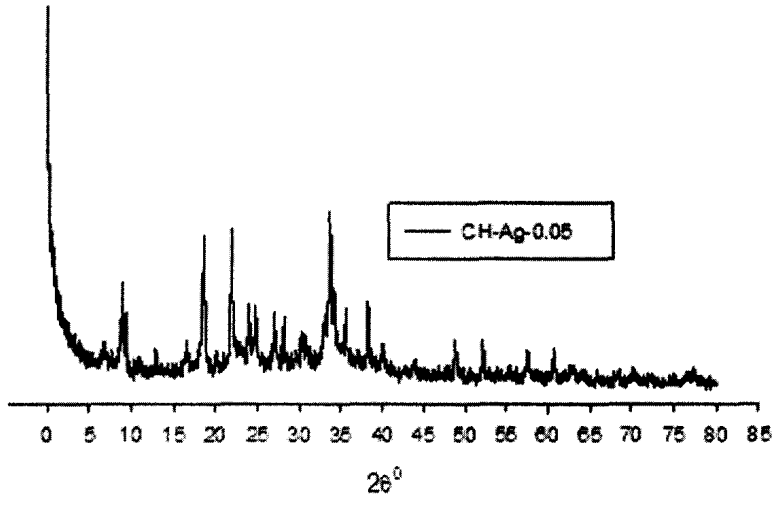

Figure 7.36: XRPD Chabazite after ion exchange (at 20°C) with 0.05 M silver nitrate

7.5 Appendix E: Bacterial Culture Propagation procedure

Freeze dried pellets of *Escherichia coli* were initially obtained from American Type Culture Collection. The vial containing the bacterium in this freeze dried form was opened according to enclosed instructions (aseptic environment). Using ATCC 294 recommended broth medium of tryptone and sodium chloride, 1 mL of broth was used, using 1000 uL pipette, to cover and rehydrate the entire pellet. 1 mL of rehydrated pellets was then transferred from the vial into a 500 mL flask containing 50 mL recommended broth. The flask was then incubated with foam stopper for 24 hours, 37°C. Two actions were then performed with the cultured flask:

i) The 50 mL cultured bacteria flask was then mixed with 50 mL glycerol and 1 mL of the mixture was transferred into 50 vials. Vials were stored in the freezer until needed. Frozen vials were propagated every few months to ensure viability of bacteria or if contamination was evident on the storage petri dishes. Contents of frozen vials, once rehydrated, would be transferred into 20-30 mL recommended broth and inoculated.

ii) Several drops of the inoculation from the flask were used to inoculate agar plates; ATCC 294 agar was used to prepare the petri dishes. Once petri dishes were pour plated the plates were inoculated for 24 hours at 37°C. In order to achieve dilution of *E. coli* and essentially achieve healthy individual colonies for storage in petri dish on recommended medium, the initial plates were then streaked onto new plates using standard microbiological practices. New plates were streaked at least once a month to guarantee a viable working strain of bacteria free of contamination.

7.5.1 Sample N_0 data from experimentation

Table 7.1: Typical Experimental Data to Calculate N_0

			E. Coli Plate Counts (10^7 CFU)					
Sample Description	**Concentration (weight %)**	**Aluminum Substrate$_n$**	**P1-N_0**	**P2-N_0**	**P3-N_0**	**Mean Ave-N_0**	**STD P_n N_0 Substrate$_n$**	**STD P_n N_0 Substrate$_{1-3}$**
	1	1	168	162	165	129.63	3	32.880
		2	103	101	83		11.015	
		3	134		121		9.192	
	0.5	1	140	134	149	139	7.549	8.544
		2	127	132	139		6.027	
		3	136	155	139		10.214	
	0.5(2) Durability	1	81	81	97	88.111	9.237	6.091
		2	92	94	88		3.055	
		3	87	81	92		5.507	
	0.5(B) Repeatability	1	105	106	114	107	4.932	8.529
		2	118	110	95		11.676	
		3	116	94	105		11	
	0.5(After) Leaching	1	85	89	86	92.625	2.081	13.383
		2	105	112	105		4.041	
		3	87	72			10.606	
	0.1	1	60	52	54	95.222	4.163	33.925
		2	129	133	133		2.309	
		3	97	113	86		13.576	
	0.05	1	75	62	71	83.556	6.658	13.010
		2	99	98	87		6.658	
		3	92	76	92		9.237	
	0.03	1	82	87	95	78.778	6.557	12.214
		2	60	64	74		7.211	
		3	72	93	82		10.503	
	0.005	1	74	81	82	77	4.358	4.949
		2	71	76	80		4.509	
Chab-20.7% Ag		3	69	77	83		7.023	

Table 7.1: [Typical Experimental Data to Calculate N_0] Continued

			E. Coli Plate Counts (10^7 CFU)					
Sample Description	**Concentration (weight %)**	**Aluminum Substrate$_n$**	**P1-N_0**	**P2-N_0**	**P3-N_0**	**Mean Ave-N_0**	**STD P_n N_0 Substrate$_n$**	**STD P_n N_0 Substrate$_{1-3}$**
Chab-4.5% Ag	1	1	128	136	133	131.13	4.041	9.876
		2		118	127		6.363	
		3	137	149	121		14.047	
	0.5	1	123	131		131.25	5.656	11.671
		2	150	127	111		19.604	
		3	134	133	141		4.358	
	0.1	1	98	99	117	93.33	10.692	14.662
		2	103	75	94		14.294	
		3	100	70	84		15.011	
	0.5(2) Durability	1	198	177	215	180.63	19.035	20.381
		2	171	174			2.121	
		3	176	146	188		21.633	
	0.5(3) Durability	1	149	140	138	145.44	5.859	12.729
		2	157	144	168		12.013	
		3	144	147	122		13.650	
	0.5(B) Repeatability	1	109	109	110	127	0.5773	15.937
		2	133	130	135		2.516	
		3	158	127	132		16.643	
	0.5(After) Leeching	1	106	115	117	127.13	5.859	25.062
		2	123	105	121		9.865	
		3		153	177		16.970	
Chab-3.4% Ag	0.05	1	94		90	77.12	2.828	15.968
		2	57	88	94		19.857	
		3	65	59	70		5.507	
	0.005	1	80	81	67	76.37	7.810	6.116
		2	80	74	70		5.033	
		3		74	85		7.778	
	0.0017	1	103	104	88	99.44	8.962	13.538
		2	111	86	79		16.822	
		3	118	113	93		13.228	

Table 7.1: [Typical Experimental Data to Calculate N_0] Continued

			E. Coli Plate Counts (10^7 CFU)					
Sample Description	**Concentration (weight %)**	**Aluminum Substrate$_n$**	**P1-N_0**	**P2-N_0**	**P3-N_0**	**Mean Ave-N_0**	**STD P_n N_0 Substrate$_n$**	**STD P_n N_0 Substrate$_{1-3}$**
Silica200C (1)- 8.6% Ag	1	1	72	59	63	59.11	6.658	14.277
		2	45	42	39		3	
		3	73	78	61		8.736	
	0.5	1	137	138	119	126.1	10.692	8.335
		2		128	121		4.949	
		3	119		121		1.414	
	0.1	1	80	80	81	92.87	0.577	22.987
		2	78	77	89		6.658	
		3	121		137		11.313	
	0.05	1	103	104	88	99.44	8.962	13.538
		2	111	86	79		16.822	
		3	118	113	93		13.228	
	0.5(2) Durability	1	125	145	151	140.5	13.613	12.511
		2	157	139	134		12.096	
		3	155	122	137		16.522	
	0.5(3) Durability	1	147		149	140.8	1.414	8.951
		2	147	137	143		5.033	
		3	125	131	148		11.930	
	0.5(B) Repeatability	1	108	90	88	98.11	11.015	10.397
		2	92	91	102		6.082	
		3	104	90	118		14	
	0.5(After) Leeching	1	91	81	78	79.88	6.806	7.928
		2	83	75	63		10.066	
		3	87	79	82		4.041	
Chab-13.0% Cu	1	1	104	87	96	97.66	8.504	10.5
		2	112	96	86		13.114	
		3	90	93	115		13.650	
Chab-4.5% Zn	1	1	121	148	132	151.6	13.576	22.945
		2	149	199	168		25.238	
		3	145	139	164		13.051	

Table 7.1: [Typical Experimental Data to Calculate N_0] Continued

			E. Coli Plate Counts (10^7 CFU)					
Sample Description	**Concentration (weight %)**	**Aluminum Substrate$_n$**	**P1-N_0**	**P2-N_0**	**P3-N_0**	**Mean Ave-N_0**	**STD P_n N_0 Substrate$_n$**	**STD P_n N_0 Substrate$_{1-3}$**
Nano particles -31% Ag	0.5	1	95	95	85	79.77	5.773	10.860
		2	78	68	81		6.806	
		3	64	72	80		8	
	0.15	1	82	99	114	98.33	16.010	17.233
		2	69	96	85		13.576	
		3	105	113	122		8.504	
	0.05	1	75	62	71	83.55	6.658	13.010
		2	99	98	87		6.658	
		3	92	76	92		9.237	
	0.005	1	81		78	80.87	2.121	6.128
		2	89	82	76		6.506	
		3	71	89	81		9.018	
	0.5(2) Durability	1	91	107	101	106.89	8.082	8.161
		2	112	109	119		5.131	
		3	111	111	101		5.773	
SynZ-A- 2.2% Ag	0.1	1	94		90	77.12	2.828	15.968
		2	57	88	94		19.857	
		3	65	59	70		5.507	
No Carrier $AgNO_3$	0.1	1	82	87	95	78.77	6.557	12.214
		2	60	64	74		7.211	
		3	72	93	82		10.503	
Tollens Metallic Ag	2	1	80	81	67	76.37	7.8102	6.116
		2	80	74	70		5.033	
		3		74	85		7.778	
	0.1	1	81	83	78	83.88	2.516	6.641
		2	87	82	76		5.507	
		3	98	89	81		8.504	
CNT- 77.2% Ag	1	1	87	74	78	118.5	6.658	33.831
		2	150	136	155		9.848	
		3	122	146			16.970	

Table 7.1: [Typical Experimental Data to Calculate N_0] Continued

Sample Description	Concentration (weight %)	Aluminum Substrate$_n$	E. Coli Plate Counts (10^7 CFU) P1-N_0	P2-N_0	P3-N_0	Mean Ave-N_0	STD P_n N_0 Substrate$_n$	STD P_n N_0 Substrate$_{1-3}$
Silica 1013.25mbar 20C- 3.6% Ag	0.1	1	100	89	89	84.88	6.350	8.550
		2	82	81	87		3.214	
		3	82	68	86		9.451	
	0.05	1	101	83	89	84.77	9.165	11.054
		2	69	89	71		11.015	
		3	97	76	88		10.535	
	0.005	1	105	92	112	99.12	10.148	7.039
		2	91	99			5.656	
		3	102	97	95		3.605	
Silica 215mbar -50C - 2.2% Ag	0.1	1	101	83	89	84.77	9.165	11.054
		2	69	89	71		11.015	
		3	97	76	88		10.535	
	0.05	1	101	83	89	84.77	9.165	11.054
		2	69	89	71		11.015	
		3	97	76	88		10.535	
	0.005	1	105	92	112	103	10.148	13.360
		2	91	99	134		22.869	
		3	102	97	95		3.605	
Company D	unknown	1	122	100		133.1	15.556	15.198
		2	142	142	141		0.5773	
		3	145	139	134		5.507	
	unknown(2) Durability	1	123	118	107	117.6	8.185	12.186
		2	128	134	132		3.055	
		3	107	109	101		4.163	
	unknown(B) Repeatability	1	144	145	106	145.6	22.233	18.001
		2	154	168	156		7.571	
		3	143		149		4.242	
	unknown(after) Leeching	1	98	112	89	98.88	11.590	7.655
		2	99	91	110		9.539	
		3	97	96	98		1	

Table 7.1: [Typical Experimental Data to Calculate N_0] Continued

			E. Coli Plate Counts (10^7 CFU)					
Sample Description	**Concentration (weight %)**	**Aluminum Substrate$_n$**	**P1-N_0**	**P2-N_0**	**P3-N_0**	**Mean Ave-N_0**	**STD P_n N_0 Substrate$_n$**	**STD P_n N_0 Substrate$_{1-3}$**
Company P	unknown	1	78	91	82	133.78	6.658	40.916
		2	130	154	148		12.489	
		3	158	180	183		13.650	
Control - Polyester TGIC Clear Coat	0(1)	1	69	53	51	71	9.865	21.336
		2	59	59	53		3.464	
		3	93	98	104		5.507	
	0(2)	1	120	152	135	163.13	16.01	26.513
		2	164	173			6.363	
		3	179	202	180		13	
	0(3)	1	101	110	109	96.66	4.932	8.558
		2	91	89	94		2.516	
		3	85	96	95		6.082	